

Azores Field Guide

August 20-30, 2017

Table of Contents:

History and economy of the Azores (Hannah Rabinowitz).....	2
General Tectonics of the Azores (Kelvin Tian)	5
Volcanic features of São Miguel Island (Dan Rasmussen).....	14
Volcanic history – Furnas (Celia Eddy).....	17
Volcanic history – Fogo (Natalie Accardo).....	24
Volcanic history – Sete Cidades (Laura Haynes).....	32
Seismicity (Genevieve Coffey).....	38
Landslides (Rachel Marzen).....	45
Tsunamis (Thomas Weiss).....	49
Coastal Erosion (Anna Barth).....	52
Paleoshorelines and vertical displacement history (Michael Sandstrom).....	56
Marine Life (Elise Myers).....	61
Terrestrial Life (Josh Russell).....	72
Agriculture (Meg Frenkel).....	76
Oceanography and the Marine Boundary Layer (Lorelei Curtin).....	82
The North Atlantic Oscillation (Alexandra Boghosian).....	87
Volcanic emissions and sulfate aerosols (Henry Towbin).....	91
Geothermal Power (Yen Joe Tan).....	103
Hydroelectric Power (Bar Oryan).....	107

The Discovery and Settlement of the Azores Islands

The Azores archipelago (Fig. 1) was discovered by humans only relatively recently, though the credit for the initial discovery remains disputed. World maps as early as the Florentine Atlas of 1351 show a group of islands at approximately the same location, which some have suggested is proof of an earlier discovery date for the Azores.

However, the most well established date of discovery is in 1432 when Gonçalo Velho

Cabral led a merchant expedition back from western Africa that landed on the island of Santa Maria during a storm. The discovery of Santa Maria was quickly followed by that of São Miguel and Terceira (named for being the third island discovered). Within seven years, all seven islands that make up the Oriental (Santa Maria and São Miguel), Central (Faial, Pico, São Jorge, Graciosa, and Terceira), and Occidental (Corvo and Flores) groups had been discovered (Fig. 1). Upon discovery, the Azores were populated only by birds, providing a challenge for the Portuguese whose primary interest in colonizing the islands was to establish a restocking harbor for their merchant ships traveling between Portugal and Africa. To address this issue, on July 2, 1439 when Prince Henry of Portugal ordered that the islands be populated with sheep prior to settlement by people.

Largely due to their distance from the mainland, the Azores islands were governed in a fairly decentralized manner. Primarily settled by disenfranchised groups from mainland Europe, each island was overseen by a Captain-Donatary, all of whom came from a group of poor nobles in Portugal. The general population was made up of Jews, Spanish, Bretons, Moors, and Africans with the Central group being settled by Flemish refugees as a favor from Prince Henry to his sister, La Infanta Isabel.

Pursuit of Autonomy

Though the Azores were largely governed locally for most of their early history, as a port established to restock merchant ships, their economy was dictated by the central government in Portugal. This arrangement quickly began to irk the islands populations who felt that the central government was profiting off of their labor but refusing to invest in infrastructure such as parks and docks, which had to be funded by private citizens. This discontent erupted into a few unsuccessful revolts on São Miguel and Faial in the early 1890s. Tensions rose further when the Portuguese government replaced the Azorean currency with that of Portugal, tried to abolish the high court on the islands so that all court cases would have to be heard on the mainland, and abolished municipal governments in 1892. The final straw came when the central government decided that alcohol prices would be set in Lisbon, further constraining the Azores economy. The Portuguese government quickly realized the strain on their relationship with the islands as local elections became dominated by candidates running on a pro-autonomy platform rather than those from traditional parties. In 1895, the Azores was granted the right to petition for autonomy. However, soon after (in 1910) the Portuguese monarchy was removed from power, causing a shift towards a recentralization of power in Portugal.



Figure 1 Maps of the Azores with the island groupings indicated on the right map. Maps from <http://www.worldatlas.com/webimage/countrys/europe/azores.htm>

This paradigm remained in place for almost another century until the Second Autonomous Movement in the 1970s. After a 1974 coup overthrew the fascist government of Portugal, the Portuguese Constitutional Assembly approved Section VII of the Constitution, which established the Autonomous Region of the Azores on March 26, 1976. This created a truly administratively and politically autonomous region within the Portuguese state. Under this system (Fig. 2), local areas in the Azores are governed as parishes (*freguesias*) and municipalities (*concelhos*). On a broader scale, the islands are governed by a Representative of the Republic who is nominated by the Portuguese head of state and has veto power. This representative has the responsibility to nominate a President of the Regional Government who is elected by the population of the Azores. The president forms the executive government and oversees the functioning of executive organizations. Finally, the Legislative Assembly is composed of members who are directly elected. This assembly monitors the Regional Government and can override the veto of the Representative of the Republic.

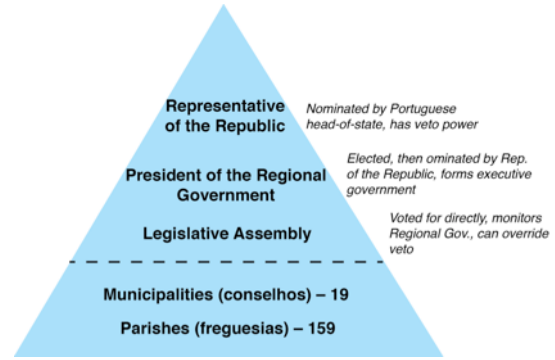


Figure 2 Schematic of the structure of the government in the Azores.

The Role of the Azores on the Global Stage

Just as the Azores were initially settled as a stopping point for ships en route to Portugal, the current geopolitical role of the islands revolves around their central location in the Atlantic between North America and Europe. The Azores were used as a reprovisioning and refueling point for transatlantic journeys, and was notably a stopping point for the first intercontinental commercial flight in 1939. The islands were also strategically important during both World Wars. For example, one of the reasons that Germany strove for Portugal to join their side during WWI was that they wanted to establish a base for their U-boat campaign on the Azores. Indeed, when Portugal declared against Germany, the U.S. took the opportunity to establish a naval base in the Azores.

Again, during WWII, the Allies campaigned to establish a base on the Azores islands. Though Portugal remained neutral in the war, in 1943, the U.S. and Britain were able to establish Lajes Airforce Base on Terceira as part of the Treaty of Windsor of 1373 between Britain and Portugal. A second air force base on Santa Maria was granted to and built up by the U.S. when the volume of flights overwhelmed Lajes. Though the bases were returned to Portugal after the war, the U.S. has maintained use of Lajes Airforce Base to the present day through a 1951 treaty, renewed in 1983/4 and 1995.

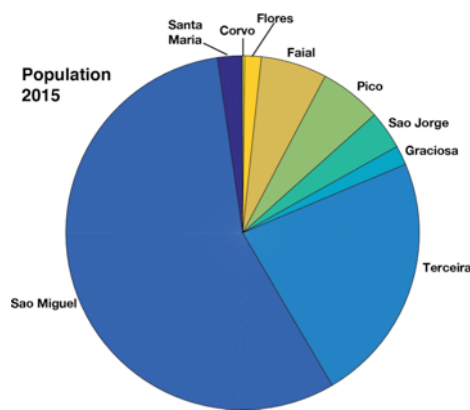


Figure 3 Population distribution in the Azores in 2015. Data from Serviço Regional de Estatística dos Açores

Population and Economy of the Azores

Over half of the population of the Azores lives on São Miguel, followed by Terceira with ~25% of the population (Fig. 3).

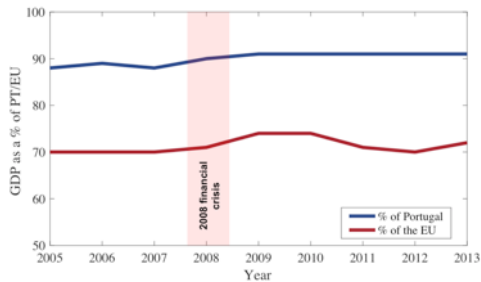


Figure 4 GDP of the Azores as a percent of the GDP of Portugal (blue) and the average EU country (red). The timing of the 2008 financial crisis is indicated on the chart. Data from Massot, 2015, *The Agriculture of the Azores Islands*

Economically, the Azores has improved significantly since the 1990s. In 1983, the GDP of the Azores was ~39% of that of the average European Union (E.U.) country, yielding a designation as a “less developed region”. By 2005, the Azores GDP had risen to ~70% that of the average E.U. country. This was largely the result of a strong overall Portuguese economy as well as a boost from E.U. structural funds. Indeed, the economy of the Azores was stable enough by 2008 to survive the financial crisis at a higher GDP than the average E.U. country (Fig. 4).

The economy of the Azores is largely focused on the services sector, which includes components such as tourism. The next largest component of the economy is industry, comprising such things as wine and cheese production. Finally, about 10% of the economy is in the primary (agricultural) sector. However, land use in the Azores is strongly focused on the agricultural sector with ~51% of the land (usable agricultural area) being dedicated to farming. Most of this (~98%) is focused on livestock, divided between grassland for grazing and farmland for growing maize used to feed cattle. The other 2% of the land is used for permanent crops, including sugar beet, banana, pineapple, tea, and yams. The most significant exports from the Azores are wine and dairy, with the largest fraction of these exports going to Portugal (Fig. 5).

The economy of the Azores is largely focused

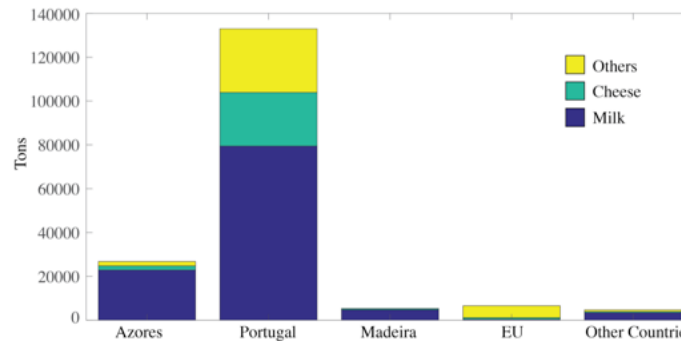


Figure 5 Dairy exports from the Azores. The majority of dairy is exported to Portugal, with the largest fraction of these exports being milk. Exports designated as “Others” include products such as dehydrated milk.

References

Massot, A., Directorate-General for Internal Policies, European Parliament’s Committee on Agriculture and Rural Development. (2015). *The Agriculture of the Azores Islands*. Brussels: European Union.

Moniz, Miguel. (1999). *World Bibliographical Series: Azores*. (Vol. 221). Oxford, England: ABC-CLIO Ltd.

65th Air Base Wing History Office. *A Short History of Lajes Field, Terceira Island, Azores Portugal*.

Statistics Azores Portugal (Estatística dos Açores). (2017, May 22). Retrieved from <http://srea.azores.gov.pt/>.

General Tectonics of Azores (Kelvin Tian)

Introduction

The Azores archipelago is located at both sides of the Mid-Atlantic Ridge (MAR) at about 39°N, 1400 km west of continental Europe, comprising nine volcanic islands: from West to East are Flores, Corvo, Faial, Pico, Sao Jorge, Graciosa, Terceira, Sao Miguel and Santa Maria (Fig. 1) [Hildenbrand *et al.*, 2014]. In addition to the East-West plate extension of MAR with a separation rate of 20~23 mm/a [Vogt and Jung, 2004], the Northwest-Southeast trending hyper-slow Terceira Rift (TR) is currently obliquely (~40°~65° angles to the rift axis) spreading with a rate of 4 mm/a (Fig. 1), which is equivalent to 2.3~3.8 mm/a in a direction orthogonal to the rift axis.

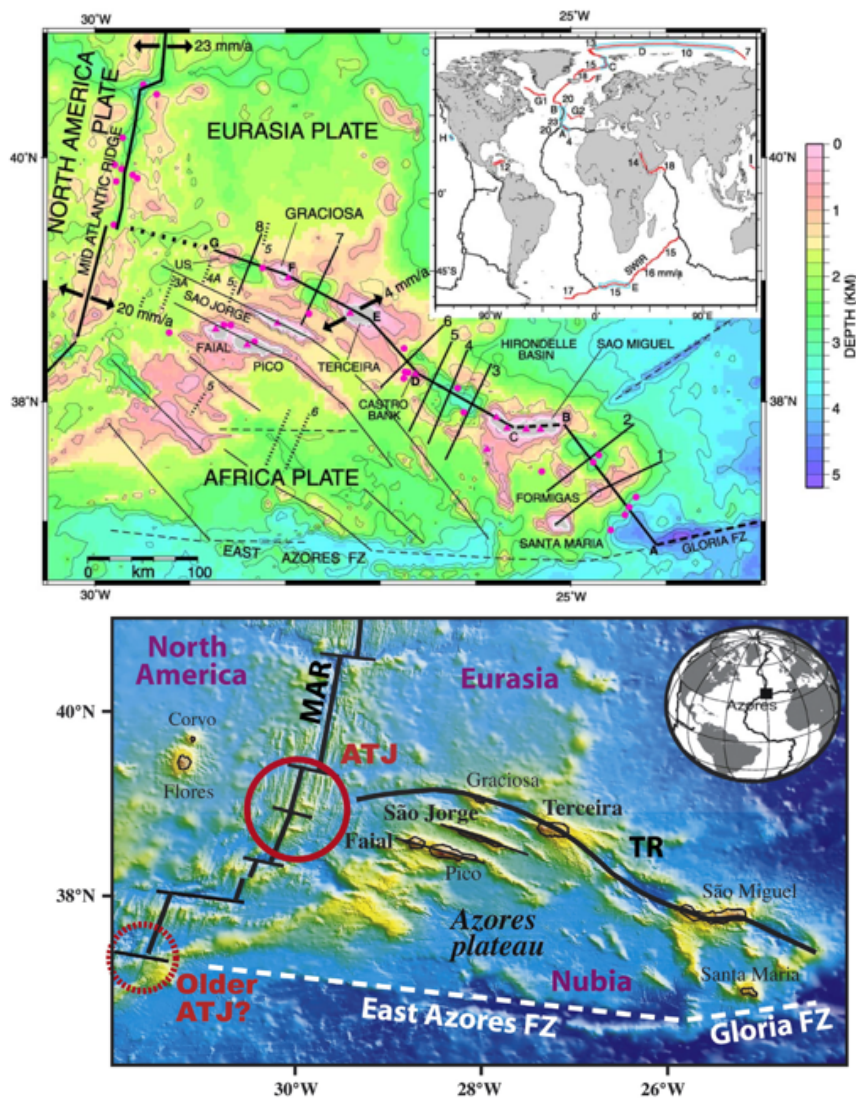


Figure 1. Up: Bathymetry around Azores triple junction with interpreted Terceira Rift (TR) and Mid-Atlantic Ridge (MAR) plate boundaries. The spreading rate of MAR varies from 20 mm/a to 23 mm/a whereas the TR is obliquely spreading with 4 mm/a. (Adapted from [Vogt and Jung, 2004]). Down: Azores islands. From [Hildenbrand *et al.*, 2014].

The TR is considered the slowest spreading ridge compared to ‘ultra-slow’ spreading ridge Southwest Indian ridge of 15~16 mm/a and Gakkel ridge of 7~13 mm/a [Vogt and Jung, 2004], joining the MAR at 30°W 39°N. The intersection of the two extensional plate boundaries is the Azores triple junction where North American plate, Eurasian plate and African plate meet. The Azores triple junction is one of the eight triple junctions around the world (Fig. 3) with a type of Ridge-Ridge-Ridge (RRR) configuration. According to [Fowler, 2005], this type of triple junction is unconditionally stable (Fig. 2).

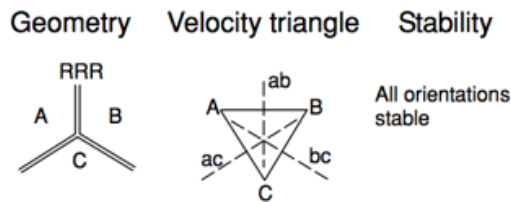


Figure 2. Stability of RRR type of triple junction according to [Fowler, 2005].

However, the existence of an active hotspot with a deep mantle plume origin at Azores triple junction [Torsvik et al., 2010](fig. 3) complicates the plate boundary between Eurasian and African plates and results in a diffused plate boundary revealed by recent GPS data [Marques et al., 2013] (fig. 4).

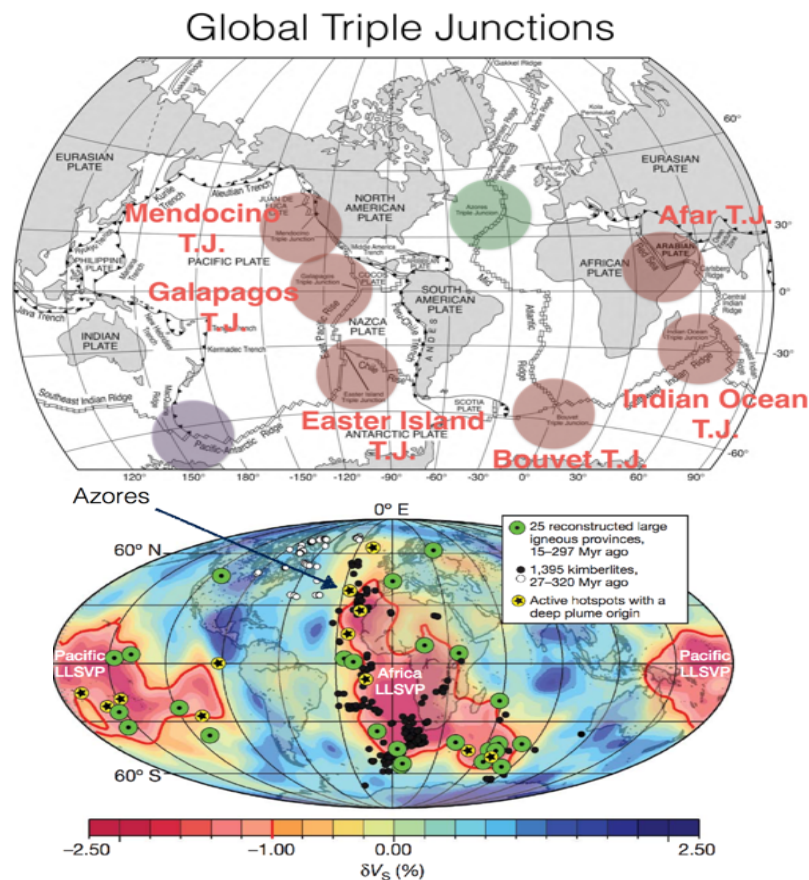


Figure 3. Up: Global triple junction distribution. Adapted from [Fowler, 2013] ; Down: Hot spots and igneous province distributions. Adapted from [Torsvik et al., 2010].

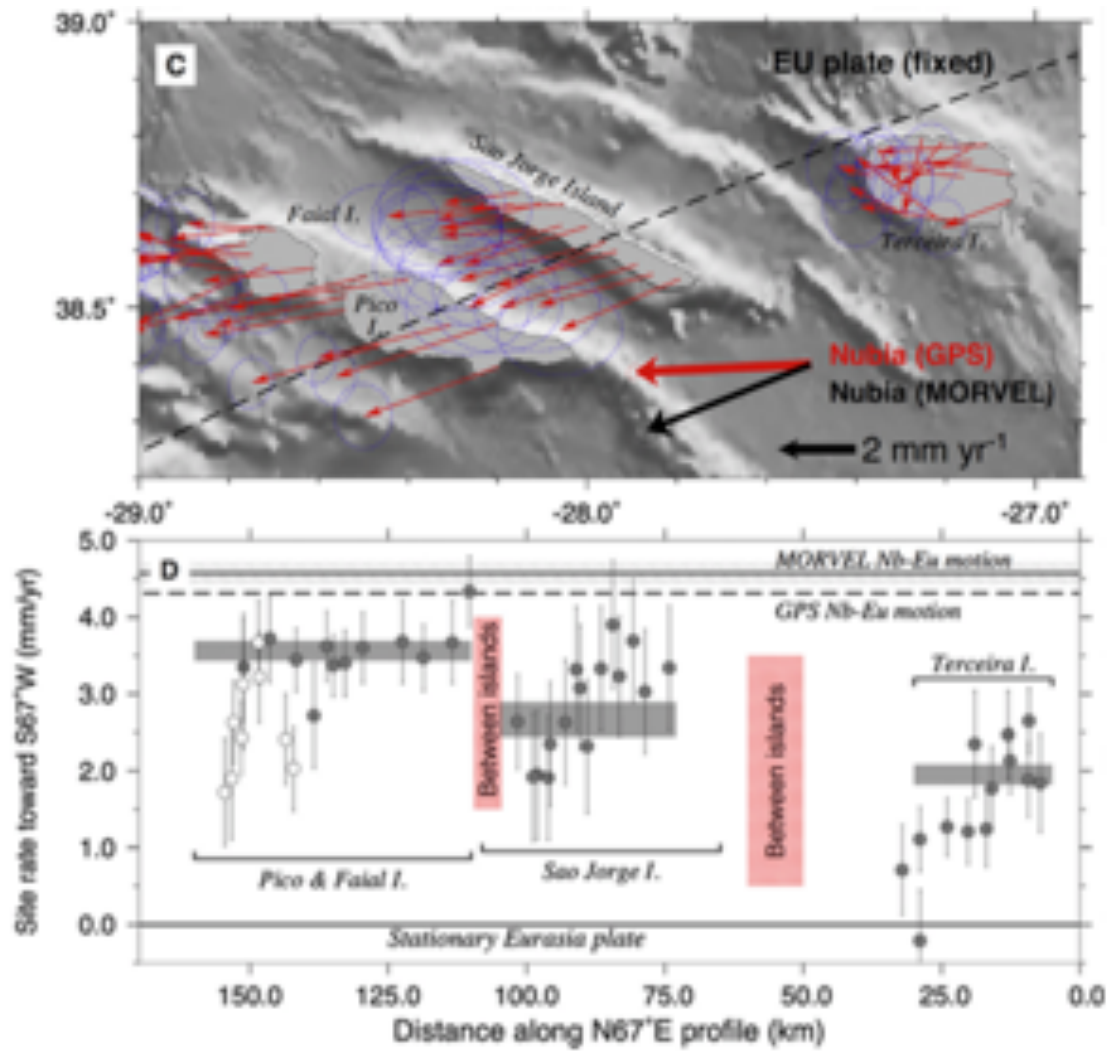


Figure 4. GPS site velocities (red arrows). From [Marques *et al.*, 2013].

Major tectonic structures around Azores are the MAR that separate the lithospheric plates between North America (NA) and Eurasia Plate (Eu) as well as African/Nubia Plate (Nu), the East Azores Fracture Zone (EAFZ), the West Azores Fracture Zone (WAFZ), the North Azores Fracture Zone (NAFZ), the TR, the East Azores Volcano-Tectonic System (EAVTS), [Gaspar *et al.*, 2015](Fig. 5).

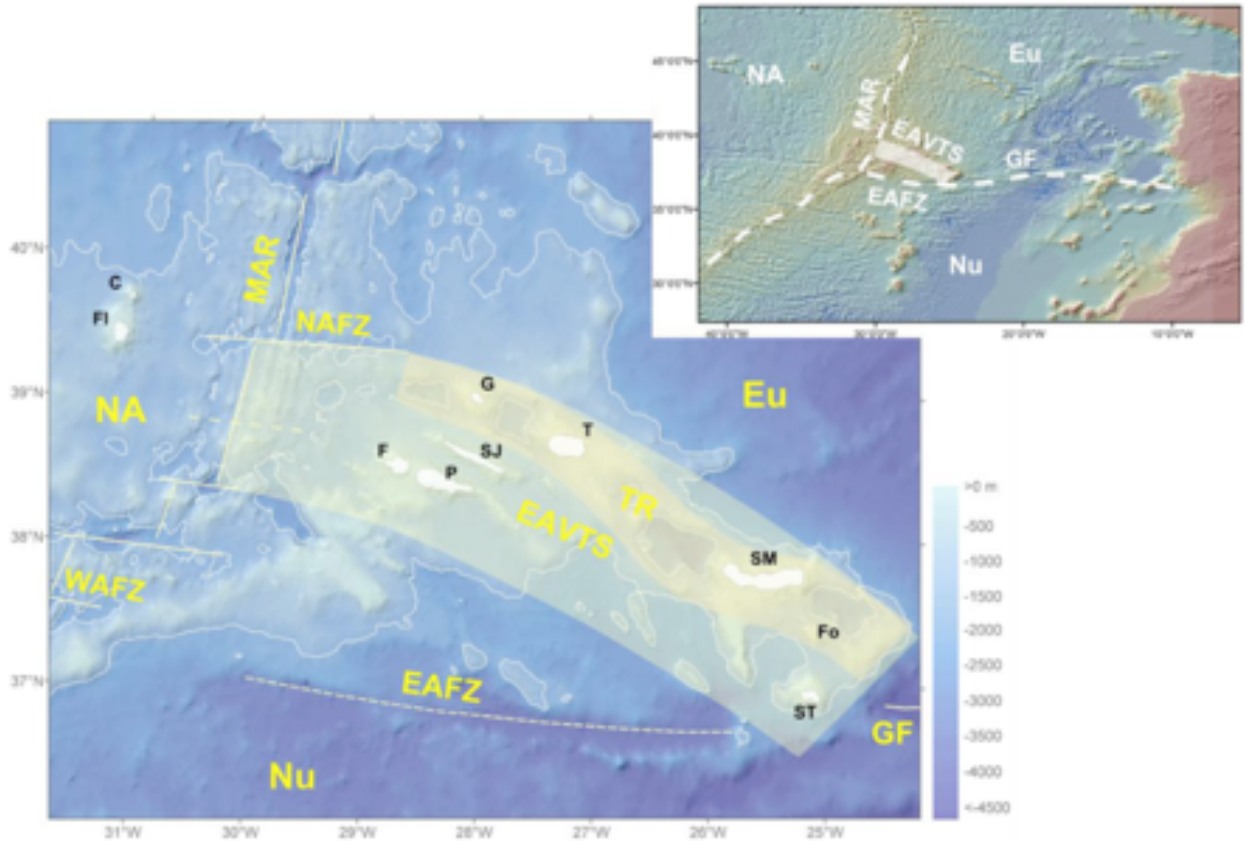


Figure 5. Main tectonic structures around Azores. The shaded area represents the sheared western segment of the Eu–Nu plate boundary. Lithospheric plates: NA, North America; Eu, Eurasia; Nu, Nubia. Tectonic structures: MAR, Mid-Atlantic Ridge; NAFZ, North Azores Fracture Zone; WAFZ, West Azores Fracture Zone; TR, Terceira Rift; EAFZ, East Azores Fracture Zone; GF, Gloria Fault; EAVTS, East Azores Volcano-tectonic System. Islands: C, Corvo; FI, Flores; F, Faial; P, Pico; SJ, São Jorge; G, Graciosa; T, Terceira; SM, São Miguel; Fo, Formigas islets; ST, Santa Maria. Adapted from [Gaspar *et al.*, 2015].

The MAR axis has an obvious bend at the Azores triple junction from NE to NEN. This bend might be related to the localization of the plume magmatism. The EAFZ is thought to be the old plate boundary between EU and NU which is currently inactive [Searle, 1980]. To the East tip of the EAFZ is the transform fault Gloria Fault (GF). According to [Argus *et al.*, 1989], the curved geometry of GF has been used to constrain the pole of rotation, which locates at around 20°W 20°N as shown in Figure 6. This result is further supported by the focal mechanism that transitions from trans-tensional at TR to strike-slip at GF to compressional east of Gibraltar strait (Fig. 6).

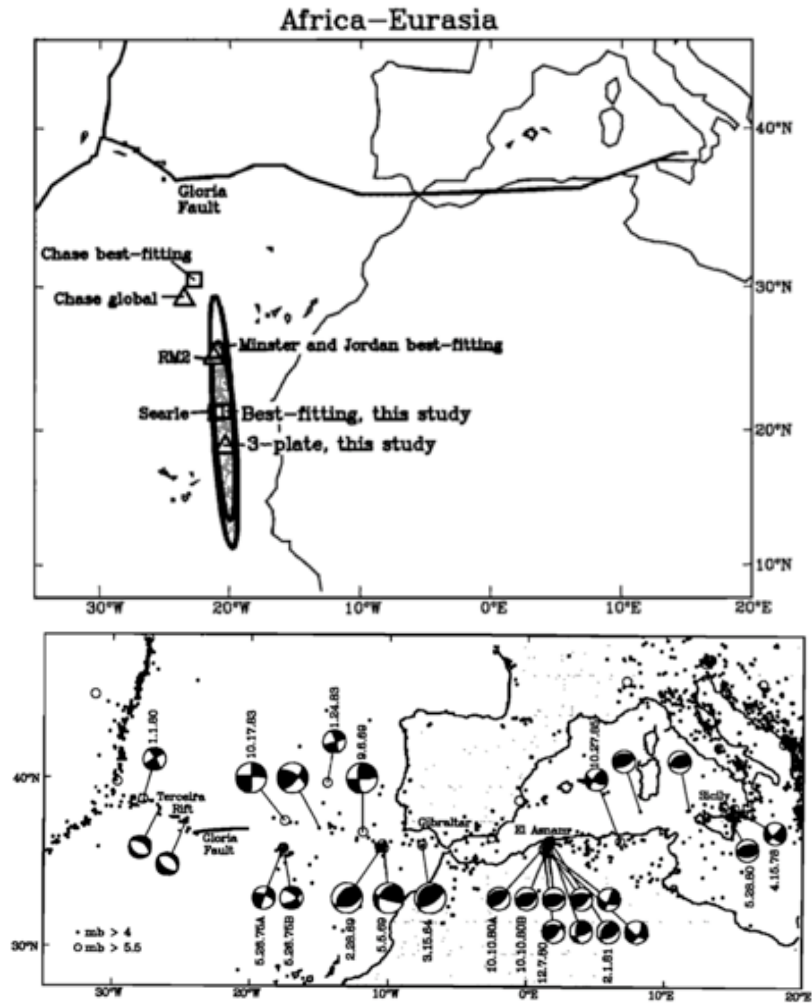


Figure 6. Up: Pole of rotation for Eu and Nu plates. Down: Earthquakes during 1964–1987 that are shallower than 100 km. 26 large events are shown with focal mechanism solutions. From [Argus et al., 1989].

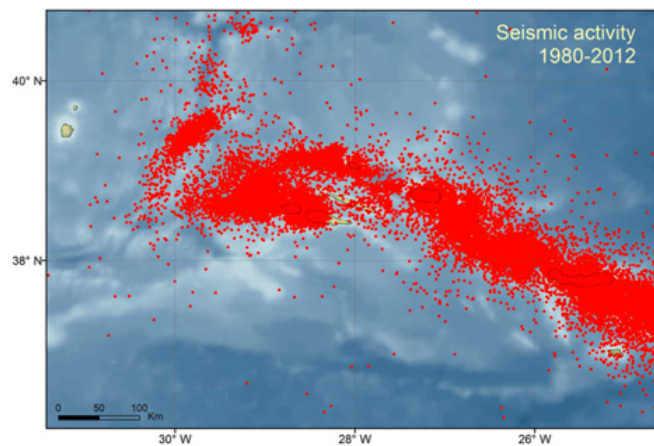


Figure 7. 30 years seismicity at Azores. From [Gaspar et al., 2015].

According to [Gaspar et al., 2015], since human started to live on the Azores islands in 1500s, there are totally 31 large earthquakes which killed about 6300 people. The past 30 years of

seismicity show a clear seismic gap (fig. 7) around São Jorge area where a magnitude 7 earthquake happened in 1757.

In addition, due to the existence of the hot plume, the bathymetry along the MAR at Azores triple junction show a clear change from median valley to axial high (fig. 8) [Searle, 1980].

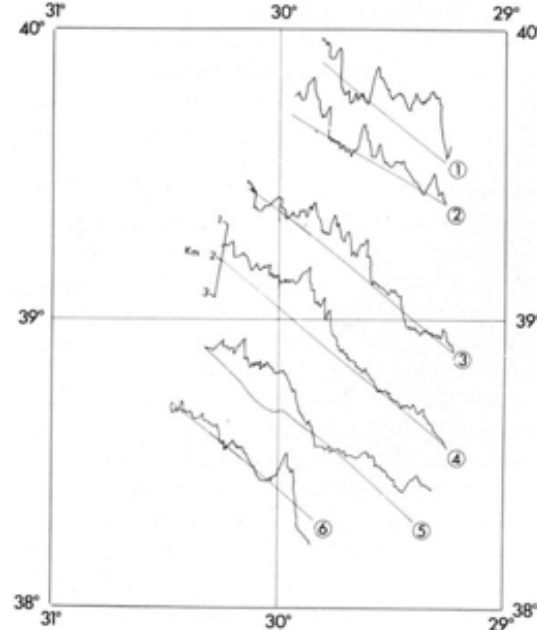


Figure 8. Bathymetric profiles along MAR near Azores trip junction. From [Searle, 1980].

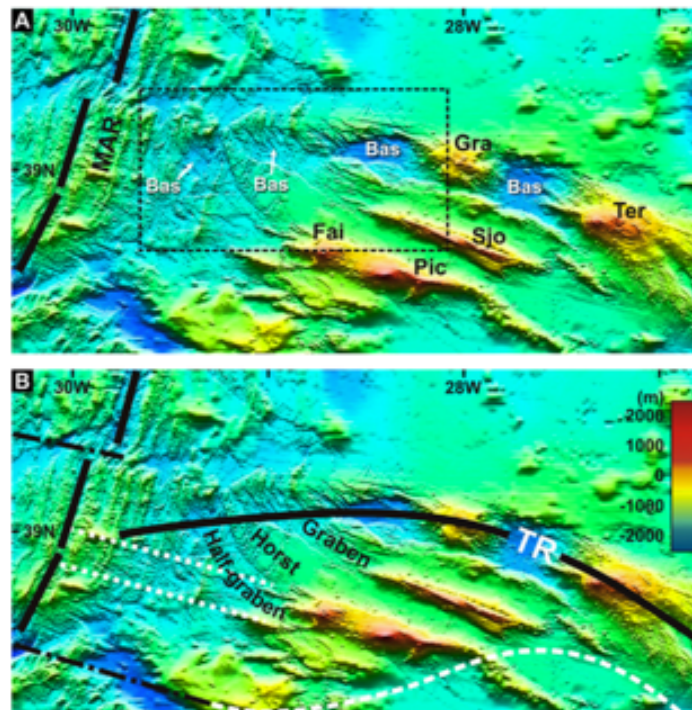


Figure 9. Bathymetry of the western end of the TR, in its junction with the MAR axis. Black heavy lines are ridge axes (MAR and TR). Dashed white line is the southern limit of deformation and seismicity. From [Marques et al., 2013].

However, for the TR, bathymetry show interesting curved graben-horst structure (fig. 9) [Marques *et al.*, 2013]. Dating of volcanic rocks indicate that this curved structure might be related to the two phases of magmatism with two orientations (N150 around 850 kyr and N110 around 750 kyr)(fig. 10) [Hildenbrand *et al.*, 2014].

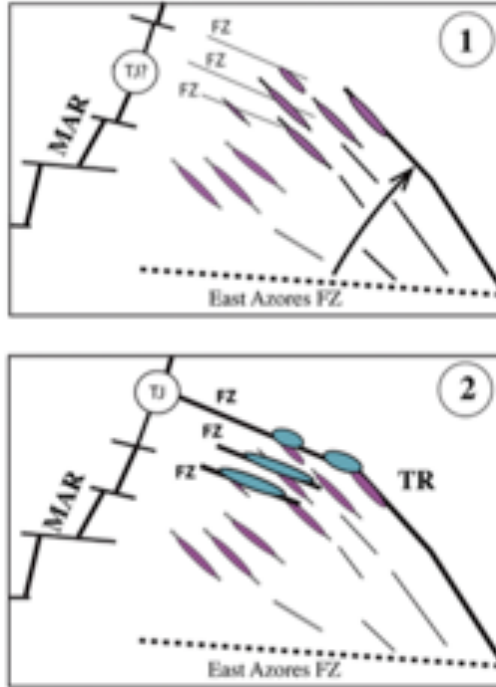


Figure 10. Two phases Eu–Nu plate boundary motion and magmatism from dating volcanic rocks: (1) diffuse stretching with N150 oblique ridges prior to 850 kyr; (2) at about 750 kyr, re-organization, with subsequent melt production/extraction controlled by re-activation of N110 FZ. From [Hildenbrand *et al.*, 2014].

To the East, one interesting phenomenon worth noting is that the island Santa Maria is the only island that is under active uplifting in Azores with a rate of ~ 60 m/Ma since the past 3.5 Myrs from Ar/Ar dating [Ramalho *et al.*, 2017]. Because Santa Maria locates to the West corner of the intersection of East end of TR and West tip of GF, where the extension of TR to the South might not be accommodated due to the sharp angle between TR and GF as well as limited by the EAFZ to the South, the Santa Maria might emerge as a result of this squeezing plate motion at the corner. This is supported by [Sibrant *et al.*, 2016] that the stress regime changes around 5 Myr due to a major reconfiguration of the Eu–Nu plate boundary in Azores. However, from current day tectonics studies that indicating trans-tensional stress regime along the TR, this hypothesis might not hold true [Marques *et al.*, 2013; Madeira *et al.*, 2015]. Alternatively, the bend at the intersection between GF and TR open a window for easier localization of plume magmatism that causes the active upwelling of the island.

Moreover, [Madeira *et al.*, 2015] note that the tectonic features (e.g. fault scarps, tectonically controlled drainage, displaced eruptive centers (cones, domes)) is much clearer morphologically during period of decreased volcanism. They present a comprehensive review on the neo-tectonic structures for the central group of the Azores islands (e.g. Faial, Pico, São Jorge, Graciosa and Terceira). For example, according to [Madeira *et al.*, 2015], there are two trends of fault scarps

on Faial island, one trending WNW-ESE and the other trending NNW-SSE with surface expression (fig. 11).

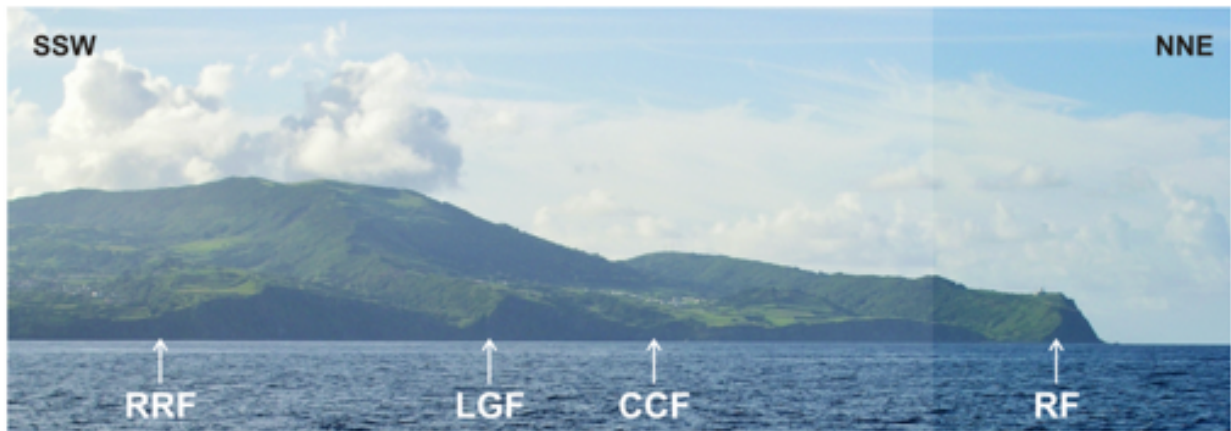
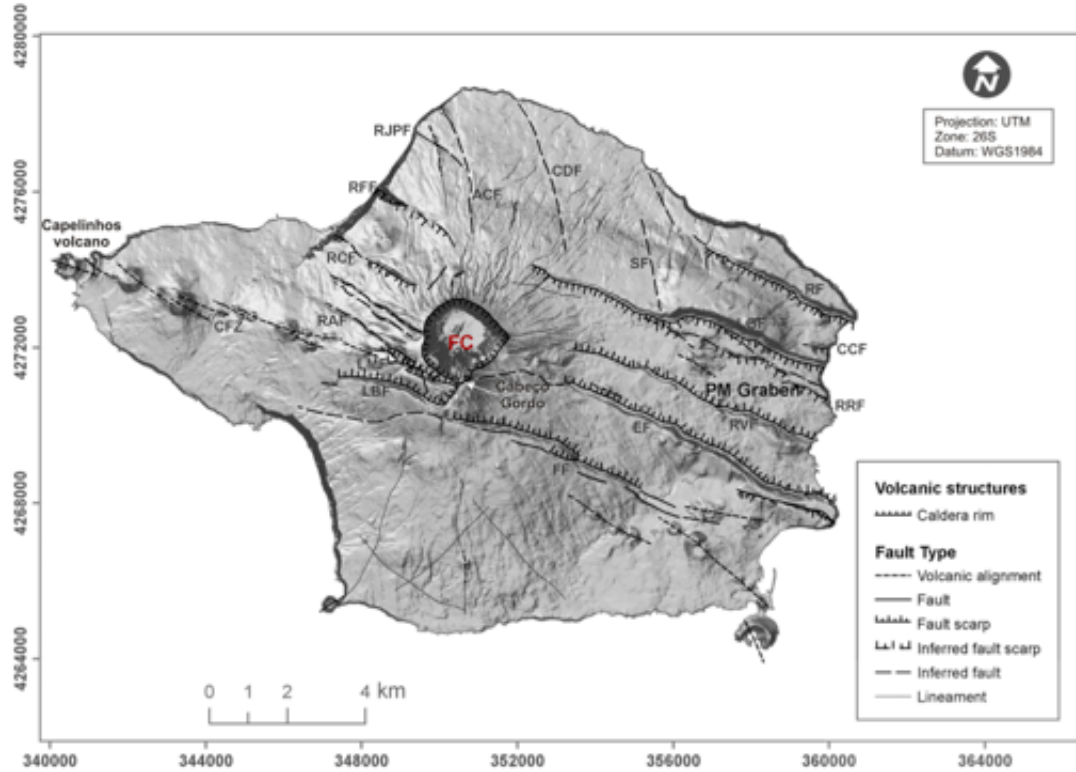


Figure 11. Up: Neo-tectonic structures of Faial island. RF, Ribeirinha Fault; CCF, Chada Cruz Fault; LGF, Lomba Grande Fault; RRF, Ribeira do Rato Fault; RVF, Rocha Vermelha Fault; EF, Espalamaca Fault; FF, Flamengos Fault; LBF, Lomba de Baixo Fault; LMF, Lomba do Meio Fault; CFZ, Capelo Fault Zone; RAF, Ribeira do Adao Fault; RCF, Ribeira das Cabras Fault; RFF, Ribeira Funda Fault; RJPF, Ribeira de Joana Pires Fault; ACF, A'gua-Cutelo-Porto do Caldeirao probable fault; CDF, Cedros-Cabouco Velho probable fault; SF, Salao probable fault; PM Graben, Pedro Miguel Graben; FC, Faial caldera. DTM (10 m resolution). Down: Photo of the northern half of the Pedro Miguel Graben, Faial Island, seen from the East, an example of major fault scarps presenting heights of tens to hundreds of metres: from north to south (right to left) the scarps of the Ribeirinha (RF), Chada Cruz (CCF), Lomba Grande (LGF) and Ribeira do Rato (RRF) south-dipping faults. From [Madeira *et al.*, 2015].

References:

- Argus, D. F., R. G. Gordon, C. DeMets, and S. Stein (1989), Closure of the Africa-Eurasia-North America Plate motion circuit and tectonics of the Gloria Fault, *J. Geophys. Res.*, *94*(B5), 5585, doi:10.1029/JB094iB05p05585.
- Fowler, C. M. R. (2005), *The solid earth: an introduction to global geophysics*, Cambridge University Press, Cambridge.
- Gaspar, J. L., G. Queiroz, T. Ferreira, A. R. Medeiros, C. Goulart, and J. Medeiros (2015), Chapter 4 Earthquakes and volcanic eruptions in the Azores region: geodynamic implications from major historical events and instrumental seismicity, *Geol. Soc. London, Mem.*, *44*(1), 33–49, doi:10.1144/M44.4.
- Hildenbrand, A., D. Weis, P. Madureira, and F. O. Marques (2014), Recent plate re-organization at the Azores Triple Junction: Evidence from combined geochemical and geochronological data on Faial, S. Jorge and Terceira volcanic islands, *Lithos*, *210*, 27–39, doi:10.1016/j.lithos.2014.09.009.
- Madeira, J., A. Brum da Silveira, A. Hipolito, and R. Carmo (2015), Chapter 3 Active tectonics in the central and eastern Azores islands along the Eurasia-Nubia boundary: a review, *Geol. Soc. London, Mem.*, *44*(1), 15–32, doi:10.1144/M44.3.
- Marques, F. O., J. C. Catalão, C. DeMets, A. C. G. Costa, and A. Hildenbrand (2013), GPS and tectonic evidence for a diffuse plate boundary at the Azores Triple Junction, *Earth Planet. Sci. Lett.*, *381*, 177–187, doi:10.1016/j.epsl.2013.08.051.
- Ramalho, R. S., G. Helffrich, J. Madeira, M. Cosca, C. Thomas, R. Quartau, A. Hipólito, A. Rovere, P. J. Hearty, and S. P. Ávila (2017), Emergence and evolution of Santa Maria Island (Azores)—The conundrum of uplifted islands revisited, *Geol. Soc. Am. Bull.*, *129*(3–4), 372–390, doi:10.1130/B31538.1.
- Searle, R. (1980), Tectonic pattern of the Azores spreading centre and triple junction, *Earth Planet. Sci. Lett.*, *51*(2), 415–434, doi:10.1016/0012-821X(80)90221-6.
- Sibrant, A. L. R., F. O. Marques, A. Hildenbrand, T. Boulesteix, A. C. G. Costa, and J. Catalão (2016), Deformation in a hyperslow oceanic rift: Insights from the tectonics of the São Miguel Island (Terceira Rift, Azores), *Tectonics*, *35*(2), 425–446, doi:10.1002/2015TC003886.
- Torsvik, T. H., K. Burke, B. Steinberger, S. J. Webb, and L. D. Ashwal (2010), Diamonds sampled by plumes from the core – mantle boundary, *Nature*, *466*(7304), 352–355, doi:10.1038/nature09216.
- Vogt, P. R., and W. Y. Jung (2004), The Terceira Rift as hyper-slow, hotspot-dominated oblique spreading axis: A comparison with other slow-spreading plate boundaries, *Earth Planet. Sci. Lett.*, *218*(1–2), 77–90, doi:10.1016/S0012-821X(03)00627-7.

Volcanic features of São Miguel Island

Dan Rasmussen

1. Overview of volcanism on São Miguel Island

São Miguel is the largest island of the Azores archipelago (Fig. 1a), and the most volcanically active. Frequent eruptions of $\sim 400 \text{ km}^3$ of material over the last ~ 4 million years have built the subaerial portion of the island. Eruptions over the last 5,000 years have occurred within 5 currently active volcanic regions (from west to east): Sete Cidades Volcano, the Picos Fissural Volcanic System, Fogo (or Agua de Pau) Volcano, the Congro Fissural Volcanic System, and Furnas Volcano (Fig. 1b). The majority of recent eruptive activity has been focused at Sete Cidades, Fogo, and Furnas. Two older, inactive volcanic centers (Povoação caldera and the Nordeste Volcanic System) occupy the east end of the island. Large eruptions that occurred in the last ~ 10 s of thousands of years have formed large collapse features known as calderas, which are the most topographically distinct features found on the island today (Fig. 1b).

Eruptions are typically basaltic or trachytic, spanning a range of explosivities, from low-energy effusive to high-energy explosive eruptions, and styles of eruption that includes Hawaiian, Strombolian, sub-Plinian, Plinian, and Vulcanian. Over the last 5,000 years, 73 eruptions have been identified (Fig. 2a), averaging to an eruption every ~ 70 years. Over the last 500 years, there have been ~ 8 significant eruptions at the three main volcanic centers (Fig. 2b). The largest eruption in recent history (< 500 years) was the Fogo A eruption, a Plinian event that launched 3.2 km^3 of material upwards of 27 km into the atmosphere.

In this chapter, I review the range of eruptive styles, magma compositions, and volcanic features found on São Miguel Island.

2. Eruptive styles and magma composition

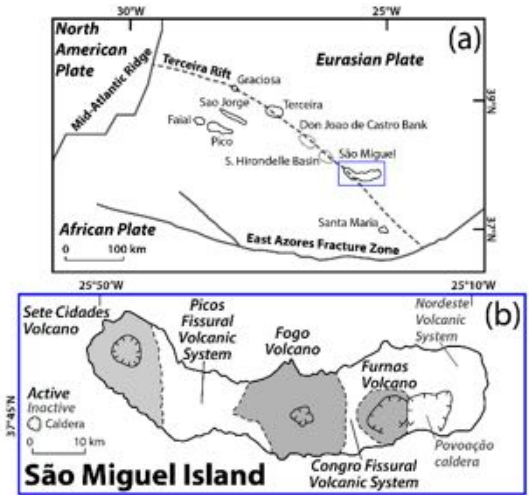


Figure 1. Map of the Azores archipelago and São Miguel Island.

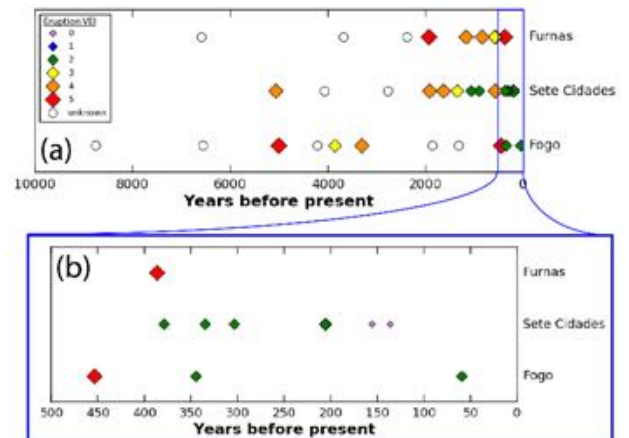


Figure 2. Volcanic eruptions that have occurred at the three main volcanic centers over the last 10,000 years. VEI is the volcanic explosivity index (a measure of the energy released in an eruption). Eruptive records are from the Global Volcanism Project of the Smithsonian Institution.

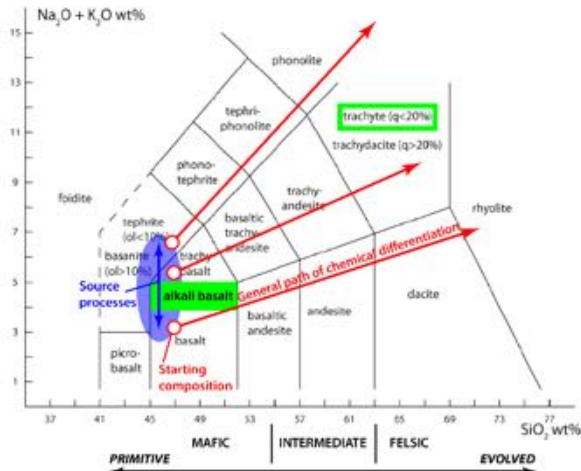


Figure 3. Total alkalis vs. silica (TAS) diagram. Red lines are generalized paths of magmatic differentiation. The blue shaded region shows the general range in initial magma composition. Common rock compositions found on São Miguel Island are indicated by green highlighting.

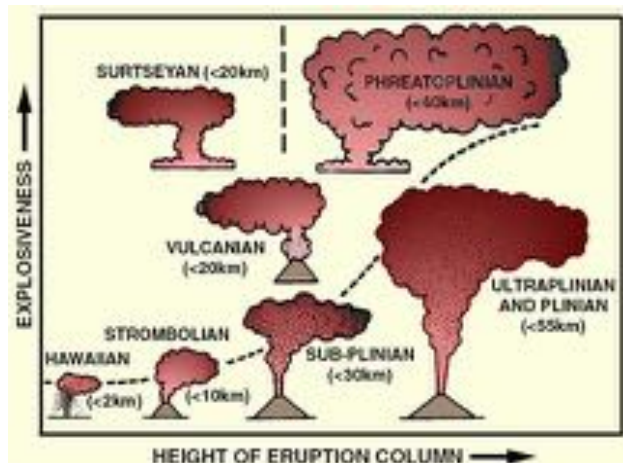
Magma Composition	Felsic	Intermediate	Mafic
Silica Content	70%	60%	50%
Eruption Temperature	750-900 °C	900-1000 °C	1100-1200 °C
Viscosity	Higher	Intermediate	Lower
Explosiveness	More Explosive		More Effusive
Volcanism	Rhyolitic Dacitic	Andesitic	Basaltic
Volcanic Products	Lava Domes Pyroclastic Deposits		Lava Flows
Volcano Types	Lava Dome Complexes	Composite Volcanoes	Shield Volcanoes Cinder Cones

Kenneth A. Bevis © 2013

the *volcanic explosivity index* (VEI; Fig. 2). Another way to describe the style of eruption is with descriptive terms (Fig. 5).

The Picos and Congro fissural systems erupt the most primitive material found on São Miguel Island. Alkali-basalts are common, but these systems also erupt minor trachyte. Most eruptions produce *lava flows* and *cinder cones* (see section 3), which have Strombolian and Hawaiian type eruptions. Some *phreatomagmatic* deposits have also been found

Figure 4. Relationship between magma composition and physical properties, eruptive style, and typical edifice types.



The styles of eruption and composition of associated magmas broadly fit into two categories: more *primitive*, lower energy eruptions of the fissural volcanic systems (Fig. 1b) and more *evolved*, higher energy eruptions of the larger volcanic systems (Sete Cidades, Fogo, and Furnas; Fig. 1b). The terms *primitive* and *evolved* are used to describe the composition of the associated magma. The most common way to classify rocks by composition is a TAS (total-alkalis vs. silica) diagram (Fig. 3). On this diagram, *primitive* compositions are at the low silica (SiO₂) end of the diagram, and more evolved magmas are at the higher SiO₂ end. Magmas may undergo chemical differentiation (e.g., crystallization, magma mixing, crustal melting) after formation (red paths in Fig. 3),

creating progressively more *evolved* magma compositions. Variation in alkali content (Na₂O+K₂O) of primitive magmas is generally due to processes occurring during magma formation (e.g., degree of partial melting or source enrichment). Composition strongly relates to the physical properties of magma, and it can also relate to the common style of eruption and edifice type (Fig. 4). Eruption energy refers to the amount of energy released in an eruption, which is controlled by the mass of erupted material and its velocity on leaving the vent. One measure of the energy released in an eruption is

the *volcanic explosivity index* (VEI; Fig. 2). Another way to describe the style of eruption is with descriptive terms (Fig. 5).

– an especially explosive eruption type that results from the interaction of magma and groundwater or surface water (e.g., phases of the 2010 eruption of Eyjafjallajökull involved magma interaction with glacial water).

Sete Cidades, Fogo, and Furnas erupt dominantly trachyte. Eruptions at the volcanoes ranges in style, but most commonly eruptions

Figure 5. Descriptive eruption styles that relate to the height of the eruptive column and energy released.

are sub-Plinian to Plinian, which is apparent in the last 10,000 years of eruptive activity (Fig. 2). Occasional Vulcanian eruptions have also been identified.

3. Volcanic features

Several volcanic features are found on São Miguel Island. The most topographically distinct landforms are calderas, but several other features can be found in the area, which include lava fields, cinder cones, and remnants of a shield volcano (Fig. 6).

Calderas are formed during large volcanic eruptions. Such eruptions occurred at Sete Cidades at 36, 29, and 16 ka (thousand years ago); Fogo at 15 ka; and Furnas at 30 and 12 ka. Caldera structures are found at Sete Cidades,

Fogo, Furnas, and Povoação volcanoes. Calderas form during large eruptions when the underlying magma reservoir is evacuated causing the overlying edifice to collapse, forming large (typically 1-50 km in diameter), circular depressions. A general model for caldera formation and evolution is shown in Fig. 7.

Also found on São Miguel Island are numerous cinder cones and lava flows, and an old, eroded shield volcano (Nordeste). These volcanic landforms are typically associated with more primitive eruptive products. The Picos and Congro fissural systems have numerous associated lava flows and cinder cones.

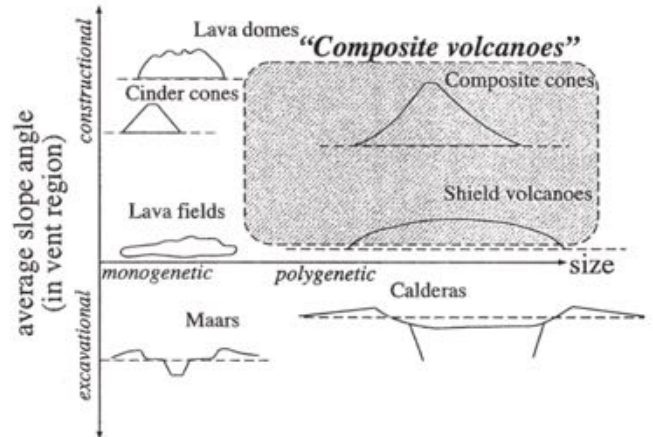


Figure 6. Volcanic edifice types.

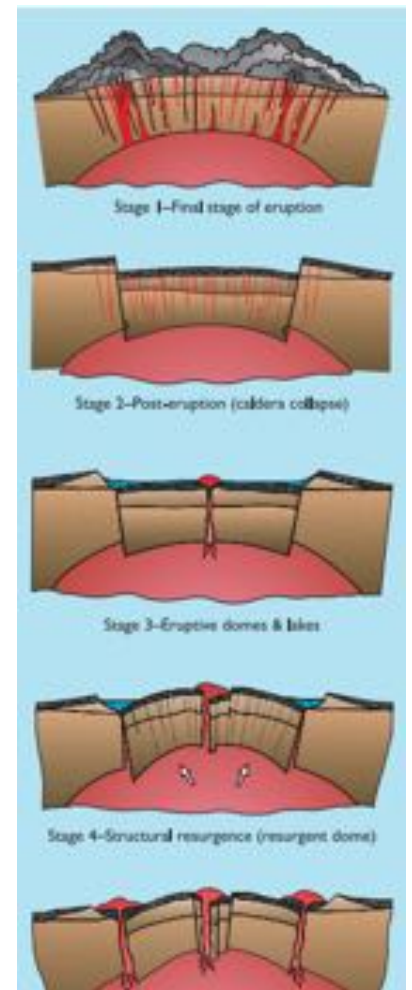


Figure 7. General model for caldera formation.

Furnas Volcanic Complex

Furnas is one of three main volcanic centers on the island of São Miguel. It is located on the east side of the island, just to the west of the older Povoação and Nordeste volcanic calderas (Figure 1). Furnas volcano rises about 800 m above sea level, though there is no clear edifice. It has a subaerial volume of 60 km³, with an average rate of increase of 0.06 km³/century (Guest et al., 1999). It was built by a series of explosive subaerial eruptions during the past 100,000 years (Figure 2). The main caldera is about 5 km by 8 km, within which sits Lagoa das Furnas and the town of Furnas, which has a population of approximately 1400 (Wikipedia). There are a large number of hot springs, mud pools, and geysers within the caldera. The area around Furnas is heavily vegetated, so most of the outcrops occur in valleys in the caldera walls or along sea cliffs on the southern coast of the island.



Figure 1. Location of main volcanic complexes on São Miguel, including Furnas (Wallenstein et al., 2007).

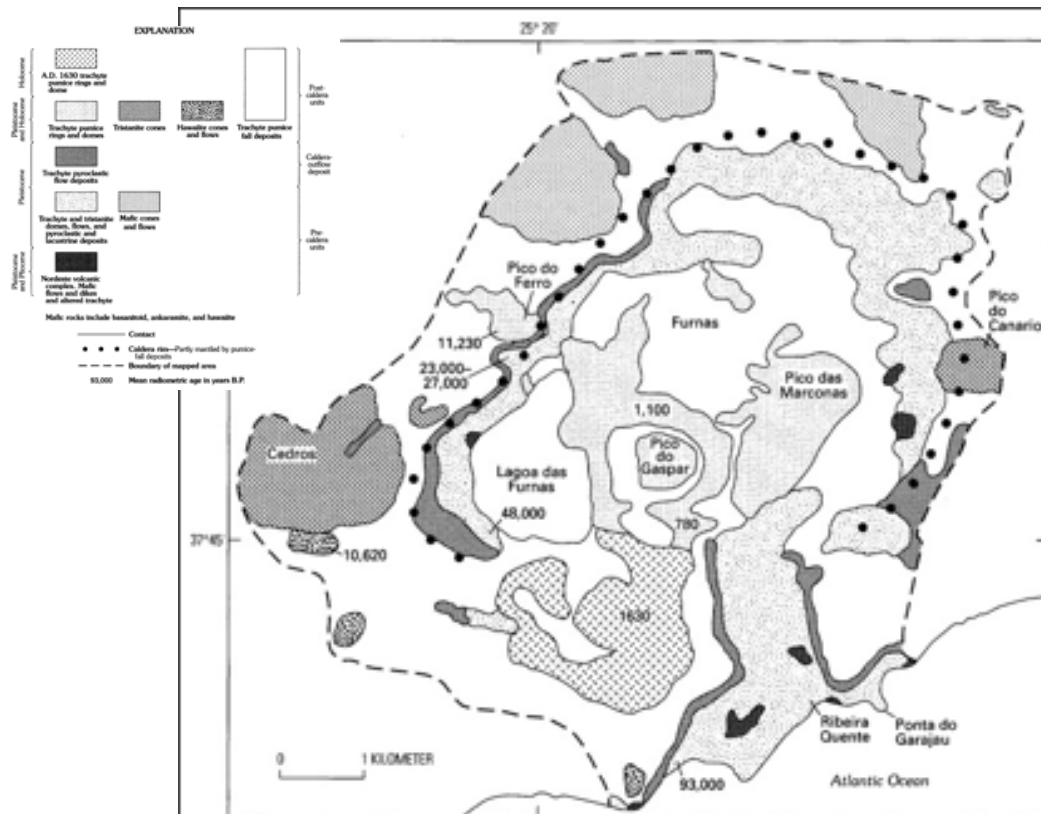


Figure 2. Geologic map of Furnas volcanic complex from Moore (1991).

There are several different fracture systems on São Miguel that intersect at the Furnas volcanic complex (Figure 3). There is one set of fractures extending across the volcanic complex with a WNW-ESE trend that has a normal dip-slip component, and some of the vents within the caldera are aligned with this fracture system. Another set of fractures consisting of conjugate faults with N-S and NNE-SSW trends is located near the coast, on the southern end of the volcanic complex. The convergence of these structures may be responsible for the location of the volcanic center at Furnas, and the locations of walls from caldera collapses can be controlled by these preexisting structural weaknesses (Guest et al., 1999).

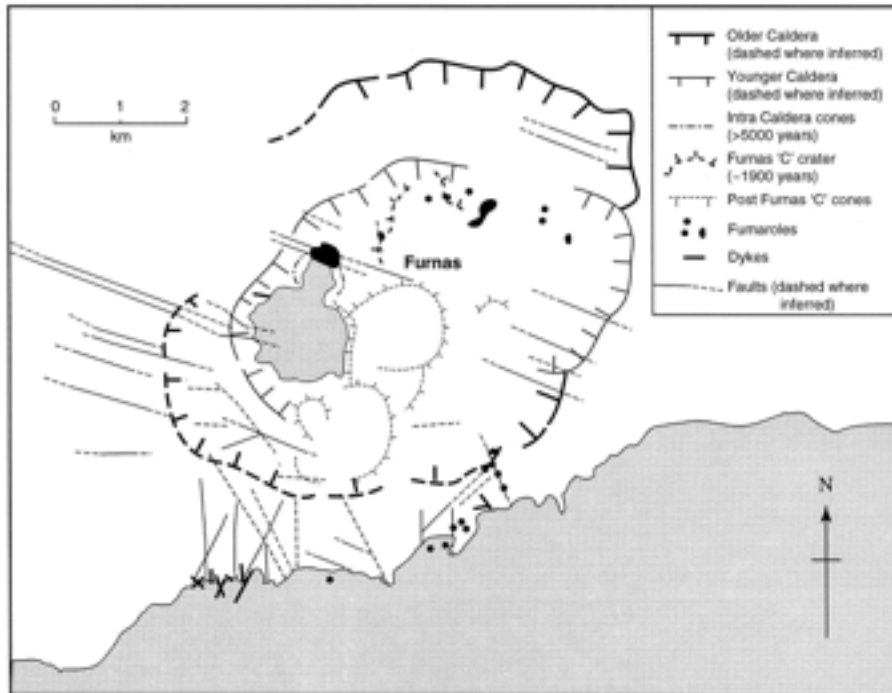


Figure 3. Locations of mapped faults in the Furnas volcanic complex from Guest et al. (1999)

Most of the lavas at Furnas have a trachyte composition, with a few more mafic lavas (Figure 4). The more trachytic lavas tend to be located within the caldera, and the mafic volcanism occurs at vents outside the caldera rim (Guest et al. 1999).

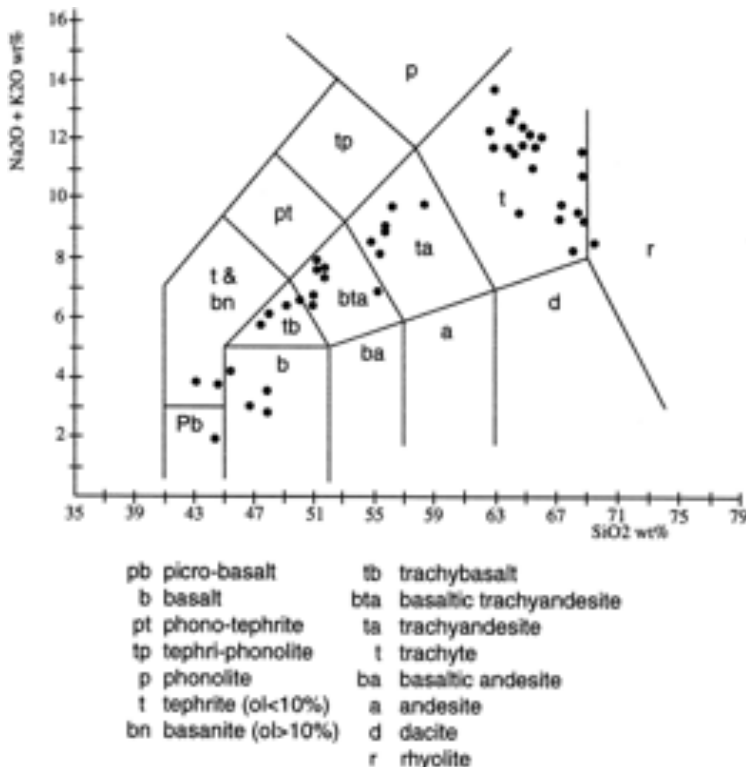


Figure 4. Composition of lavas of the Furnas volcanic complex.

Furnas volcano sits on top of the Povoação/Nordestes volcanic complex, which was active between 1-4 Myr ago. There is an initial basaltic pile underlying the volcano, and the oldest eruptions at Furnas are dated to 93,000 years (Moore, 1991). Since then, there have been a series of tristanite and trachyte flows, lapilli and ash deposits, and mudflows between then and 30,000 years ago reflecting mostly explosive activity. This series of lavas is known as the Lower

Furnas Group, and is exposed in sea cliffs on the southern coast of the island and in a canyon in the caldera wall. This exposure has a section of lacustrine sedimentary rocks with algal mats, showing evidence for earlier crater lakes within the caldera.

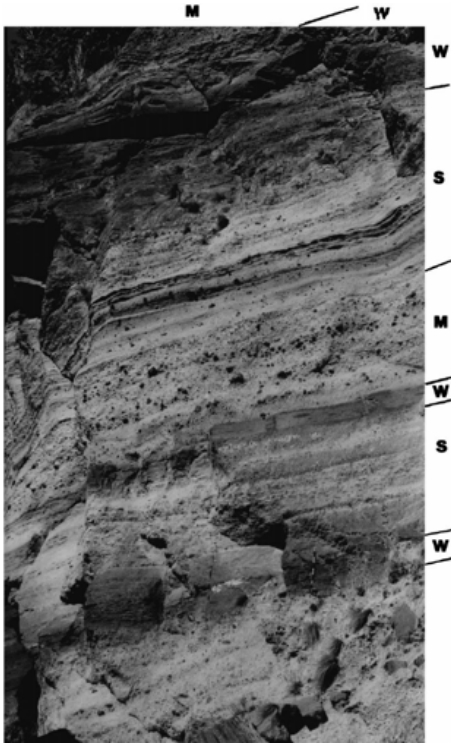


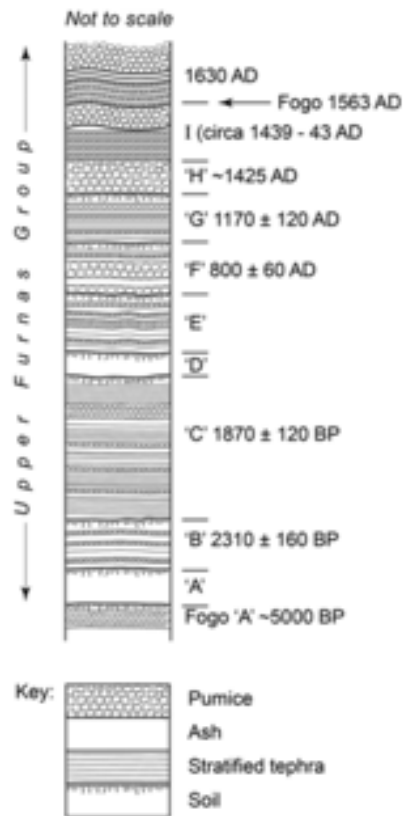
Figure 5. Povoação Ignimbrite Formation, from Duncan et al. (1999)

The caldera formed in two stages, creating an older, outer, caldera wall and an inner, younger, caldera wall (Figure 7). The older caldera formed about 30,000 years ago during a trachyte pumice eruption. This produced the Povoação Ignimbrite Formation, a welded tuff outflow deposit that is exposed in a few locations around the caldera and is typically 25-50 m thick (Figure 5, Duncan et al. (1999)). This formation marks the top of the Lower Furnas Group. For the next 20,000 years, a series of eruptions filled the caldera with ignimbrites, surge and fall deposits, and some lavas. This series of deposits is known as the Middle Furnas Group. The inner caldera collapsed about 12,000 years ago, marking the end of this formation.

At least ten Plinian and sub-Plinian eruptions of trachyte pumice occurred within the caldera after it formed, and these make up the Upper Furnas Group (Guest et al., 2015).

Alternating episodes of magmatic and phreatomagmatic activity produced interbedded volcanic ash and lapilli deposits (Figure 6). Multiple trachyte domes also formed within and outside the rim of the caldera. The largest eruption produced the Furnas C deposits around 1900 years ago. This eruption produced a pumice ring and thick mudflows covering the north part of the caldera, and alternating layers of ash and lapilli reflect transitions between phreatomagmatic and magmatic eruptive styles within the eruption.

Figure 6. Stratigraphy of Upper Furnas Group, from Guest et al. (2015).



There have been two historic eruptions at Furnas that were recorded. The first occurred in the 15th century soon after the island had been settled, and is thought to have occurred

around 1440 be approximately a VEI 4. This eruption occurred at the Pico do Gaspar dome, located in the center of the caldera. Early settlers to the area observed “tongues of fire” coming from the valley, in addition to loud noises and lightning. The second historic eruption occurred in 1630 when there were significantly more people living on the island. It was a VEI 5, and killed at least 191 people from a combination of earthquakes preceding the eruption, pyroclastic flows, and mudflows. The eruption had both effusive and explosive phases, and produced three nested pumice rings and a central trachyte dome on the southern caldera floor (Cole et al., 1995). Figures 7 and 8 show the location of the historic eruptions relative to the caldera walls and present day caldera lake, Lagoa das Furnas.

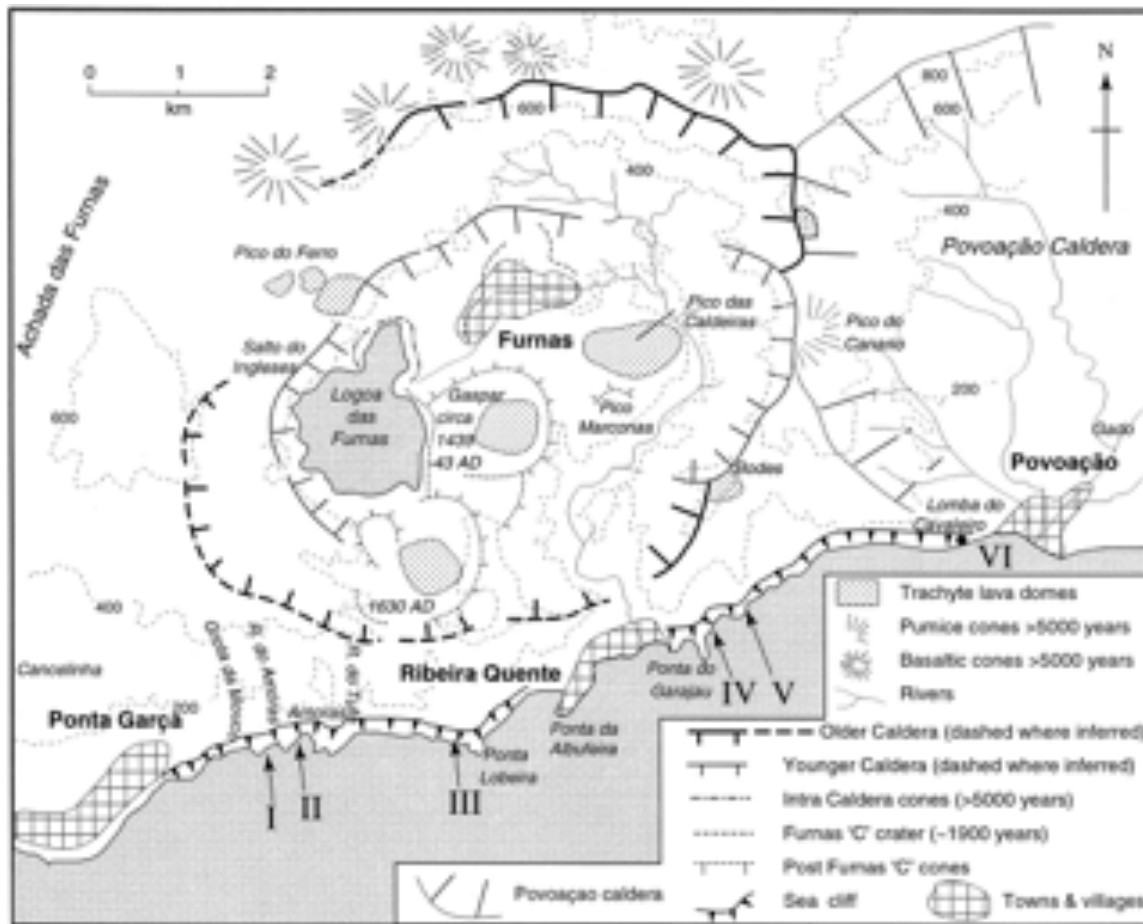


Figure 7. Locations of caldera walls and historic eruptions in the Furnas volcanic complex (Guest et al., 1999).

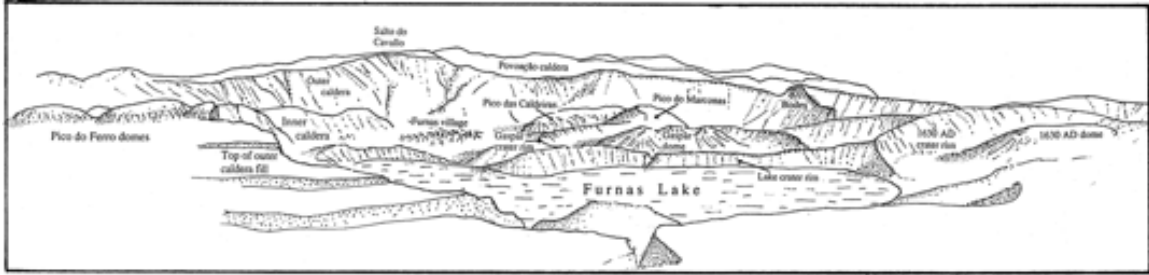
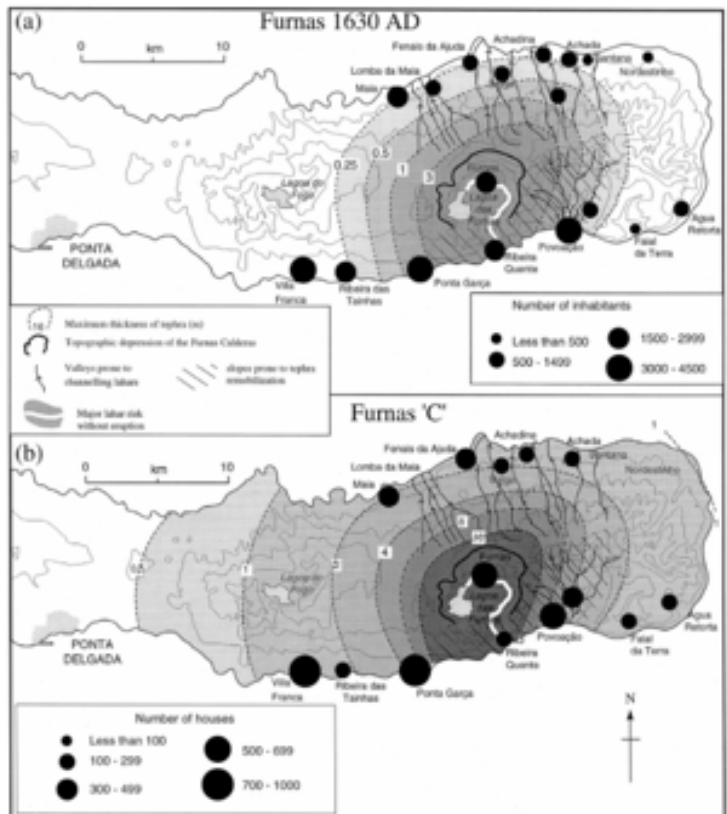


Figure 8. View of Furnas caldera and cartoon from Guest et al. (1999)

Figure 9. Modeled impact of the 1630 AD and Furnas C eruptions, from Cole et al. (1999).



There is significant risk to people living around the Furnas volcanic complex due to the active volcano. Furnas has erupted on average every 369 years since the Furnas C eruption 1900 years ago (Cole et al, 1999). Areas within the caldera are at risk of pyroclastic flows, and towns at the mouths of rivers are particularly vulnerable to pyroclastic flows and mudflows. Figure 9 shows that eruptions like those that in 1630 AD and Furnas C would impact a large number of people on São Miguel, particularly those living within and around the caldera. In addition, there are high CO₂ concentrations within the town of Furnas that are an environmental hazard to the people living there; lethal concentrations of CO₂ have been measured in houses in Furnas (Baxter et al. (1999).

Residents of Furnas and the surrounding areas are also at risk of landslides; steep caldera slopes are especially prone to failure. Small earthquakes, volcanic eruptions, and precipitation can all trigger slope failure. On October 31, 1997, a series of landslides triggered by extreme rainfall killed 29 people in the village of Ribeira Quente, located at the mouth of a river along the southern coast of São Miguel.

References

P. J. Baxter, J.-C. Baubron, Rui Coutinho, Health hazards and disaster potential of ground gas emissions at Furnas volcano, São Miguel, Azores, *Journal of Volcanology and Geothermal Research*, Vol. 92, 1-2, 1999, 95-106.

P. D. Cole, G. Queiroz, N. Wallenstein, J. L. Gaspar, A. M. Duncan, J. E. Guest, An historic subplinian/phreatomagmatic eruption: the 1630 AD eruption of Furnas volcano, São Miguel, Azores, *Journal of Volcanology and Geothermal Research*, Vol. 69, 1-2, 1995, 117-135.

P. D. Cole, J. E. Guest, G. Queiroz, N. Wallenstein, J. M. Pacheco, J. L. Gaspar, T. Ferreira, A. M. Duncan, Styles of volcanism and volcanic hazards on Furnas volcano, São Miguel, Azores, , *Journal of Volcanology and Geothermal Research*, Vol. 92, 1-2, 1999, 39-53.

A. M. Duncan, G. Queiroz, J.E. Guest, P. D. Cole, N. Wallenstein, J.M. Pacheco, The Povoação Ignimbrite, Furnas Volcano, São Miguel, Azores.

J. E. Guest, J. L. Gaspar, P. D. Cole, G. Queiroz, A. M. Duncan, N. Wallenstein, T. Ferreira, and J.-M. Pacheco, Volcanic geology of Furnas Volcano, São Miguel, Azores, *Journal of Volcanology and Geothermal Research*, Vol. 92, 1-2, 1999, 1-19.

J. E. Guest, J. M. Pacheco, P. D. Cole, A. M. Duncan, N. Wallenstein, G. Queiroz, J. L. Gaspar, and T. Ferreira, Chapter 9: The volcanic history of Furnas Volcano, São Miguel, Azores, Geological Society, London, *Memoirs*, 44, 125-134, 2015.

Nicolau Wallenstein , Angus Duncan , David Chester and Rui Marques , Fogo Volcano (São Miguel, Azores): a hazardous edifice, *Geomorphology: relief, process, environment* , vol. 13 - n3, 2007, 259-270.

Overview of Agua de Pau (aka Fogo) Volcano

Natalie Accardo

1 Introduction

Agua de Pau is the largest active volcano on Sao Miguel rising to over 1000 m and covering ~ 150 km² (Moore 1990a). Located in the center of the island, the caldera of Agua de Pau contains Lagoa do Fogo, a large freshwater lake. The volcano is characterized by two nested calderas, the inner one of which remains active today. Volcanic and tectonic structures dominate the landscape of Agua de Pau with many volcanic features aligning with inferred tectonic lineaments. Like the two other primary volcanoes on Sao Miguel, Agua de Pau is a trachytic volcano that is associated with numerous hot springs.

2 Stratigraphy of Agua de Pau

The geologic history of Agua de Pau and associated stratigraphy is commonly separated into two main phases (Upper and Lower groups) separated by the formation of the outer caldera. For a detailed review of the stratigraphy of Agua de Pau see Wallenstein et al. (2015). The Lower Group was deposited beginning at ~ 200 Ka with the oldest onshore dated units associated with the Eira Velha trachyte dome (Gandino et al. 1985). There is some indication that older submarine deposits dating to ~ 280 Ka are associated with Agua de Pau however, error bars with those measurements are quite large (Wallenstein et al. 2015). The Lower Group is associated with numerous eruptions identified now from dated trachyte domes, tuffs, mudflows, and pyroclastic deposits (Booth et al. 1978; Gandino et al. 1985). The Lower Group ends when the outer caldera is hypothesized to have begun forming at ~ 46 Ka (Moore 1990b). The formation of this outer caldera continued until 26 kyr and may be associated with an eruption that deposited a large offshore tephra package dated to ~33 Ka (Huang et al. 1979).

The Upper Group is separated into the time prior to the formation of the inner caldera (dated to ~ 5 Ka) and the time after the formation of the inner caldera. While more is known about the Upper Group, complex stratigraphic relations exist between these deposits and similar flows associated with the two nearby volcanos (Furnas and Sete Cidades) (Wallenstein et al. 2015). Several eruptions occurred prior to the formation of the inner caldera. Deposits from

these eruptions are primarily limited to the northern and southern flanks of the volcano. Most of these deposits are heavily weathered and associated with pyroclastic flows. From this group is the Coroa da Mata Formation (~ 18.6 Ka), outcropping 2.5 km from Ribeirinha Village on the northern flank, which contains abundant Obsidian fragments (Moore & Rubbin 1991; Wallenstein 1999). On the southern flank, a prominent formation is the Roida da Praidá, exposed along sea cliffs and a road cut near the village of Pisao (Figure 2). This formation is primarily a pumice fall deposit associated with as many as 65 individual events beginning ~ 34.2 Ka (Booth et al. 1978). Another prominent formation with good outcrops is the Ribeira Cha Formation also along road cuttings and sea cliffs on the southern flank. This formation is primarily a pumice fall deposit as well as pyroclastic flow and ignimbrite deposits broadly dating to 8-12 Ka (Wallenstein 1999).

The formation of the inner caldera marks the separation of the two primary phases of the Upper Group. The most widespread formation associated with Agua de Pau, named Fogo A, occurred during this time. Fogo A resulted from a Plinian eruption, notably the only Plinian eruption to have occurred in the Azores. Dating studies broadly agree that the eruption occurred at 4.66 Ka (e.g. Moore & Rubin 1991; Wallenstein 1999). This formation is well exposed along sea cliffs on the southern flank and is most notably known for abundant loose feldspar crystals.

While the previous discussion has focused solely on primarily felsic volcanic deposits, basaltic deposits are associated with Agua de Pau. These basaltic deposits all date to < 5 ka and are primarily expressed as scoria cones on the northern and southern flanks of the volcano. Notably, a lava flow erupted towards the north formed a lava tube (Gruta do Esqueleto) and also created a lava delta that separates the Santa Barbara and Ribeira Grande beaches (Wallenstein 1999).

3 Historical Eruptions

Agua de Pau has erupted three times since humans first populated Sao Miguel. In 1563 two eruptions occurred 4 days apart with the first being a sub-Plinian eruption and the second being a Hawaiian style eruption (e.g. Wallenstein et al. 1999). The first eruption originated

from the summit caldera while the second erupted originated from a trachytic dome on northern flank. The Hawaiian eruption (named Pico do Sapateiro) created two separate lava flows one that reached the Santa Barbara beach (Figure 3). A third eruption is thought to have occurred in 1564 in the same location as the first 1563 eruption (Wallenstein 1999).

4 Morphology and Tectonics of Agua de Pau

The most distinctive features of Agua de Pau are related to the abandoned outer and presently active inner calderas. These calderas are clearly seen in topographic maps as arcuate scarps with significant topography (Figures 1 & 4). Remnants of the outer caldera are only observed north of the inner caldera. A prominent valley (the Lombadas valley) separates the two calderas (Figure 1). Several CO₂ rich hot springs are located within Lombadas Valley. Water temperatures in these hot springs are commonly near 100° C which may indicate that hot rock or event magma is shallow in the region (Moore 1990a).

Large tectonic structures also define the landscape of Agua de Pau volcano. Tectonic structures are dominantly NW-SE to NNW-SSE and are expressed by linear trends of volcanic domes and cones as well as linear segments of drainage systems (e.g. Carmo et al. 2015). The most prominent tectonic feature of Agua de Pau volcano is the Ribeira Grande Graben which transects the northwest side of the northern flank. The West Ribeira Grande Fault bounds the graben to the west and the Falca Fault to the east (Figure 4). Surface features with linear trends that continue south of the summit caldera may suggest that the graben extends to the south across the summit of Agua de Pau (Carmo et al. 2015). The summit caldera as well as surrounding valleys of Agua de Pau are likely tectonically controlled as these features align with observed faults.

FIGURES

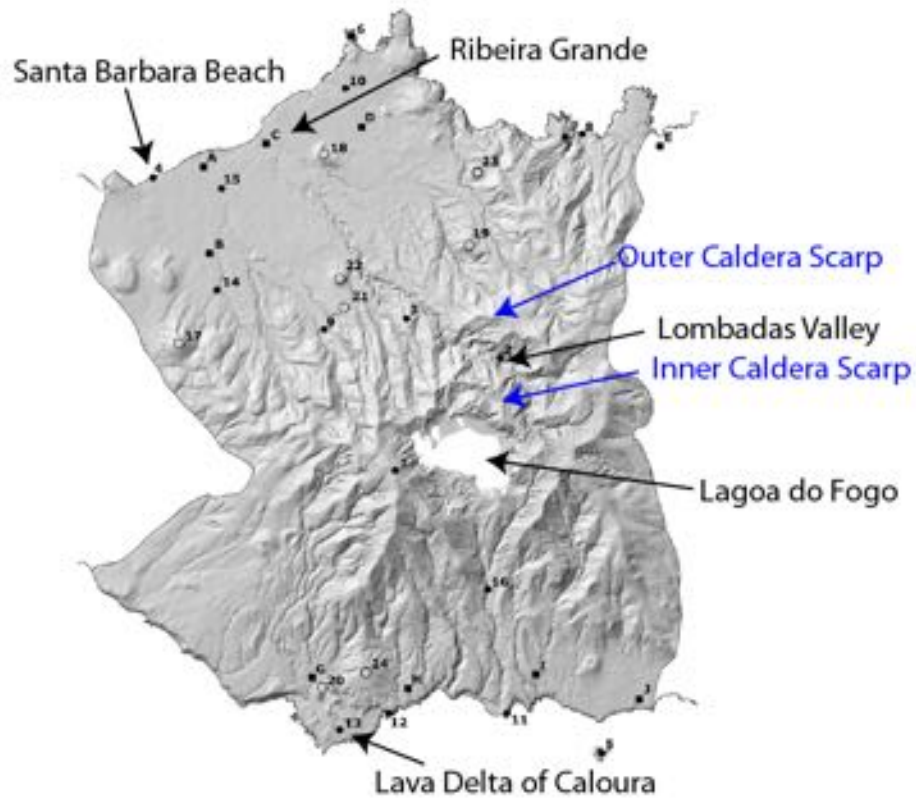


Figure 1. Digital elevation map of the Agua de Pau from Wallenstein et al. 2015. Locations and structures of interest are labeled.



Figure 2. Image of road cut from the southern flank near the town of Pisao. Labels a1-b2 represent different deposits of the Roida da Praia Formation, c represents the Pisao formation, and d represents the ubiquitous Fogo A Formation. From Wallenstein et al. 2015.



Figure 3. (a) Google Earth view of the two separate lava flows associated with the Hawaiian 1563 eruption. (b) View of basaltic lava on the Santa Barbara beach associated with the 1563 Hawaiian eruption. From Wallenstein et al. 2015.

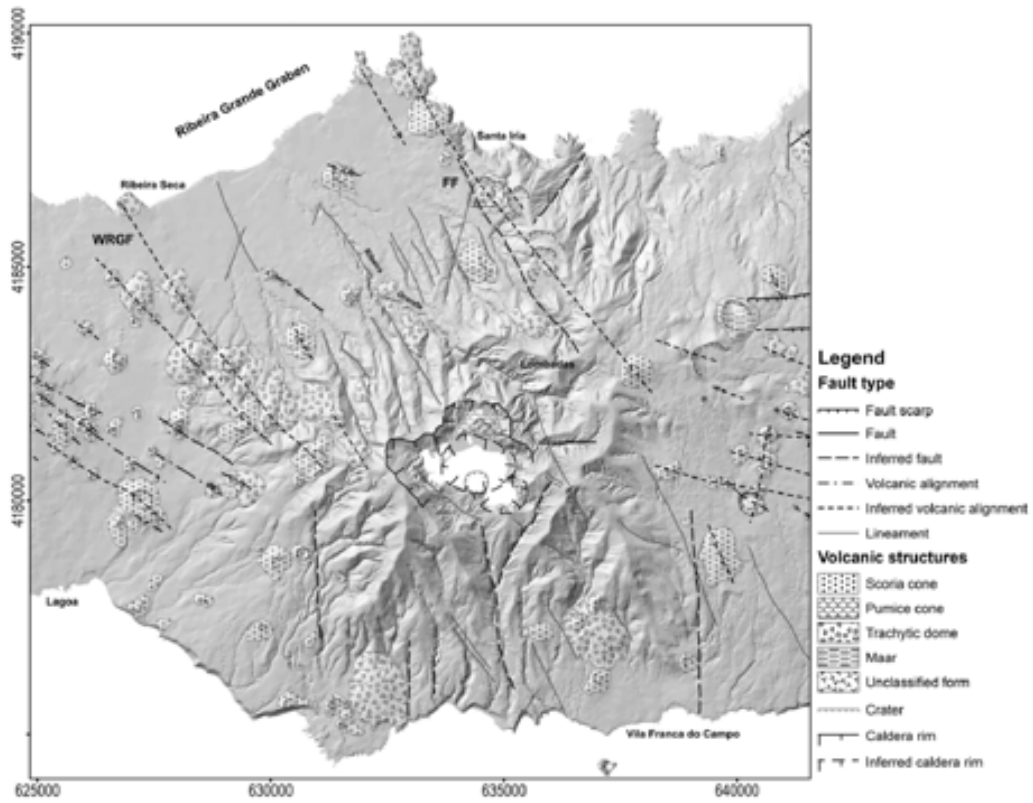


Figure 4. Digital elevation map with structural and volcanic features overlain. Locations of interest are labeled. From Carmo et al. (2015).

REFERENCES:

- Booth B., Croasdale R., & Walker G. P. L. (1978). A quantitative study of five thousand years of volcanism on Sao Miguel, Azores. *Phil. Trans. R. Soc. London* 288:271-319
- Carmo, R., Madeira, J., Ferreira, T., Queiroz, G., & Hipolito, A. (2015). Chapter 6 Volcano-tectonic structures of Sao Miguel Island, Azores, Geological Society, London, *Memoirs*, 44(1), 65–86, doi:10.1144/M44.6.
- Gandino, A., Guidi, M., Merlo, C., Mete, L., Rossi, R. & Zan, L. (1985). Preliminary model of the Ribeira Grande geothermal field (Azores Islands). *Geothermics*, 14, 91–105.
- Huang, T. C., Watkins, N. D., & Wilson, L. (1979). Deep-sea tephra from the Azores during the past 300000 years: eruptive cloud height and ash volume estimates. *Geol. Soc. Am. Bull.* 90:131-133
- Moore, Richard B. (1990a). Volcanic geology and eruption frequency, Sao Miguel, Azores. *Bull. Volcanol.*, 52, 602-614.
- Moore, Richard B. (1990b). Geology of three late Quaternary strato- volcanoes on Sao Miguel, Azores. *US Geol. Survey Bull.*
- Wallenstein, N. (1999). Study of the recent history of volcanic eruptions from Fogo Volcano (S. Miguel, Azores). *Avaliacao preliminar do hazard*. PhD thesis, University of Azores, Ponta Delgada,
- Wallenstein, N., Duncan, A., Guest, J. E., & Almeida, M. H. (2015). Chapter 8 Eruptive history of Fogo Volcano, Sao Miguel, Azores, Geological Society, London, *Memoirs*, 44(1), 105–123, doi:10.1144/M44.8.

Introduction to The Sete Cidades Volcanic System

One of three major volcanic systems on the island of Sao Miguel, Sete Cidades is the westernmost and most active stratovolcanic complex on the island (Queiroz et al., 2008). The volcanic region became active around 220,000 years ago, and has since evolved to include volcanic features such as scoria cones, maar lakes, and volcanic domes, in addition to a central caldera that formed between 36,000-16,000 years ago (Beier et al. 2006). The caldera floor is ringed by pyroclastic cinder cones that resulted from Holocene trachytic eruptions. In the past 5,000 years, there have been 17 trachytic intracaldera eruptions and 12 basaltic flank eruptions (Queiroz et al. 2008). At the caldera's center, the modern landscape features a lake system that is characterized by two smaller lakes that are bisected by a strait at its center. The lakes are characterized by differences in water chemistry and biological productivity, causing one to be blue and the other to be green.

General Topography & Tectonic Setting

In contrast to the other volcanic systems on Sao Miguel, which are situated parallel the East Atlantic Fracture Zone (EAFZ), the Sete Cidades Massif is located along the slow-spreading Terceira Rift Axis (Figure 1). In addition to this slow spreading ridge (extending at a rate of 2-4 mm/yr), the Azores Plateau is also situated on top of a zone of slow seismic velocity, suggesting melting due to a possible small mantle plume beneath the islands (Beier et al. 2008). However, a connection to the deeper mantle has not been located, suggesting that the system represents a relatively small and short-lived dying mantle plume system (Silveira et al. 2006).

The caldera has a basal area of about 15 km², with average wall heights of 350 m (Queiroz et al. 2008). On the northwestern flank, the Mosteiros graben is an extensional feature that has scarps with displacement of up to 70 m and is associated with the Terceira Rift (Queiroz et al. 2008, Figure 3.)

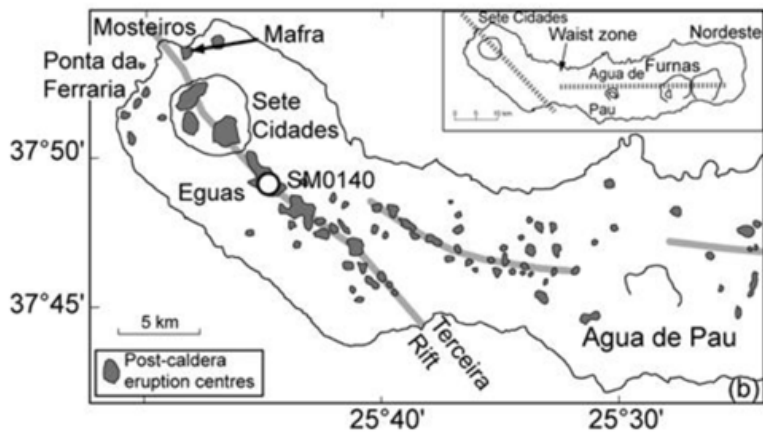


Figure 1. Location of the Sete Cidades volcanic complex in the regional tectonic setting. From Beier et al. 2006. Note the along-axis eruption centers that correspond to the Terceira Rift, which is distinct from the Agua de Pau system.

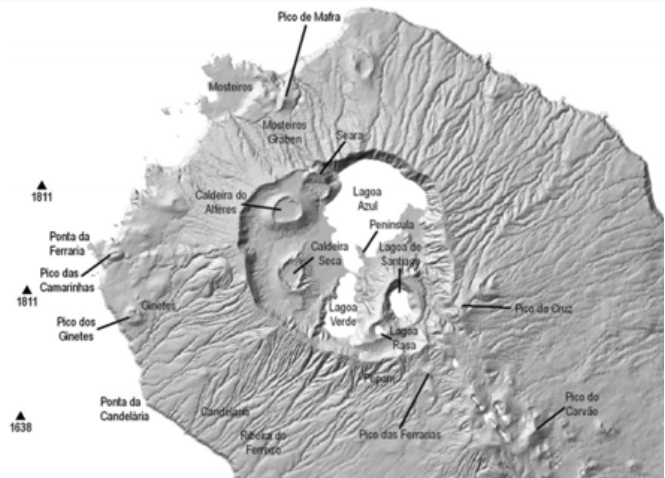


Figure 2. Topography and volcanic features of Sete Cidades. From Queiroz et al. 2008.

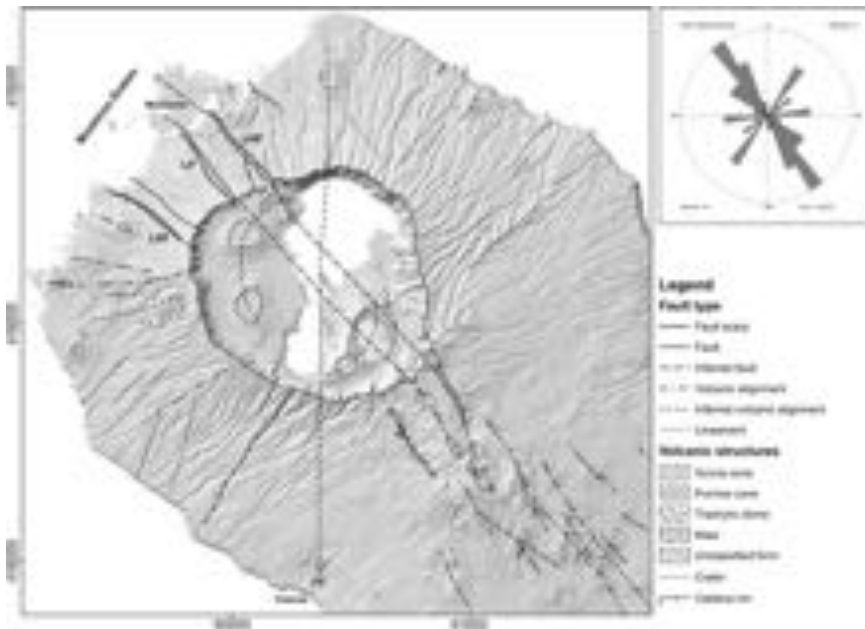


Figure 3. Regional fault structures and surface expression of the Mosteiros Graben (below). From Carmo et al. 2015.



Stages of Volcanic Activity and Associated Deposits

In general, the stages of volcanic activity at Sete Cidades can be grouped into three major intervals (Beier et al. 2006, Figures 4, 5, 6):

1. **220-36 ka, Pre-caldera phase:** During this period, the volcano underwent its basaltic shield-generating phase. Eruptions were effusive (not explosive), and volcanoclastic deposits are more rare than in later intervals. This interval is the thickest due to its long temporal duration, comprising approximately 200m of volcanic deposits. While the overall composition is dominantly basaltic, fractionation cycles between basalt and more felsic (silica rich, Mg/Fe poor) trachytic magmas can be observed within this thick unit. Many of these outcrops can be seen along the coast, particularly at Moisteros and Ponta de Ferrara. In particular, at Ponta de Ferrara, four fractionation cycles from basalt to the more felsic trachyte/pumice can be observed in the upper section.

2. **36, 29, 16ka, Caldera-forming eruptions:** During this period, the explosive, more felsic (trachytic) eruptions occurred that caused the large caldera feature at the volcano's center to form. Beier et al. (2006) hypothesize that this eruption was triggered by the injection of basaltic magma into the trachytic magma chamber, causing rapid heating and an increase in pressure in the magma chamber and leading to an explosive eruption. At the eastern edge of the caldera, the ash-fall deposits from these eruptions are approximately 50-60 m thick.
3. **16 ka-present: post-Caldera forming eruptions:** The most recent volcanic eruptions at Sete Cidades have been characterized by explosive trachytic events that are intercalated with smaller-scale, effusive basalt eruptions that emanate from the flanks of the volcano. In contrast, the trachytic magmas mainly erupted through the ring fault around the caldera, which served as a conduit to this felsic magma chamber. This pattern of inner caldera trachyte eruptions and flank basaltic eruptions has been hypothesized to result from two distinct magma chambers that have conduits to their respective outlet regions (Figure 4). One of these younger flank deposits is the Mafra deposit, which is visible on the northwest coast of the island (Figure 5). Also included in the more recent features is the northwest-southeast striking lineament of cinder cones that lies to the southeast of the caldera, which based on $^{87}\text{Sr}/^{86}\text{Sr}$ evidence are linked to the Sete Cidades system and are likely caused by extension along the Terceira rift zone (Figure 1). The most recent volcanic eruption occurred approximately 800 years ago and resulted in the formation of the Caldeira Seca cone (Figure 2).

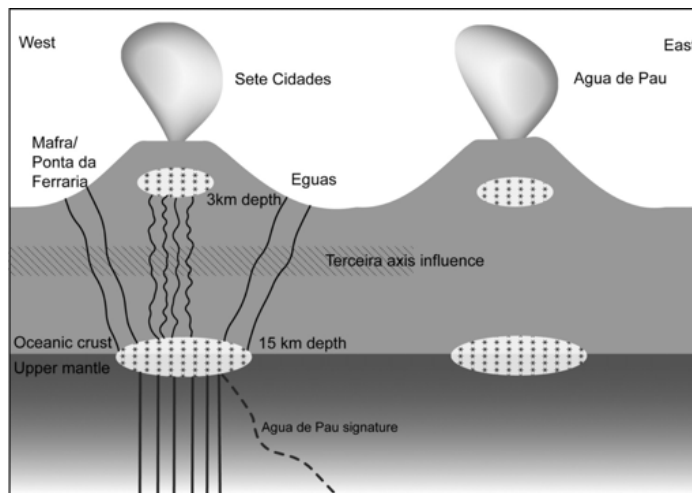


Figure 4. Schematic of possible magma chamber structure feeding Sete Cidades volcanism in the post-caldera phase. From Beier et al. 2006. The authors hypothesize that a deeper, isolated basaltic magma chamber feeds flank eruptions, while a more evolved trachytic chamber feeds eruptions that are released from the ring fault in the center of the caldera.

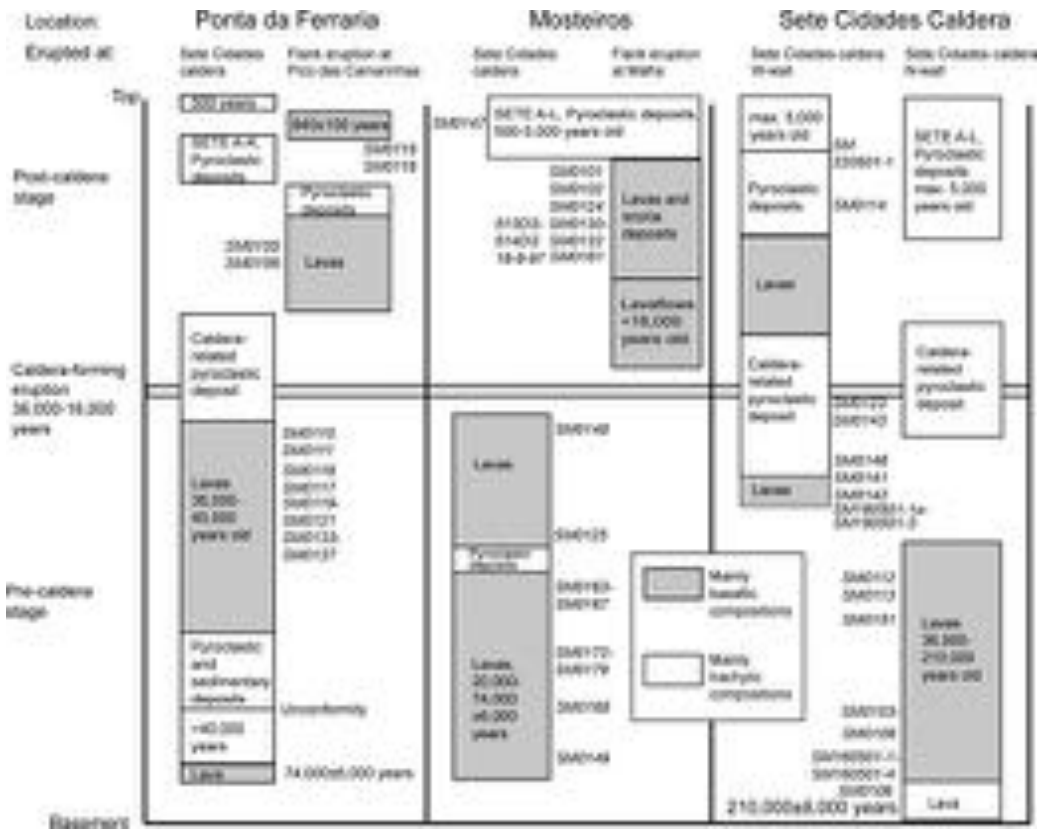


Figure 4. Stratigraphy of volcanic deposits at major outcrops in the region. From Beier et al. 2006.

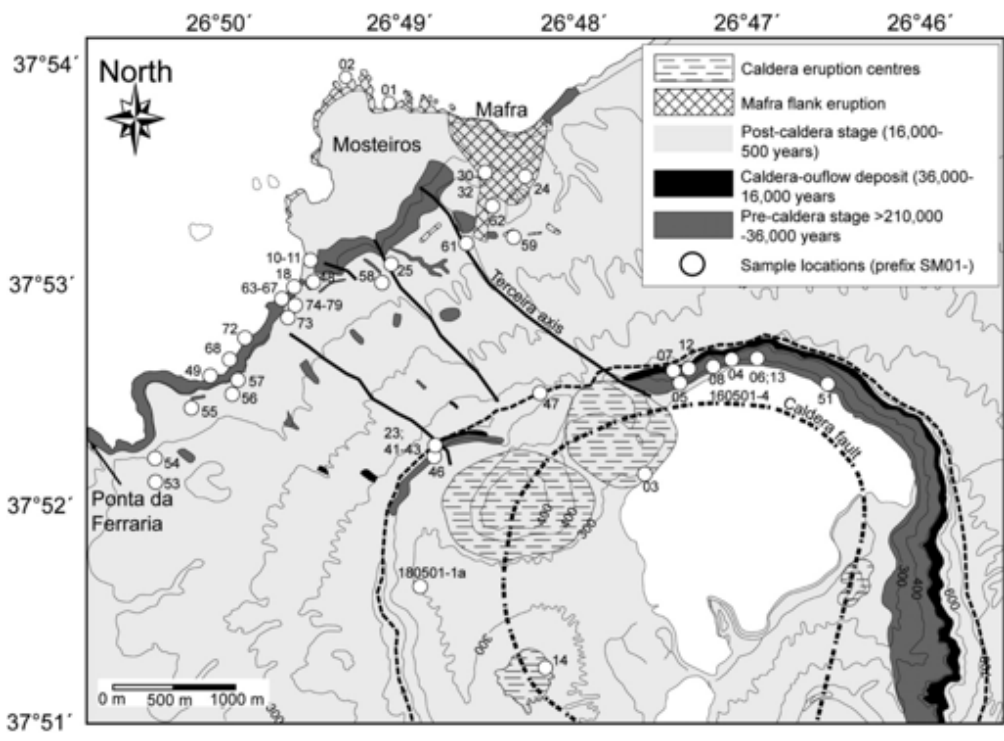


Figure 5. Geologic map of the NW region of Sete Cidades. From Beier et al. 2006. Shading indicates the deposits that are associated with each eruptive phase.

Geochemistry and Relation to Proximal Volcanic Systems

Compared to other island volcanic systems such as the Hawaiian chain, the three major volcanic complexes of Sao Miguel are unique due to their unusually high inter-system geochemical variability (Beier et al. 2006). The chemical dissimilarity of Sete Cidades volcanic deposits compared to the neighboring Agua de Pao system suggest that there is a physical barrier between the two magma chambers. If there were some diffusion of magmas between them, a chemical gradient would be expected; however, this is not observed, and the magmas are chemically distinct and do not suggest mixing (Beier et al. 2006). While the island's volcanic systems show great spatial variability in their geochemistry, the primitive magmas erupting from Sete Cidades have remained geochemically similar throughout its 220 kyr eruptive history (Beier et al. 2006). This may be because the slow-spreading Terceira rift has been relatively stable over this time, causing similar depths of melting and consistent mechanisms for magmagenesis.

Modern environment and Water Quality

While the volcanic system is geologically fascinating, the Sete Cidades region also plays a key role as a water reservoir for the population of Sao Miguel. Since the 1980's, eutrophication resulting from agricultural activities has plagued the Azores islands' water resources, causing a general deterioration in water quality (Virgílio Cruz et al. 2015). Eutrophication results from the excess input of nutrients into a water supply, often from use of industrial fertilizers or increased animal waste runoff. As the nutrients reach water bodies, they encourage blooms of algae and cyanobacteria. These organisms die and sink, causing consumption of oxygen in bottom waters and ultimately leading to anoxia. The most prominent example of this phenomenon globally is currently occurring in the Gulf of Mexico. Due to the pre-existing predisposition to algal growth in Green Lake, it generally shows greater eutrophication than Blue Lake (Virgílio Cruz et al. 2015).

In the Sete Cidades catchment, 24% of the land is dedicated to pasturelands, and the input of nutrients into the catchment is predominantly associated with the livestock grazing these lands (Virgílio Cruz et al. 2015). In the early 2000's, local governments recognized this problem and started implementing solutions to reduce nutrient runoff into the lake systems. These efforts mainly focused on building infrastructure to divert nutrient-laden waters away from the lake systems and into the sea (Virgílio Cruz et al. 2015).

REFERENCES

- Beier, C. Hasse, K.M. and Hansteen, T.H. (2006). Magma Evolution of the Sete Cidades Volcano, Sao Miguel, Azores. *Journal of Petrology* 47(7), 1375-1411.
- Beier, C., Haase, K.M., Abouchami, W., Krienitz, M-S., and Hauff, F. (2008). Magma genesis by rifting of oceanic lithosphere over anomalous mantle: Terceira Rift, Azores. *Geochemistry, Geophysics, Geosystems* 9(12).
- Carmo, R., Madeira, J., Ferreira, T., Queiroz, G., and Hipólito, A. (2015) Chapter 6: Volcano-tectonic structures of Sao Miguel Island. In *The Geological Society of London Memoirs*, 44, 65-86.
- Queiroz, G., Pacheco, J.M., Gaspar, J.L., Aspinall, W.P., Guest, J.E., and Ferreira, T. (2008).

The last 5000 years of activity at Sete Ciades volcano (Sao Miguel Island, Azores): Implications for hazard assessment. *Journal of Volcanology and Geothermal Research* 178: 562-573.

Virgilio Cruz, J., Pacheco, D., Porteiro, J., Cymbron, R., Mendes, S., Malcata, A., and Andrade, C. (2015). Sete Cidades and Furnas lake eutrophication (Sao Miguel, Azores): Analysis of long-term monitoring data and remediation measures. *Science of the Total Environment* 520, 168-186.

Overview

The Azores sit upon the Azores Gibraltar Fracture Zone (AGFZ, *figure 1*) and experiences high rates of seismicity, owing to a combination of tectonic stresses along the AGFZ and volcanism generated by rifting. Near the Azores, the AGFZ is a wide shear zone that accommodates for different rates of spreading north and south of the triple junction. Deformation along the AGFZ is variable and transitions from transpression in the west (central islands of the Azores) to transtension in the east (near Sao Miguel and Santa Maria).

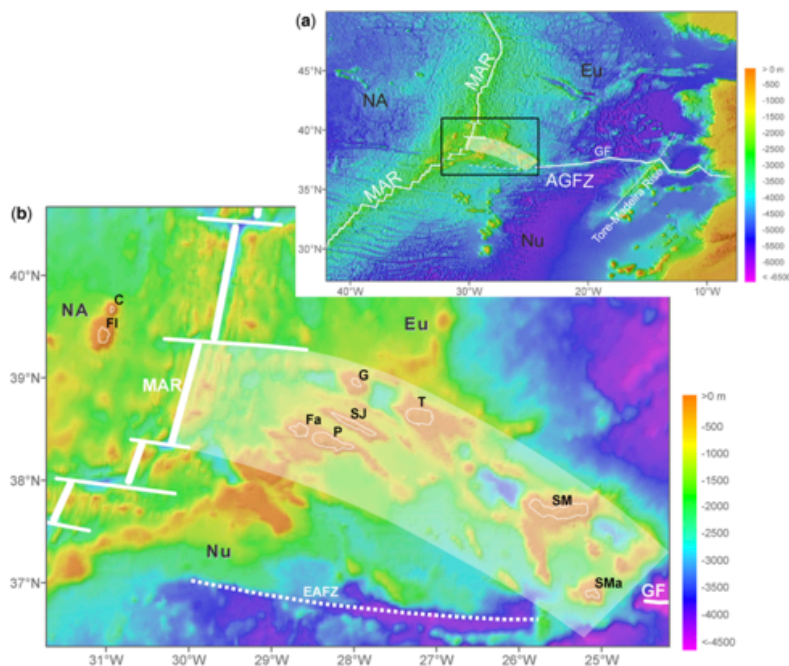


Figure 1 – tectonic setting of the Azores showing the central and eastern islands position along the AGFZ. The shaded region is the location of the Terceira rift, a slow oblique spreading center. Figure from Madeira et al. (2015)

Seismic monitoring began in 1902 with installation of the first station on Sao Miguel. Since then, the network has grown to comprise 37 short period and 12 long period stations. 16 of these short period stations were deployed on the island of Sao Miguel, focused around the main volcanoes (*figure 3*). Between 1997 – 2010, 17,000 events have been detected either on or near Sao Miguel and of these events, 13,000 are associated with one of the main volcanic centers on the island.

High rates of seismicity in the Azores include events up to magnitude 7 and these are focused primarily along plate boundaries with particularly abundant seismicity along the Terceira Rift (*figure 2*), an intensely faulted region of the AGFZ that consists of aligned tectonic basins and volcanos. In addition to larger magnitude events, seismic swarms (lower magnitude earthquakes, which are temporally and spatially clustered, but lack a mainshock) are a consequence of consequence of volcanic activity and are thought to be associated with magma migration and/or circulation of hydrothermal fluids.

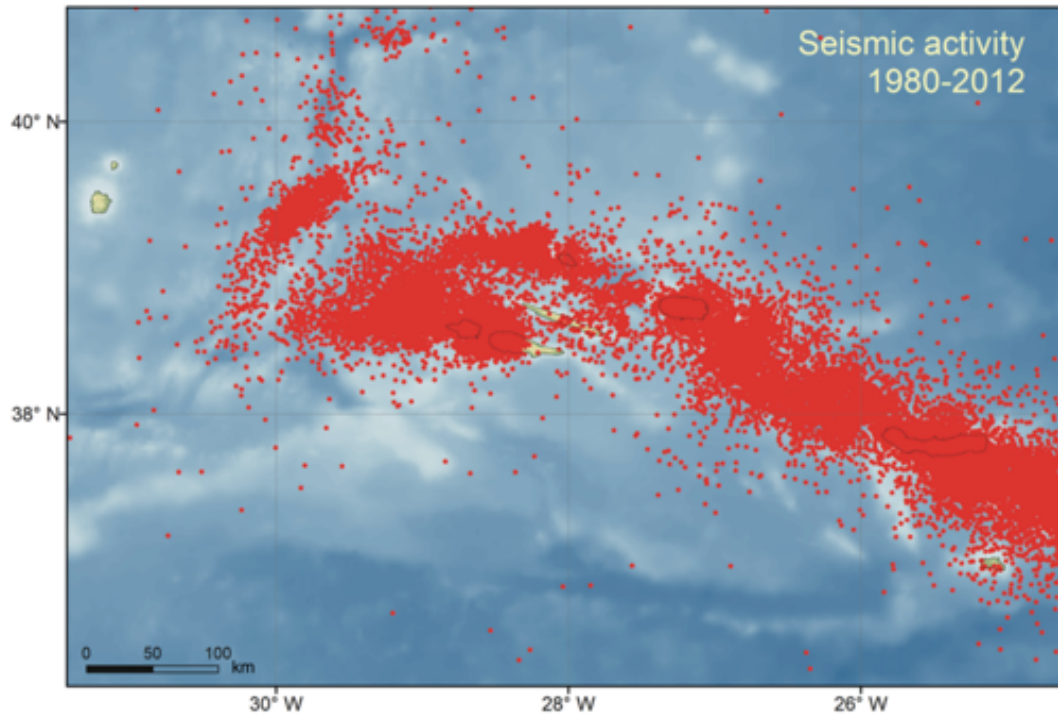


Figure 2 – All seismicity of all sizes near the central and eastern Azores between 1980 and 2012. Figure from Madeira et al. (2015)

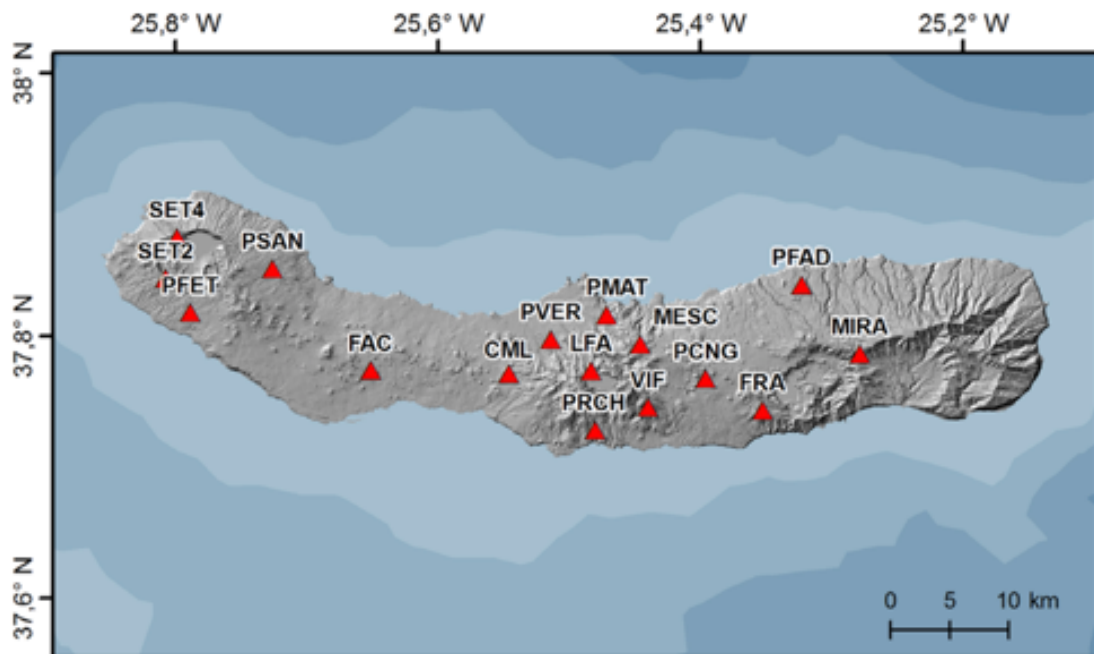


Figure 3 – Locations of the 16 short-period seismic stations that are part of the CIVISA network installed on Sao Miguel. Figure from Silva et al. (2015)

Volcanism and seismicity

The main volcanic centers on Sao Miguel are shown in *figure 4* and include from west to east: Sete Cidades Volcano, Picos Fissural Volcanic system, Fogo Volcano, and Furnas Volcano. Each of these centers is characterized by slightly different volcano-tectonic structures and fault orientations. Fault mapping is achieved using volcanic alignments, geomorphology, and exposure in road cuts. Additionally, the pattern of seismicity through time differs between these centers, which is outlined below along with structural their structural characteristics and good examples of exposures that have been referenced in scientific literature.

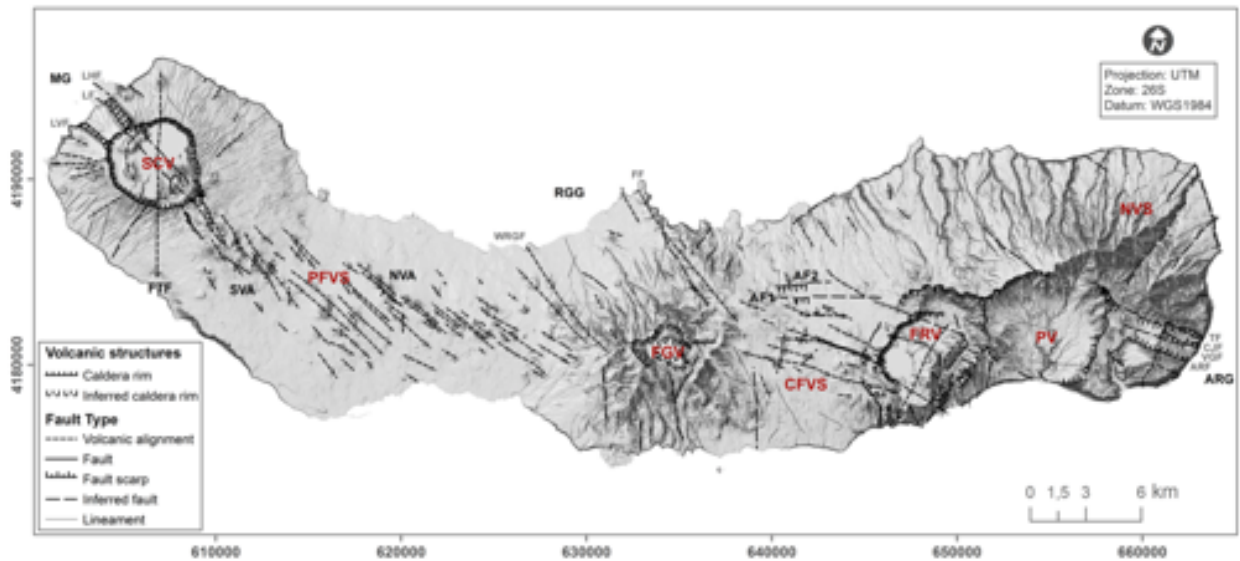


Figure 4 – digital elevation model of Sao Miguel with tectonic and volcanic structures indicated as well as the main volcanic centers (labelled in red). The four centers we’re focusing on are SCV, PFVS, FGV, and FRV. Figure from Madeira et al. (2015).



Figure 5 – Feteiras fault exposed in a road cutting in

Sete Cidades is dominated by NW-SE striking faults with the exception of the N-S striking Feteiras Fault (FTF, *figure 5*). The Feteiras fault is one of the better characterized faults on Sao Miguel, estimated to have accommodated 30 – 40 m of vertical displacement with a slip rate of 0.14 – 0.19 mm/yr. Other notable faults associated with Sao Miguel are the Lombinha (LF) and Lomba dos Homens (LHF) faults, which bound the Mosteiros graben and have hosted ~55 m and 65 m of vertical displacement

Feteiras village. Figure from Carmo et al. (2015)

The Picos Fissural Volcanic System is the least seismically active of the volcanic centers. It is dominated by lava flows and scoria cones with NW-SE striking faults, which are delineated by volcanic alignments. In contrast Fogo Volcano is the most seismically active region and is dominated by NW-SE and NNW-SSE striking faults. The Ribeira Grande Graben extends to the northwest of Fogo Volcano. It is bound by the Ribeira Grande and Falca faults and is estimated to have experienced ~ 650 m of subsidence (*figure 6*).

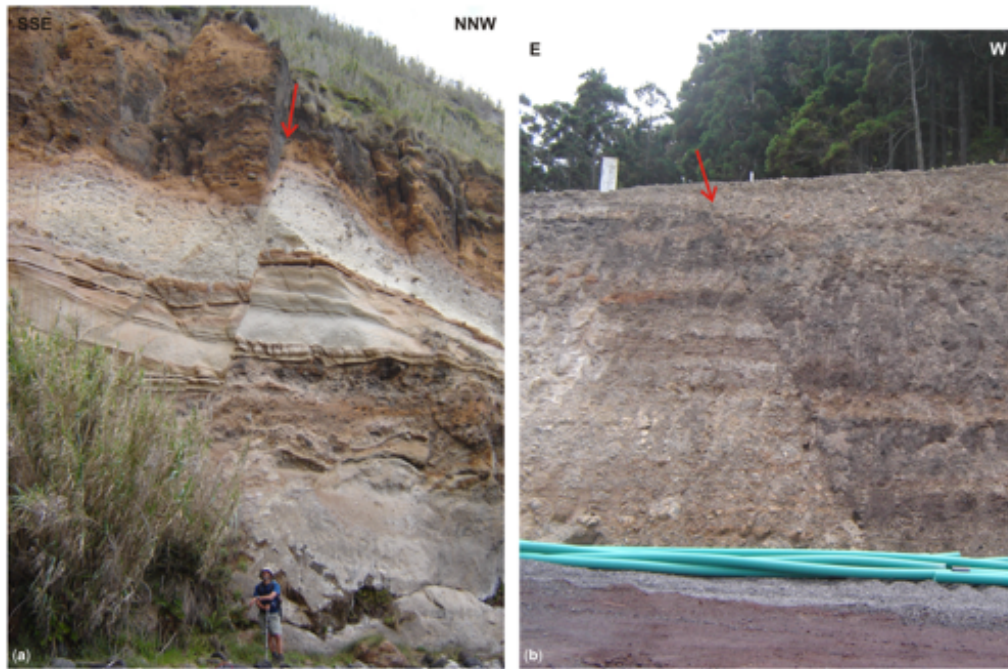


Figure 6 – Falcas fault, the eastern bounding fault of the Ribeira Grande graben exposed in sea cliffs north of Fogo Volcano. Photos from Carmo et al.

The final volcanic center, Furnas Volcano, demonstrates more variability in the strike of faulting with mostly WNW-ESE and SW-NE striking faults. The Amoras fault is located here near the southwestern edge of the crater and is estimated to have hosted 75 m of vertical displacement. It can be seen to offset ignimbrites in sea cliffs on the southern coast (*figure*



Figure 7 – Offset resulting from faulting along the Amoras fault in a sea cliff on the south coast. Photo from Carmo et al., (2015)

Temporal patterns of seismicity

Seismicity across Sao Miguel has evolved through time with certain volcanic centers turning on during different periods. This can be seen in *figure 8* which displays the seismicity broken down by volcanic center during the 1997 – 2010 period. It can be seen that seismicity was low during 1997 before a small uptick in seismicity occurred in 1998 for all volcanic centers but the PFVS. The second significant rise in seismicity occurred in 2002 at Fogo Volcano, reaching a maximum in 2005, which was also coincident with a rise in seismicity at Sete Cidades, before decreasing again.

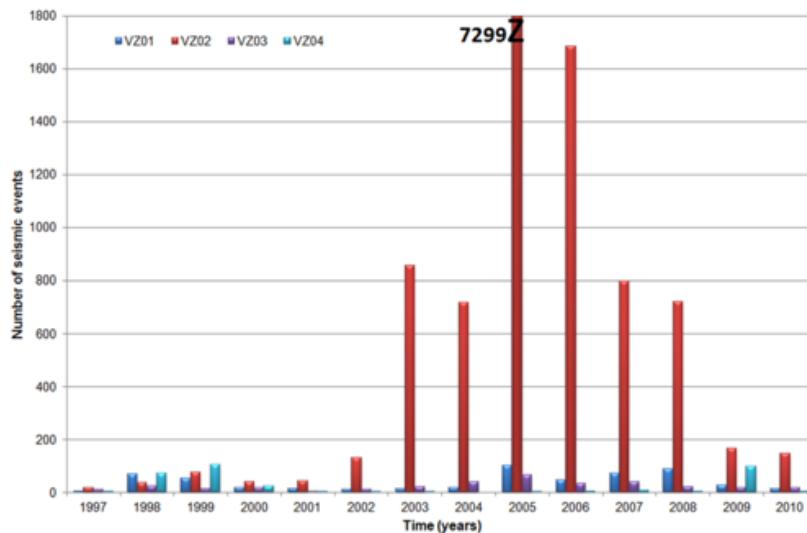


Figure 8 – seismicity through time in Sao Miguel during 1997 – 2010 broken down by volcanic center. Colors correspond to each volcanic center (dark blue is Sete Cidades, red is Fogo Volcano, purple is PFVS, and light blue is Furnas Volcano). Figure from Carmo et al. (2015).

The main driver of this temporal variation in seismicity is thought to be inflation and deflation events caused by magma migration. Inflation events may enhance circulation in highly fractured volcanic centers. As a result, the presence of fluids decreases the effective normal stress, leading to increased seismicity. In contrast, deflation may lead to compaction of pore space and discharge of fluid, resulting in periods of seismic quiescence.

Historical seismicity

The largest earthquakes to have occurred on Sao Miguel had intensities of 8 – 10 on the European Macroseismic Scale (EMS), a qualitative magnitude scale. These intensities correspond to severe (partial collapse of ordinary buildings and overturning of furniture) to extreme (well-built wooden and masonry structures destroyed) damage. All of these earthquakes had epicenters located offshore apart from one. The onshore event occurred in 1522 just north of the once capital, Vila Franca do Campo, and is the most damaging earthquake the Azores has experienced. What led destructiveness is the extensive landsliding it triggered. It is believed that during the days leading up to the earthquake there was considerable rain saturating the soil. As a result of this weakening, many landslides and lahars were triggered that travelled towards the village. The volume of debris involved in these landslides is estimated to be 6.75 m^3 , travelling at a speed of about $1 - 3 \text{ ms}^{-1}$, completely burying Vila Franca do Campo and resulting in the

death of 3000 – 5000 civilians. The remaining earthquakes were not as large nor as deadly as the 1522 event, but still caused significant damage and landsliding.

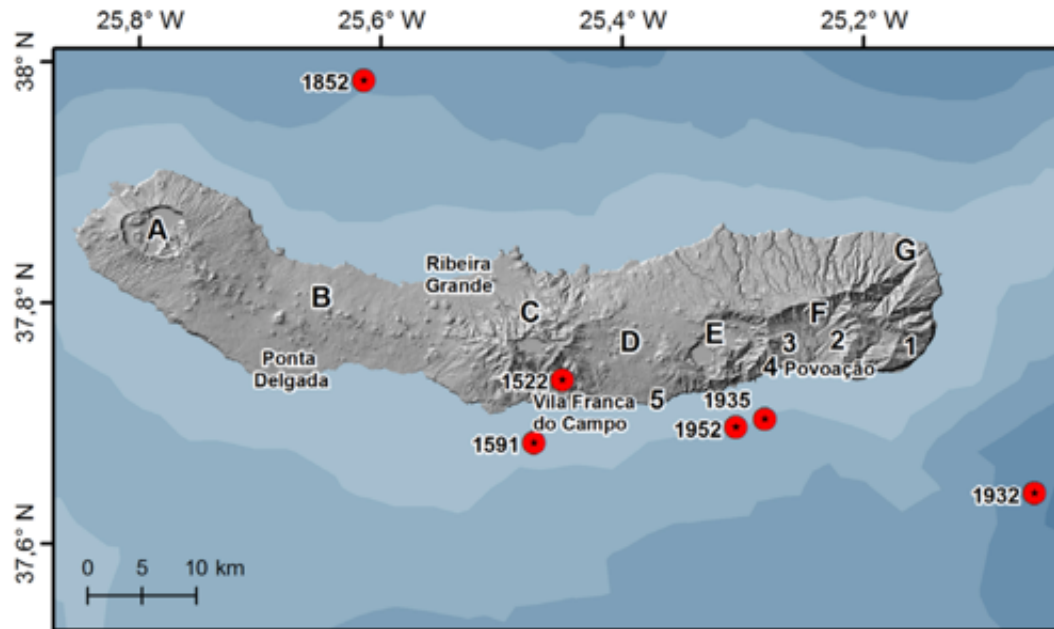


Figure 9 – historical seismicity in and near São Miguel. Figure from Silva et al. (2015)

References:

Carmo, R., Madeira, J., Ferreira, T., Queiroz, G., & Hipólito, A. (2015). Volcano-tectonic structures of São Miguel island, Azores. *Geological Society, London, Memoirs*, 44(1), 65-86.

Gaspar, J. L., Queiroz, G., Ferreira, T., Medeiros, A. R., Goulart, C., & Medeiros, J. (2015). Earthquakes and volcanic eruptions in the Azores region: geodynamic implications from major historical events and instrumental seismicity. *Geological Society, London, Memoirs*, 44(1), 33-49.

Madeira, J., da Silveira, A. B., Hipólito, A., & Carmo, R. (2015). Active tectonics in the central and eastern Azores islands along the Eurasia–Nubia boundary: a review. *Geological Society, London, Memoirs*, 44(1), 15-32.

Silva, R., Ferreira, T., Medeiros, A., Carmo, R., Luis, R., Wallenstein, N., ... & Sousa, R. (2015). Seismic activity on São Miguel Island volcano-tectonic structures (Azores archipelago). *Geological Society, London, Memoirs*, 44(1), 227-238.

Trota, A., Mendes, V., Amaral, P. (2009) - Deformation source modelling of a probable magma intrusion in the Fogo/Congro area (S. Miguel Island, Azores). 13th IAIN World Congress, Estocolmo, Suécia, 27 – 30 de Outubro (Comunicação Oral).

Landslides in the Azores

Landslides occur when large amounts of rock, debris and/or soil move down slope. These events vary in the composition of the material that is displaced, the way in which the material moves (examples include rotation and translation of material across a surface), and the speed at which the material travels. Because landslides can destroy large amounts of infrastructure, trigger other natural disasters like tsunamis, and take lives, understanding landslide triggers and where landslides are most likely to occur is a crucial area of research in landslide-prone areas like the Azores. Figure 1 shows photographs of landslides on Sao Miguel.



Figure 1. Photographs of landslides from (a,b) Furnas Volcano, and (c,d) Fogo Volcano in Sao Miguel [Marques et al., 2015]

Landslides are a frequent occurrence in the Azores (Figure 2) and pose significant risk to lives and infrastructure. Landslides in the Azores between 1990 and 2008 have killed 67 people [Marques et al., 2015]. One particularly devastating event on Sao Miguel

in 1997 resulted from prolonged rainfall affecting vulnerable slopes and already saturated soils to form ~1000 translational slides and debris flows containing water, pumice, ash, trees and branches, and lava blocks. This event killed 29 people dead and left 114 people homeless [Valadao et al., 2002; Gaspar et al., 2011].

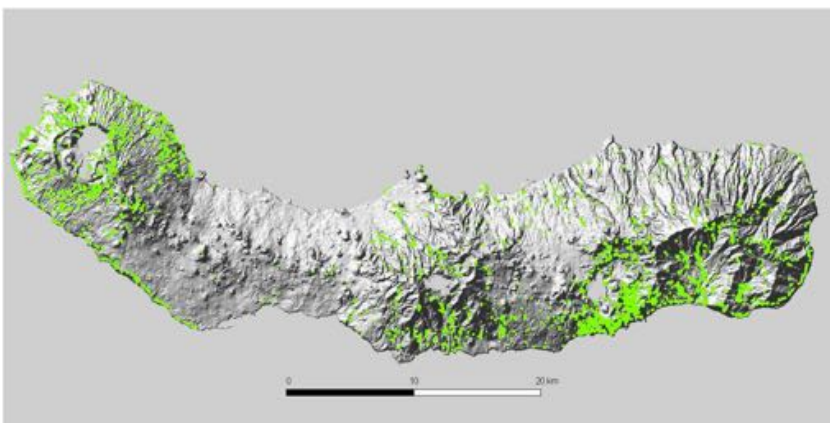


Figure 2. Landslide density map for Sao Miguel Island showing the locations of 2818 events. Landslide density is highest near volcanic complexes where steep slopes or thick, unconsolidated pyroclastic deposits increase landslide risk [Valadao et al., 2002].

Figure 3 shows an example of how debris flows from this event damaged houses. This event also impacted bridges, communication, transportation, and left land that was fertile for agriculture covered in mud. While landslide events of this scale do not occur frequently in the Azores, this event was not unique to Azores history. For example, an earthquake-triggered landslide at Villa Franca do Campo in 1522, then the island capital, buried the village and killed 4000 to 5000 people [Andrade et al., 2006].



Figure 3. Photograph of houses buried by debris flows from the 1997 event [Valadao et al., 2002].

The frequency of landslides in the Azores results from the co-occurrence of several landslide risk factors including rainfall-induced slope saturation, seismicity, and volcanic activity.

Slope saturation leaves steep slopes more prone to failure, and 75% of recent landslides and 76% of recent landslide-related casualties in the Azores are triggered by precipitation (Figure 5 [Marques et al., 2015]). Because the Azores is located at a triple junction, frequent seismicity leading to ground motion is also an important landslide trigger. Additionally, volcanoes contribute to the region's landslide hazard by building up thick, unconsolidated pyroclastic deposits and generating steep slopes along caldera walls, fault scarps, valley margins and sea cliffs that are more prone to failure [Valadao et al., 2002]. Further, landslides that send debris offshore can become dangerous tsunami triggers. Historic records suggest that a tsunami resulted from earthquake-triggered offshore landslides in 1614 [Andrade et al., 2006].

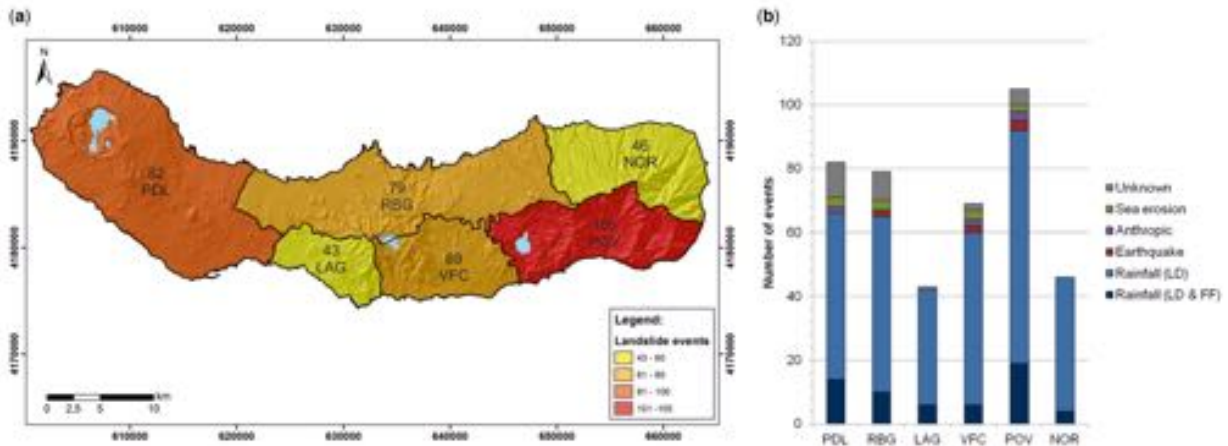


Figure 4. (left) Map of the spatial distribution of damaging landslides on Sao Miguel from 1900-2008 by region and (right) the triggers of landslides by region from [Marques et al., 2015]. Most damaging landslides are triggered by precipitation in susceptible regions (LS: landslide, FF: flash flood).

Recent research has advanced our understanding of the risks that landslides pose to lives and infrastructure in the Azores. A first step in calculating the landslide hazard is determining the spatial variation in landslide susceptibility, which is a subset of the landslide hazard calculation that only considers how likely the terrain in a given region will experience a landslide and not when or how frequently landslides occur or how destructive the landslides are. Figure 5 shows a recent landslide susceptibility map for Sao Miguel based on a statistical model using the locations of 9890 individual rupture areas and geospatial data on factors expected to influence landslide behavior [Marques et al., 2015]. This study identified slope, altitude, insolation, wetness, geology and land use to be the most important factors in predicting landslide susceptibility.

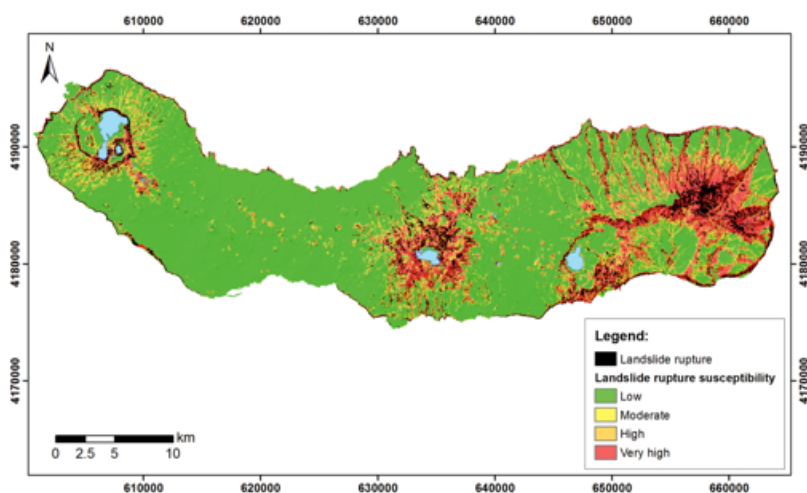


Figure 5. Map of landslide rupture susceptibility [Marques et al., 2015]. On Sao Miguel, 23% of land is classified as high to very high landslide susceptibility.

In the Azores, we are most likely to find evidence of landslides near the steep slopes of calderas and at sea cliffs at the edge of Sao Miguel. Because rainfall, the dominant landslide trigger in the region, is highest in the winter months, landslides are less likely to occur during our August visit.

References

- Andrade, C., P. Borges, and M. C. Freitas (2006), Historical tsunami in the Azores archipelago (Portugal), *J. Volcanol. Geotherm. Res.*, 156, 172–185, doi:10.1016/j.jvolgeores.2006.03.014.
- Gaspar, J. L., G. Queiroz, T. Ferreira, P. Amaral, F. Viveiros, R. Marques, C. Silva, and N. Wallenstein (2011), Geological Hazards and Monitoring at the Azores (Portugal), *Earthzine*, 1–8.
- Marques, R., P. Amaral, I. Araujo, J. Gaspar, and J. Zezere (2015), Landslides on Sao Miguel Island (Azores): Susceptibility Analysis and Validation of Rupture Zones Using a Bivariate GIS-based Statistical Approach, in *Volcanic Geology of Sao Miguel Island (Azores Archipelago)*, edited by J. Gaspar, J. Guest, A. Duncan, F. Barriga, and D. Chester, pp. 167–184, The Geological Society of London.
- Valadao, P., J. Gaspar, G. Queiroz, and T. Ferreira (2002), Landslides density map of S. Miguel Island, Azores archipelago, *Nat. hazards Earth Syst. Sci.*, 2, 51–56.

Azores Tsunamis

The Azores archipelago is especially exposed to tsunamis for two primary reasons. First, because the islands are centrally located in the Atlantic Ocean, they are vulnerable to tsunamis generated throughout the basin, including the islands themselves and the Terceira Rift in the near field, as well as North America and the Portuguese coast in the far field (Andrade., 2006). Such vulnerability is to the benefit of those of us living on the east coast of the United States, as the Azores archipelago deflects any tsunamis generated east of it, effectively shielding the US from those volcanoes (ten Brink et al., 2008). Second, the two primary modes of tsunami generation, seismic activity and mass movements, occur frequently in the North Atlantic. Earthquakes of magnitude ≥ 7 that involve vertical offset are likely to generate tsunamis. Historically, such events have occurred on the Terceira Rift and seismically active regions off the Portuguese coast, generating significant tsunamis that have made landfall on the Azores (Barkan et al., 2009). Mass movements, either subaerially or submarine, including landslides, volcanic eruptions, and caldera collapses have also been known to generate significant tsunamis (Andrade et al., 2006). As a volcanic island chain, the Azores frequently experiences tsunami-generating landslides, eruptions, and caldera collapses (Andrade et al., 2006). Furthermore, the Azores have been hit by a tsunami generated by a submarine landslide from the coast of Canada (Fine et al., 2005).

The magnitude of modern tsunamis in the Azores is measured by tide gauges (Andrade et al., 2006). Historical records of Azores tsunamis on the other hand, are generated from personal accounts and news articles of the islands' inhabitants. Because these personal accounts were written by individual civilians rather than trained geologists using a network of monitoring systems, there is some ambiguity in the extent, amplitude, and even existence of the reported tsunamis (Andrade et al., 2006). For example, evidence of a tsunami could be as minimal as "damaging earthquake on Fayal and Pico islands.... The people aboard the ships in the harbor [Horta–Faial Island] felt violently the earthquake, but only small waves nearly two feet high were formed which vanished in a few minutes. No tsunami was remarked in any other of the islands" (Andrade et al., 2006). Additionally, many tsunamis are recorded based only on ships feeling shaking "as if they had struck shoals," with no reports of any wave making landfall (Andrade et al., 2006).

Twenty-three tsunamis have been reported to hit the Azores since the early 1500's, with a recurrence interval of ~ 18 years (Table 1). Conversely, the recurrence interval of magnitude ≥ 6.5 earthquakes on the Azores plateau is ~ 70 years. Many tsunamis that hit the Azores were landslide-generated, while \sim half had distal sources (landslide or seismic) (Andrade et al., 2006). The earliest reported potential tsunami occurred in 1522 on the island of Sao Miguel. The report describes an earthquake that triggered a landslide characterized as a "...loosening of the whole of the mountain side hanging over this town, pouring mud and rocks [over the town] and covering it entirely down to the sea...and throwing enormous boulders into the port" (Andrade et al., 2006). The event killed 4,000-5,000 people, $\sim 25\%$ of the Azorean population at the time, though most if not all of the deaths were results of the landslide (Andrade et al., 2006). The first credible report of an Azorean tsunami is from 1571. The report was of shaking felt offshore in a boat and no wave was reported on land (Andrade et al., 2006). In 1591, a tsunami destroyed all ships within 20 leagues of the Azores (Andrade et al., 2006). Most Azorean tsunamis have no reported deaths; however, a 1641 tsunami with a run-up of 9 m resulted in 50 fatalities. Among the most notable Azorean tsunamis was the 1755 tsunami generated by a magnitude 8.5 earthquake on the Gorringe Bank east of the Mediterranean Sea (Barkan et al., 2009). The tsunami

was most destructive in Portugal (Baptista et al., 1997), but had an 11-15 m run-up on Terceira Island and there are many reports of damage and fatality (Andrade et al., 2006). No tsunami with a run-up greater than 1 m has hit the Azores since 1899 (Andrade et al., 2006).

In 1929, a magnitude 7.2 earthquake off the coast of eastern Canada generated a landslide and turbidity current that traveled 1,000 km east at a rate of 60-100 km/hour for 4-11 hours. The slope landslide generated a tsunami that had a run-up ranging from 3-7.5 m in Canada and killed 28 Canadians while generating \$400,000 in damage. The tsunami was one of the few landslide generated tsunamis to reach the opposite coast of the Atlantic from where it was generated and was recorded in Azores tide gauges (Fine et al., 2005)

Flank margin collapse of volcanic islands in the eastern Atlantic has been proposed as a potential generator of tsunamis that could have massive impact on the east coast of the United States (Mitchell et al., 2003; ten Brink et al., 2014). Preliminary research of the flanks of South Pico Island in the Azores shows evidence of several flank margin collapses (Mitchell et al., 2012). Furthermore, there is evidence of collapse debris on the ocean floor surrounding South Pico Island (Mitchell et al., 2012).

Date	Source	Cause	Origin	Seismic intensity/ Magnitude	Tsunami intensity		Run-up height/ tsunami height (m)	Recorded
					Alexander (1993)	Papadopoulos and Imamura (2001)		
??.07.1571	L	S		VII?	II	III-IV?	1	Smg, Ter? Gra? Sjz? Pix? Fay?
26.07.1591	L	S	37.4N/25.3W	VIII-IX	II-III	IV-V	1	Smg+ other unspecified islands
24.05.1614	L	S→Ls	38.7N/27.0W	IX	III?	IV-V	3	Ter
21.12.1641	L	S	38.4N/28.1W		III-IV	VI-VII	9	Sjz
???.?.1653	L/D				III-IV?	V-VI	4	Ter
23.11.1668	L	S?	38.5N?/28.1W?		III-IV	V-VI	7	Sjz
???.?.1676	L	S	38.4N/27.1W		III-IV	V-VI	4	Ter
26.07.1691	L	S			II-III?	III-IV	1	Ter
01.11.1755	D	S	38.0N/10.0W	8.5-8.8	IV-V	VII-VIII	11-15	All islands
09.07.1757	L	S+Ls?	38.6N/28.0W	XI/7.4	II-III	IV-V	1	Ter, Gra, Fay (only)
31.03.1761	D	S	37.0N/10.0W		III	IV-V	1	Ter
???.?.1787					II?	III?	1	
23.01.1792					III-IV	V-VI	8	Sjz
17.02.1855	L/D				III?	V?	5*-10	Ter
06.01.1856	L/D	Ss? S?			III-IV	V-VI	10	Sjz
03.02.1899	L/D	Ss? S?			III-IV	V-VI	10	Sjz
31.08.1926	L	S	38.5N/28.4W	X/5.6-5.9	I-II	II-III?	0.5	Fay
31.08.1931	L	S?	38.4N?/27.1W?		II-III	IV-V?	1	Fay
08.05.1939	D	S	34.3N/27.2W	VII/7.1	I	II	0.5	Ter
25.11.1941	D	S	37.5N/18.5 W	8.2	I	I-II	0.5	Ter
28.02.1969	D	S	36.0N/10.6W	7.3	II	II-III	1	Smg, Ter, Fay
26.05.1975	D	S	37.4N/17.7W	IV-V/7.9	II-III?	III-IV	1	Smg, Fay
01.01.1980	L	S	38.8N/27.8W	VIII/7.2	I	I-II	0.5	Ter

Notes: Smg — S. Miguel; Ter — Terceira; Gra — Graciosa; Sjz — S. Jorge; Pix — Pico; Fay — Faial. L — local; D — distal; S — seism; Ls — landslide; Ss — submarine slide. Tsunami run-up/height — see text for explanation.

Table 1—List of historical tsunamis. Blank spaces indicate lack of or inconclusive data. (Andrade et al., 2006)

References:

- Andrade, C., Borges, P., & Freitas, M. C. (2006). Historical tsunami in the Azores archipelago (Portugal). *Journal of Volcanology and Geothermal Research*, 156, 172–185.
- Baptista, M. A., Miranda, P. M. A., & Mendes Victor, L. (1998). Constrains on the source of the 1755 Lisbon tsunami inferred from numerical modelling of historical data on the source of the 1755 Lisbon tsunami. *Journal of Geodynamics*, 25(2), 159–174.
- Barkan, R., ten Brink, U. S., & Lin, J. (2009). Far field tsunami simulations of the 1755 Lisbon earthquake: Implications for tsunami hazard to the U.S. East Coast and the Caribbean. *Marine Geology*, 264, 109–122.
- Fine, I. V., Rabinovich, A. B., Bornhold, B. D., Thomson, R. E., & Kulikov, E. A. (2005). The Grand Banks landslide-generated tsunami of November 18, 1929: preliminary analysis and numerical modeling. *Marine Geology*, 215, 45–47.
- Mitchell, N. C. (2003). Susceptibility of mid-ocean ridge volcanic islands and seamounts to large-scale landsliding. *Journal of Geophysical Research*, 108, EPM 7-14.
- Mitchell, N. C., Quartau, R., & Madeira, J. (n.d.). Assessing landslide movements in volcanic islands using near-shore marine geophysical data: south Pico island, Azores. *Bulletin of Volcanology*, 74, 483–496.
- ten Brink, U. S., Chaytor, J. D., Geist, E. L., Brothers, D. S., & Andrews, B. D. (n.d.). Assessment of tsunami hazard to the U.S. Atlantic margin. *Marine Geology*, 353, 31–54.
- ten Brink, U. S., Twichell, D., Geist, E., Chaytor, J., Locat, J., Lee, H., ... Sansoucy, M. (2008). Evaluation of tsunami sources with the potential to impact the U.S. Atlantic and Gulf Coasts. USGS.

Coastal Erosion

Basics of Coastal Erosion

Coast erosion is the process of wearing away material from a coastline due to imbalance in the supply and export of material from a certain section. Coastal erosion takes place mainly during strong winds, high waves, high tides and storm surge conditions, and results in coastline retreat and loss of land. Over longer timescales, coastal erosion is promoted by sea-level rise, since this creates an increase in sediment demand. If this additional sediment is not supplied, the coastline retreats.

Sao Miguel

Sao Miguel relies heavily on the coast for tourism and fishing, and currently ~60% of the island's population live within 1 km of the coast. The coastline of Sao Miguel contains a varied range of landscapes, including bluffs, steep cliffs, pocket beaches, dunes and lagoons. Several factors about the location and geomorphology of Sao Miguel make it prone to severe coastal erosion.

Firstly, the Azores has a long fetch (the distance over which wind is travelling in the same direction and can build up waves), which results in a high-energy wave climate. Due to wind patterns, the northern coast of all the Azores islands is typically more exposed to high-energy waves than the south coast. Despite this, average coastal erosion rates in the north and south of Sao Miguel are similar (0.25 m/yr and 0.23 m/yr respectively). This is because although the south westerlies affecting the south coast are less frequent, they are more extreme when they do hit (Ng., et al 2014).

All Azores islands are characterized by steep submarine slopes with minimal shallow shelves. This creates localized patterns of wave shoaling, refraction and diffraction, which causes segmentation of the coast into discrete cells with limited sediment movement between them (Borges et al. 2002).

Tide gauge data between June 1978 and May 2007 at Ponta Delgada, Sao Miguel has shown a local sea level rise of 2.5 ± 0.4

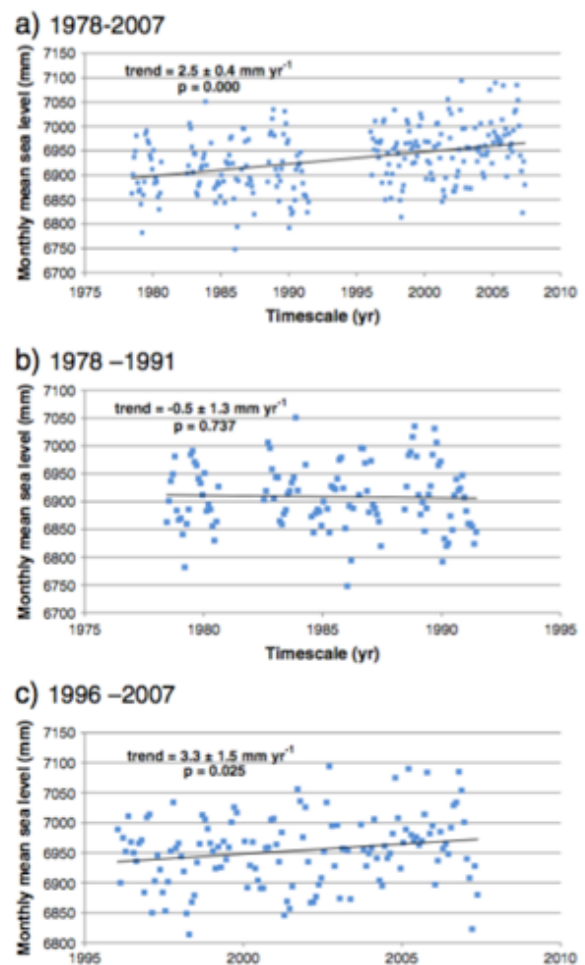


Figure 2. Mean Sea Level trends from Ponta Delgada tide gauges: a) 1978-2007; b) 1978-1991 and c) 1996-2007. From Ng., et al 2014. (Using monthly data retrieved from PMSML, 2013.)

mm/yr. Combined with rising wave energy, this will amplify storm effects, causing frequent flooding and coastal erosion.

In addition to the natural pressures on the coastline, human activity has also played a large role in coastal erosion on Sao Miguel. During the 20th century, dunes were mined for sand for industrial use, causing near complete destruction of these features. ~950,000 m³ of sand was removed from Sao Miguel, with about half of this coming from dunes. On Santa Barbara beach, the removal of the coastal dunes triggered a retreat of the bluff at very high rates (0.6 m/yr). Although sand mining was put to a halt in 1995 by legal enforcement, the system had already been disturbed beyond its natural resiliency, and continues to retreat at a fast rate. Currently, the sandy beach has been reduced in width to a single swash ramp which floods during half of the tidal cycle.

Due to the importance of the coastline for the habitants of Sao Miguel, and the increase in sea level and storm intensities, coastal engineering has been playing an increasingly important role in the protection of Sao Miguel's coastal populations. Several coastal locations have been the focus of coastal engineering projects to maintain the way of life in these communities, and these case studies will be outlined below.

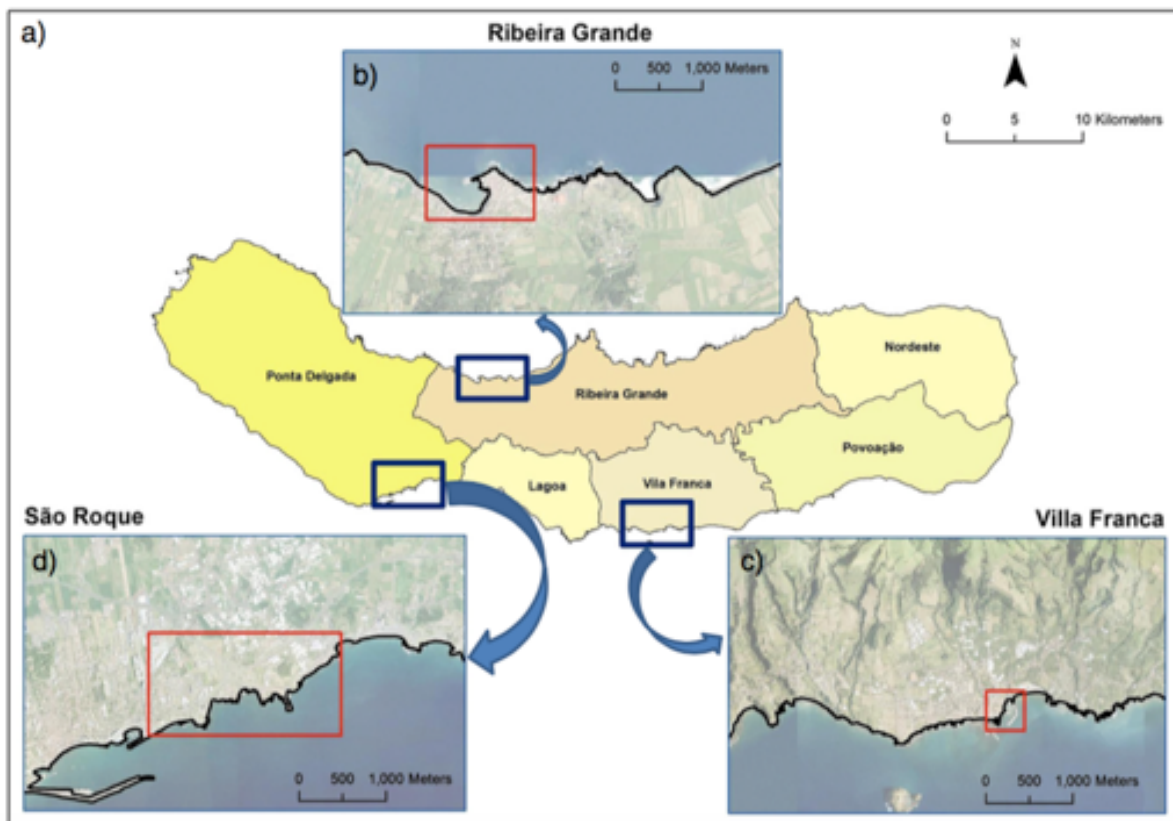


Figure 3. Case study areas for coastal engineering work. From Ng., et al 2014

Coastal engineering on Sao Miguel: case studies

Ribiera Grande

Located along the north coast of the island, Ribeira Grande is the second largest city on Sao Miguel, with a population of 32,112 (as of 2011). Waves up to 10 m high hit the shore from the NW. Storm deposits, such as huge boulders, can be found along the sandy beaches and attest to the northern coast's high wave energy. The focus of the coastal engineering project was a public bathing area that provides access to a swimming pool and small sandy pocket beach. In 2005, an emerged breakwater was constructed to protect this area, and since then that



Figure 4. Public beach at Ribeira Grande. (a) Emerged breakwater to protect swimming pool. (b) Pocket beach formed by sediment trapping. From Ng., et al 2014

portion of coastline has remained stable and safe with no observed negative downdrift impacts.

In addition to the protection it offers, the breakwater also traps local littoral drift sediments, forming a small pocket beach. Under certain wave conditions, however, the breakwater can cause depletion of this pocket beach since it refracts NE swells towards the beach which causes scouring and sediment loss during storms. These sediments are not transported far though, and periodic dredging and beach nourishment helps to maintain the beach.

Villa Franca do Campo

Villa Franca do Campo, was the first capital of São Miguel Island, before it was devastated in 1522 by a major earthquake and landslide. It is one of the three most important fishing villages in São Miguel Island and is a very popular tourist destination due to its good nautical facilities and a beautiful natural islet for bathing and snorkelling. Dominant swells arrive from the SW, although the effects are partially lessened due to the sheltering effect of the islet to southwesterly storms. In 2009, a harbor for local fishermen was built



Figure 5. Antifer cubes line the breakwater at the outer port to absorb wave energy. From Ng., et al 2014

alongside the existing marina. An emerged breakwater consisting of antifer cubes absorbs wave energy to provide safe shelter for fishing and recreational boats.

São Roque

São Roque is a coastal village just east of Ponta Delgada, the most populated city in São Miguel. Along this coastal stretch, dominant swells from the SW can reach heights of up to 12 m. The major coastal hazards are therefore storm inundation and erosion. Homes along this coast used to be flooded during winter storms and extreme events such as the 1996 Christmas Day storm when considerable damage was caused. Some locations experienced severe coastal erosion that resulted in major damage to infrastructure such as the historic fortress.



Figure 6. Tetrapods line the boardwalk buffer zone to absorb wave energy. From Ng., et al 2014

In 2002, the coastline was extended seaward and public spaces were constructed on higher ground to reduce flooding and protect existing houses and cultural heritage further inland. Most of this coastal stretch is now protected by seawalls and in some cases with concrete tetrapods to absorb wave energy. Since this engineering work was completed, several major storms have hit the south coast. Some roads and public areas were flooded but the houses all remained safe and dry. A new drainage system is in the works to improve runoff and should reduce flooding in public spaces.

Paleoshorelines and vertical displacement history on São Miguel and Santa Maria Islands, Azores.

By Michael Sandstrom

Fossil shorelines document changes in past sea level, and are also often used to reconstruct vertical displacement history along coastal regions. Sea level markers are particularly important on volcanic islands as records of past uplift or subsidence as one of the only past indicators available. Volcanic islands typically subside over long timescales, due to plate cooling away from the mid-ocean ridge, hotspot swell decay and surface loading (Ramalho et al., 2017). The island of São Miguel closely follows this trend and has no paleoshorelines from previous warm periods because it is slowly subsiding at a rate of ~ 0.6 mm/yr (Weiss et al. 2016), meaning all sea level (SL) highstands from previous warm periods would be well under water today. Evidence for long-term subsidence comes from bathymetry analysis of the shelf break around the island, which is thought to record the Last Glacial Maximum (LGM) SL low-stand (Quartau et al., 2015). The average shelf break at São Miguel is 142 m below modern SL (**fig. 1**), while the eustatic SL lowstand at the LGM should be around 130 m, thereby implying that ~ 12 m of subsidence has occurred over the last 20 ka (Weiss et al., 2016). In order to find preserved paleoshorelines, we turn our attention to the nearby island of Santa Maria.

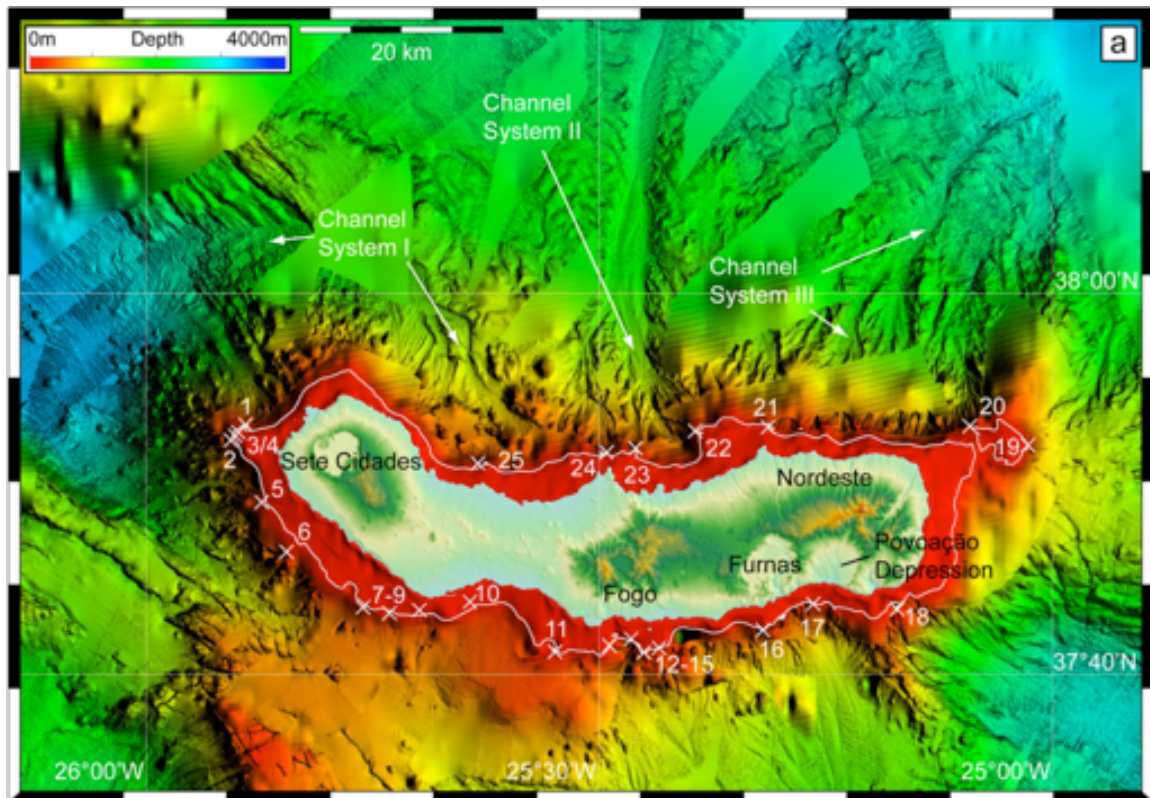


Figure 1: Bathymetry map of São Miguel [Weiss et al., 2016]. The shelf break is shown by the white line at an average depth of ~ 142 m, and is thought to represent the sea level low-stand during the last glacial maximum (LGM). Because global eustatic sea level was ~ 130 m lower during the LGM, Weiss et al. (2016) assume 12 m of subsidence over 20 ka.

Only 100 km southeast from São Miguel, is the island of Santa Maria (**fig. 2**), which is currently uplifting at a rate of ~ 0.057 mm/yr, with 200 m of total uplift since ~ 3.5 Ma (Ramalho et al., 2017). Uplift of a volcanic island is highly unusual in this region, and as a consequence, Santa Maria has the oldest sub-aerial rocks in the Azores, dating back to the Miocene. The mechanism for uplift at Santa Maria must be local in origin, as nearby islands and ocean crust are subsiding, but further investigation is necessary. The island sits on the southeast corner of the Azores Plateau, and could be subject to localized neotectonics from migration of the Nubian-Eurasia plate against the Terceira Rift (Miranda et al., 2015), however a more feasible proposal is that intrusive edifices (possibly in the upper mantle or lower crust) starting in the Pliocene have caused crustal thickening and long-term uplift (Ramalho et al., 2017).

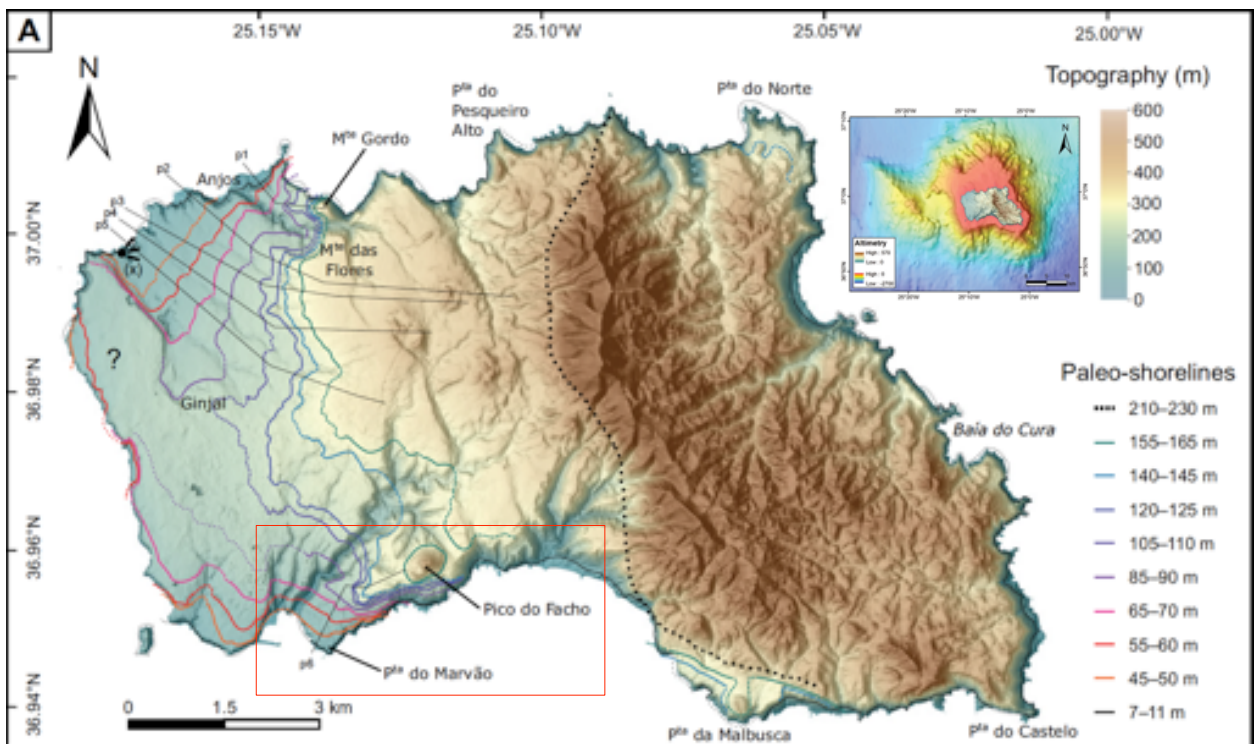


Figure 2: Map of Santa Maria showing elevation and location of paleoshorelines [Ramalho et al., 2017]. Inset at top right shows bathymetry surrounding the island. The red box on the lower left demarcates the region and paleoshorelines explored in this field guide.

The vertical displacement on Santa Maria is complex, with emergence from the ocean through volcanic accretion occurring at ~ 6 Ma, followed by subsidence and re-submergence of most of the island until 3.5 Ma (Ramalho et al., 2017). Following this time is a pronounced uplift trend that extends into the present, as is evidenced by a number of preserved shorelines on the island ranging from 7 – 230 m in elevation (**fig. 2**).

Directly dating paleoshorelines is exceeding challenging, especially in volcanic settings where few coral reefs exist and timescales are longer than > 500 ka (maximum age measurable

with U-Series dating), $^{87}\text{Sr}/^{86}\text{Sr}$ marine isotopes are often altered, and cosmogenic dating is difficult due to lack of quartz. However, Santa Maria has successive sea level markers preserved through interbedded volcanic deposits, which can be dated quite accurately, providing age brackets for relative sea level. These bounding units have been dated using $^{40}\text{Ar}/^{39}\text{Ar}$ geochronology (**fig. 3A**) and used to accurately constrain relative sea level at the time of each eruption (Ramalho et al., 2017). From this information, sea level can be estimated from a reference curve and the vertical displacement history obtained (Miller et al., 2005). One complication to this method is that eruptions don't necessarily occur during a sea level highstand, which increases the uncertainty on vertical movement, but general trends can still be acquired by averaging long-term sea level changes.

The sea level markers that exist in Santa Maria include beach and shallow subtidal deposits, along with associated tidal notches (**fig. 3B**) and intertidal marine fauna. There are also numerous subtidal pillow basalts and hyaloclastites directly overlain by aurally deposited lava flows (**fig. 3C**). Because of the complex history of subsidence and uplift in Santa Maria, fossil shoreline ages do not necessarily correspond to elevation, with the oldest Miocene shorelines actually near modern sea level (**fig. 3A**) and cut into by the last interglacial highstand (Ramalho et al. 2017). Shorelines preserved after 3.5 Ma do follow a trend of increasing elevation with age. These constraints allow for an accurate vertical reconstruction history of Santa Maria and help provide insight into unique uplift mechanisms on volcanic islands.

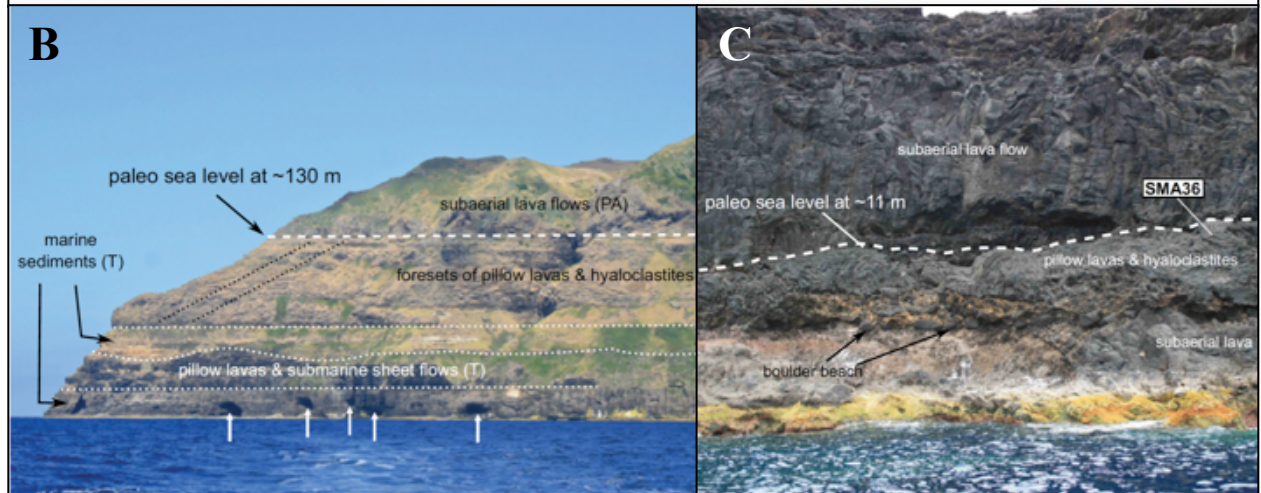
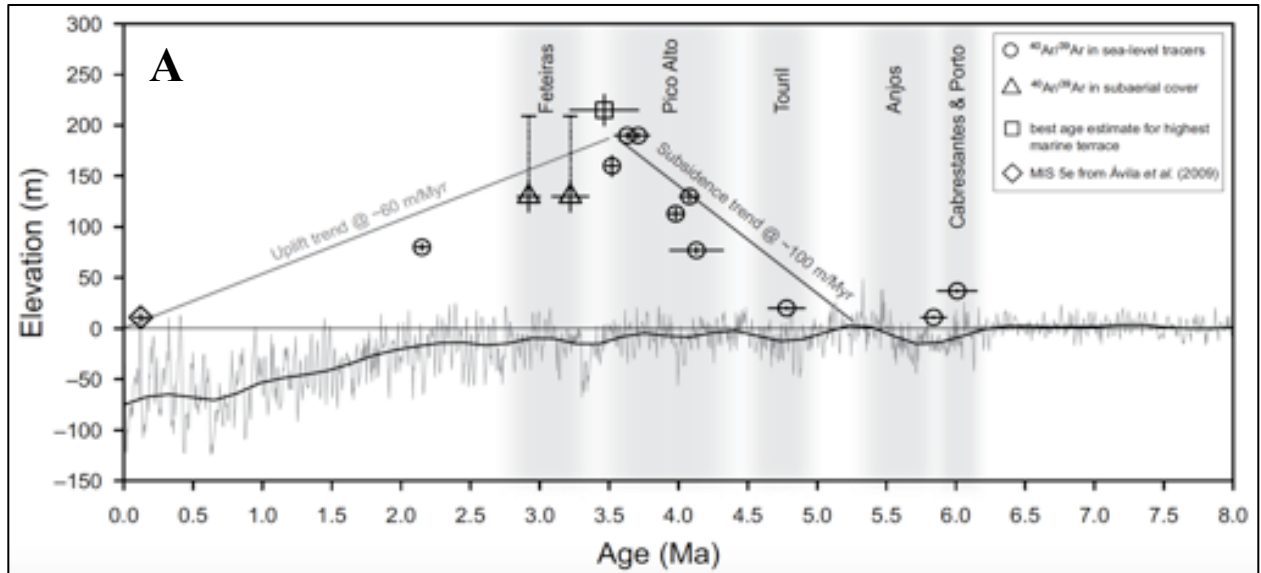


Figure 3: A.) Graph of sea level markers showing vertical movement over time based on sea level markers dated using Ar/Ar methods and compared to a LOWESS smoothed eustatic sea level curve [Ramaldo et al. 2017]. B.) Image of marine markers at Santa Maria, generally showing underwater pillow lavas and hyaloclastites overlain by marine sediments and capped with subaerial lava flows. White arrows show MIS 5e wave notches, indicative of an intertidal zone. C.) Close-up image of subtidal pillow lava deposits capped by subaerial lava flow [Ramaldo et al. 2017].

Bibliography:

Miller, K., Kominz, M., Browning, J., Wright, J., Mountain, G., Katz, M., Sugarman, P., Cramer, B., Christie-Blick, N., and Pekar, S. (2005). The Phanerozoic record of global sea-level change: *Science*, v. 310, 5752, p. 1293–1298, doi:10.1126/science.1116412.

- Miranda, J.M., Luis, J.F., Lourenco, N., and Fernandes, R.M.S. (2015). The structure of the Azores triple junction: Implications for São Miguel Island, in Gaspar, J.L., Guest, J.E., Duncan, A.M., Barriga, F.J.A.S., and Chester, D.K. *Volcanic Geology of São Miguel Island (Azores Archipelago): Geological Society of London Memoir 44*, p. 5–13, doi: 10.1144/M44.2.
- Quartau, R., Madeira, J., Mitchell, N.C., Tempera, F., Silva, P. F., and Brand, F. (2015). The insular shelves of the Faial-Pico Ridge (Azores archipelago): A morphological record of its evolution, *Geochem. Geophys. Geosyst.* 16, 1401–1420, doi:10.1002/2015GC005733.
- Ramalho, R., Helffrich, G., Madeira, J., Cosca, M., Thomas, C., Quartau, R., Hipólito, A., Rovere, A., Hearty, P., and Ávila, S. (2017). Emergence and evolution of Santa Maria Island (Azores)— The conundrum of uplifted islands revisited. *GSA Bulletin*; March/April 2017; v. 129; no. 3/4; p. 372–391; doi: 10.1130/B31538.1
- Weiss, B., Hübscher, C., Lüdmann, T., Serra, N. (2016). Submarine sedimentation processes in the southeastern Terceira Rift - São Miguel region (Azores). *Marine Geology*, 374 : 42–58.

Marine Life in the Azores Islands

Elise M. Myers

The Azores (Açores) Islands are home to a wide diversity of marine life, with particular regions called seamounts housing particularly high densities of biota. These features support the unique flora and fauna that are still only being discovered in this rich ecosystem. Unfortunately, as is increasingly common throughout the world, human activity threatens the tenuous balance in ecosystems with high biodiversity. The anthropogenic consequences coupled with still nascent marine biodiversity exploration raises fear that much of the biodiversity in the Azores Islands will disappear, even before it is fully captured.

I. Seamounts

Essential to much of the Azores Islands' marine life are geological features called seamounts. Seamounts are underwater mountains that result from hotspots underneath tectonic plates, making them common in seafloor that is volcanic and tectonically active [4]. These underwater mountains, which didn't extend vertically enough to form islands, are found near the Azores Islands at a density of about 3.3 peaks per 1000 km² [4]. Seamounts form deep summits, ranging from 800-1500 meters, and can be from 200-1,000 meters in width [4]. Currently, bathymetric map estimations suggest that about 15,000 seamounts exist around the Azores Islands, though less than 1% of them have been characterized (Figure 1).

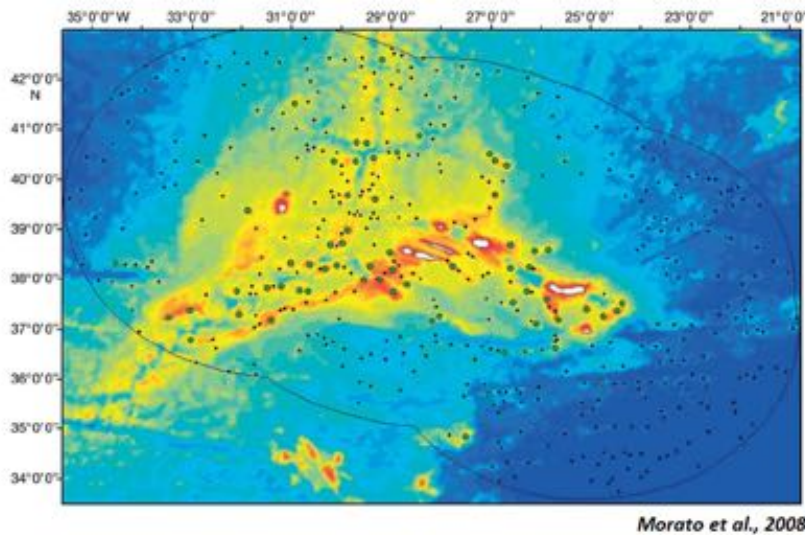


Figure 1
Many seamounts exist around the Azores Islands; this map denotes those seamounts that are known. The black line marks the Economic Exclusive Zone (EEZ), within which the rights to explore and exploit the ecosystem are given to the state (Portugal/Azores).

The seamount called Dom João de Castro Bank (Figure 2a-b), between Terceira Island and São Miguel Island, is unique in its high tectonic active that is well documented. Dom João de Castro Bank rises from 1000 meters depth to 13 meters below the surface, though the interior crater is about 50 meters deep. Its last major volcanic eruption was in 1720, when a small island called Ilha Nova (i.e. "New Island") formed with a 1.5 km diameter and reaching 250 meters in altitude. However, by 1722, the island had disappeared below the ocean's surface, causing its existence to be disputed until when it was located and mapped in 1941 [2]. While no eruptions have been recorded since then, Dom João de Castro Bank has abundant hydrothermal activity, with vents being located at depths of only 20 meters [2]. The vent exhaust reaches 120°C and,

when passing above shallow regions of the seamount, one can see gases, mainly CO₂, rising from the water [2].

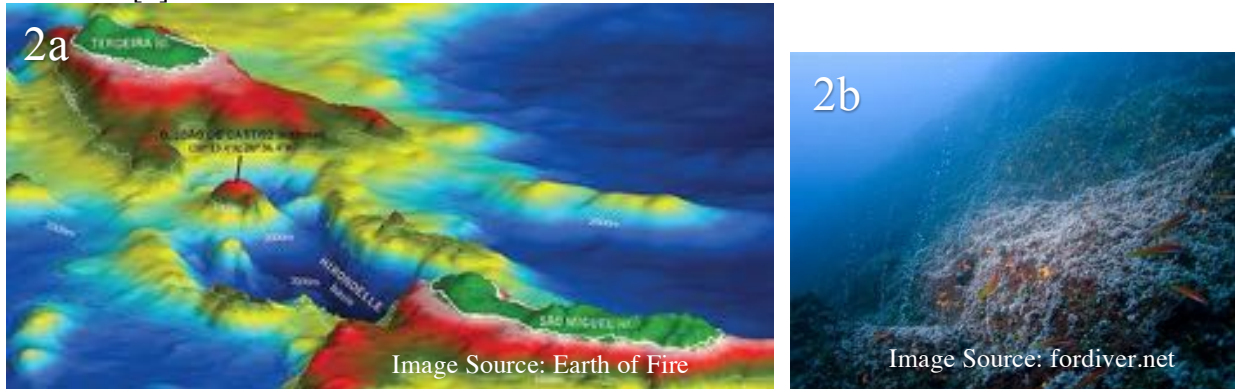


Figure 2a-b

Dom João de Castro Bank is visible in bathymetric maps and is located between the main islands of São Miguel and Terceira (2a). This seamount is unique due to its hydrothermal activity (2b).

II. Biological Hotspots

In addition to forming over mantle hotspots, seamounts form a different kind of hotspot: one of biodiversity. Seamounts are located in the open ocean where biological productivity is reduced due to limited nutrients, upwelling, and organic matter repurposing [12]. Their presence disturbs the natural flow of ocean currents, causing water to roll up the sides and stretch along the seamount (Figure 3). This small-scale upwelling provides nutrients for phytoplankton and other microorganisms, forming the base of a complex biological community. For much of the year, autotrophic cells, those microbes that fix their own carbon, are predominately small. However, during the spring when upwelling along the seamounts increases [3], the autotrophic biomass has a much larger fraction of large cells, as documented on the seamount Seine [10]. This relates to the principle of surface area to volume ratios. When nutrients are low, it is ideal for phytoplankton to have a larger ratio to allow for more nutrient uptake. Contrastingly, when nutrient concentrations are high, larger cells with a lower ratio of surface area to volume will still be able to take up adequate nutrients. Despite mesoscale variability on different seamounts causing unique conditions at different seamounts, there is still an overlying trend of an above-average abundance of phytoplankton during the spring and summer [10].

Currents rolling across the top of seamounts create turbulent eddies, which are thought to hold zooplankton and other organisms that, normally, freely move through the water [3] (Figure 3a). This stagnation of microorganisms creates a stable food source for benthic fish communities, which, in turn, support larger marine predators [11] (Figure 3b). In seamounts, there are commonly aggregations of skipjack fish, bigeye tuna, and the common dolphin, while the predatory bird, Cory's shearwater, is often spotted nearby [4]. Seamounts provide both important habitat and spawning grounds for these marine predators. The strong currents over seamounts expose the base of volcanic rock, which favors the growth of invertebrates that feed on suspended organic material. Commonly found here are gorgonians (sessile colonial cnidarians) and corals [3, 11]. Deep corals found on seamounts can grow up to 3 meters tall and live for around 300 years [3].

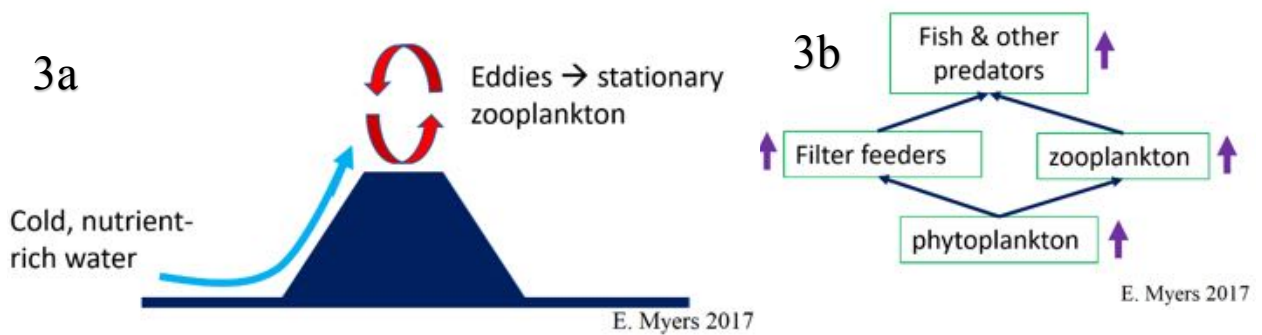


Figure 3a-b

Seamounts disturb the local ocean currents, causing localized, small-scale upwelling that provides nutrients for the base of the marine food web (3a). An increase in phytoplankton causes a cascading effect, supporting zooplankton and filter feeders, which in turn support the higher trophic level organisms, like predatory fish and dolphins (3b).

Though not emerging from the sea, seamounts function similar to islands with each seamount containing its own endemic species, like in the Galápagos Islands. The theory of island biogeography, established in the 1967 book by Robert MacArthur and Edward Wilson [9], explains species richness on islands of different size and isolation (distance from other islands or the mainland). The islands themselves, seamounts in this case, provide a habitat with open niches, while being surrounded by inhabitable or minimally supportive ecosystems, like the open ocean. Organisms can then colonize the space, with higher rates of immigration for those islands that are larger or closer to other viable ecosystems. Seamounts, surrounded by the open ocean and at a density of 3.3 peaks per 1000 km² [4] are ideal for species colonization and the subsequent evolution of distinct benthic flora and fauna. The vast majority of unexplored seamounts in the Azores Islands could harbor incredible diversity of marine organisms that have yet to be discovered.

III. Anthropogenic Threats to Seamount Marine Biology

Unfortunately, anthropogenic activities, particularly fishing, threatens seamounts and the unexplored biodiversity they harbor. In the 1990s, marine tourism in the Azores Islands dramatically increased, including whale watching, scuba diving, and big game fishing [6]. At the same time, people began shifting fishing efforts from the overfished continental platforms to the rich, pristine seamounts of the Azores Islands [3]. As large fish return in large groups for feeding and breeding, visible via simple sonar, seamounts are an easy target for large trawlers [3] (Figure 4a-b). Generally, deep-sea fisheries, especially seamounts, have high fish yields during the first few years of exploration, but then collapse within 10 years from overexploitation [6]. The strategy for maintaining deep-sea fisheries in this region is not to practice sustainability, but to exhaust one seamount and then move to a new, unexplored seamount [3]. Scientists warn that, as less than 1% of the anticipated 15,000 seamounts on the ocean floor have been studied, commercial fishing could prevent the world from discovering or benefitting from numerous species.

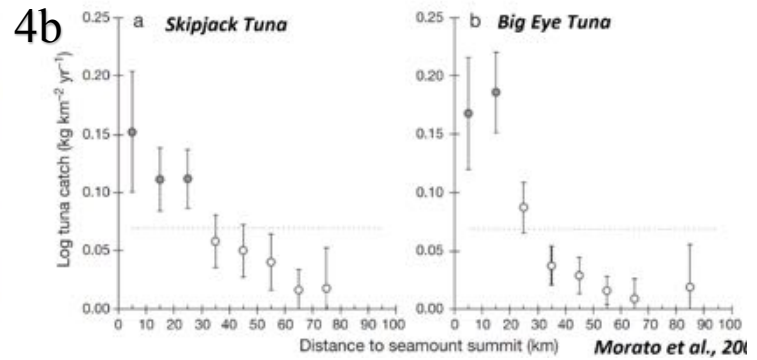
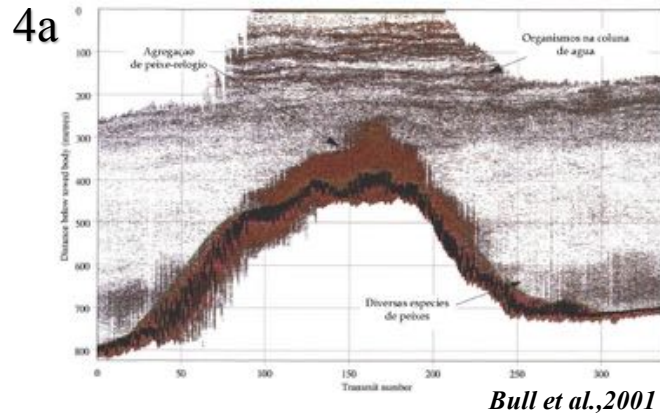


Figure 4a-b

High abundances of deep-water fish are easily visible via sonar (4a), including orange roughy (peixe relógio - left), general fish (bottom right), and other organisms (top right). Fishing yields (i.e. “catch”) demonstrate that larger, predatory fish are concentrated over seamounts (4b).

In the mid-2000s, the regional government implemented a variety of incentives that increased fishing effort via commercial fleets, despite scientific warnings in 1999 that benthic fish species were approaching critical levels of exploitation [6]. One highly endangered deep-sea fish species, the orange roughy (peixe relógio), is highly vulnerable to fishing because of its slow growth and long lifespan of up to 150 years [5]. Since 2003, the whole European deep-water fleet can fish within 100 nautical miles from the Azores Islands [3], which threatens marine conservation efforts [4]. Through these legal provisions, Azores Islands fishing has increased to yield 80 million tons of fish per year [3].

Particularly devastating is bottom trawling, which entails dragging a large net along the sea floor to catch all organisms. This practice results in high amounts of bycatch, the unintended capture of marine organisms, and deep coral reef destruction. Damage from bottom trawling to the structures on top of seamounts is long-lasting and possibly permanent. To combat this damage, the Portuguese government has enacted a temporary ban on bottom trawling and increased regulation to protect deep water coral reefs in much of the Azorean Exclusive Economic Zone (EEZ) [6] (Figure 1). An EEZ is defined by the United Nations Convention on the Law of the Sea and grants a coastal state special rights over the exploration and use of marine resources within 200 miles of shore [7].

In addition, Portugal has established Marine Protected Areas (MPAs) in 2 pristine seamounts for scientific exploration, Altair and Antialtair, 3 deep hydrothermal areas, and on shallow hydrothermal area. The government states that these MPAs are designed to preserve habitat, biodiversity, and geological history [5]. The hydrothermal vents vary, with one black smoker (fluid oversaturated in salts and metals), a submarine volcano with various crustaceans, and the collapsed Dom João de Castro Bank [5]. Hopefully, with these MPAs, the Azores rich biodiversity can be preserved for generations to come.

IV. What Marine Life to Expect

During the late summer/early fall, shallow water temperatures should be between 22-25°C with visibility of 15-30+ meters [1]. Sightings while diving or snorkeling will vary by

habitat. Sandy habitats are best for spotting Common stingrays, Madeira Skates, Cleaner wrasse, and conger eels [1]. Rocky reefs will instead have an abundance of moray eels and grouper fish. Seamounts and other local topographic highs are a good location for spotting eagle rays, tunas, jacks, Bluefish, mobulas (devil ray), mantas, or even Wahoo in the late summer [1]. In the shallows, there are many smaller marine organisms, including “blennies, gobies, small wrasse, damsels, scorpion fish, nudibranchs,” and crustaceans [1].

In deeper, open waters, it is common to see sperm whales, common dolphins, bottlenose dolphins, Atlantic spotted dolphins, fin whales, risso’s dolphin, sicklefin devil rays, loggerhead turtles, leatherback turtles, ocean sunfish, (comb) jellyfish, salps, blue sharks, and even blue or white marlin [8]. While some species might only be glimpsed near the water’s surface, others may leap from the water, including the dolphins and devil rays. Using August 2016 as a guide, the most likely macrofaunal to spot in August include the Common dolphin, the Common bottlenose dolphin, the Sperm whale, and the Atlantic spotted dolphin (Figure 5).

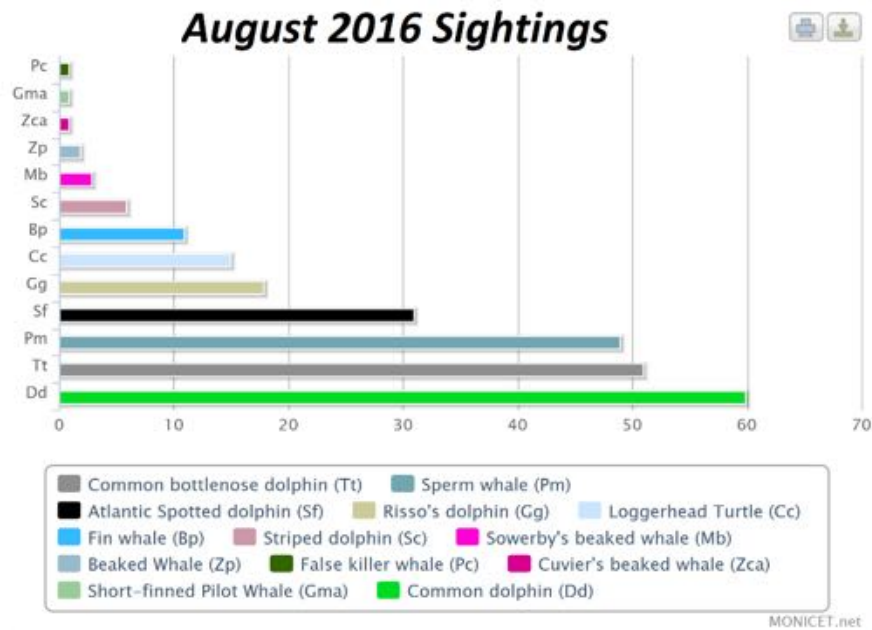


Figure 5

According to MONICET.net, a marine tourism organization, these were the sightings of large marine fauna in August 2016.

Works Cited

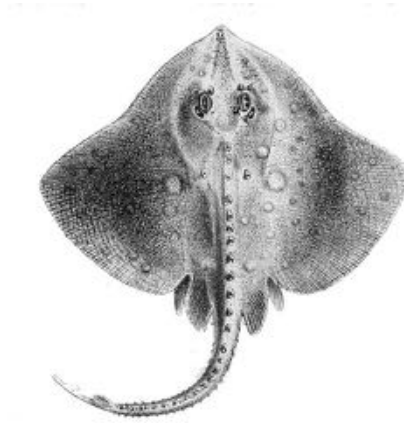
1. “Coastal Diving in the Azores on Pico Island.” *CW Azores*, Cetacean Watching Lda, 2008.
2. “Hydrothermal Vents.” *MPAs Portugal*, WAITT Foundation, 2011.
3. “Montes Submarinos – Oásis De Vida Marinha.” *Mundo Submerso-Projetos*, Department of Oceanography & Fish - IMAR Center of the University of Azores, December 2005.
4. “Seamounts in the Azores.” *CONDOR: Seamount Management and Research Tools*, Department of Oceanography & Fish - IMAR Center of the University of Azores, 27 June 2014.
5. “Seamounts.” *MPAs Portugal*, WAITT Foundation, 2011.
6. Abecasis, R. C., Longnecker, N., Schmidt, L., & Clifton, J. (2013). Marine conservation in remote small island settings: factors influencing marine protected area establishment in the Azores. *Marine Policy*, 40, 1-9.
7. Directorate, OECD Statistics. “Exclusive Economic Zone.” *Glossary of Statistical Terms - Exclusive Economic Zone (EEZ) Definition*, OECD, 4 Mar. 2003.
8. Eriksson, Ida. “São Miguel Is Surrounded by Marine Life.” *Azores Whale Watching Futurismo*, 31 May 2014.
9. MacArthur, R. H., & Wilson, E. O. (2015). *Theory of Island Biogeography*. (MPB-1) (Vol. 1). Princeton University Press.
10. Mendonça, A., Aristegui, J., Vilas, J. C., Montero, M. F., Ojeda, A., Espino, M., & Martins, A. (2012). Is there a seamount effect on microbial community structure and biomass? The case study of Seine and Sedlo Seamounts (Northeast Atlantic). *PLoS One*, 7(1), e29526.
11. Morato, T., Varkey, D. A., Damaso, C., Machete, M., Santos, M., Prieto, R., ... & Pitcher, T. J. (2008). Evidence of a seamount effect on aggregating visitors. *Marine Ecology Progress Series*, 357, 23-32.
12. Sigman, D. M., & Hain, M. P. (2012). [The biological productivity of the ocean](#). *Nature Education Knowledge*, 3(10), 21.

Marine Life Guide – Azores (Açores) Islands

Coastal/Shallow Waters



Common Stingray (*Dasyatis pastinaca*)
(otilibrary.com)



Madeira Skate (*Raja Maderensis*)
(iNaturalist.org)



Cleaner Wrasse
(shallowreefaquarium.com)



Conger Eel
(fishbase.org)



Black spot moray eel
(justgottadive.com)



Grouper
(diveworld.com)



(Red) Blenny
(marinewildlife.co.uk)



(iStock)



Devil Ray/ Mobula
(bestspotazores.com)



Goby Fish
(marinewildlife.co.uk)



Ornate Wrasse
(alamy.com)



Damselfish
(alamy.com)



Scorpionfish
(flyingsharks.eu)



Nudibranch
(*alamy.com*)

Deeper Waters/Open Ocean



Sperm Whale
(*nwf.org*)



Sperm Whale tail flukes
(*cwr.org.au*)



Common Dolphin
(*wsknow.com*)



Atlantic Spotted Dolphin
(*becuo.com*)



Risso's Dolphin
(pinterest.com)



Loggerhead Turtle
(animalspot.net)



Blue shark
(becuo.com)



Blue Marlin
(billfishreport.com)



White Marlin
(billfishreport.com)



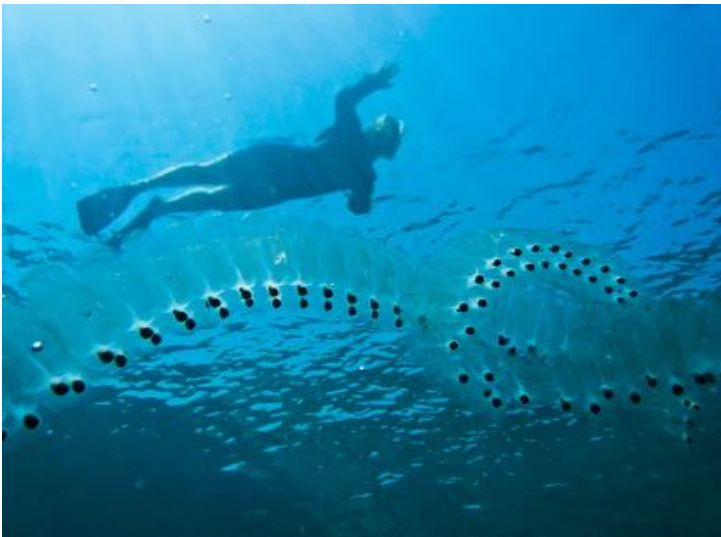
Comb Jellyfish
(texasstateaquarium.org)



Ocean sunfish
(*gettyimages.net*)



Ocean sunfish fin
(*azoreswhales.blog – Ida Eriksson*)



Salps Chain
(*nereusprogram.org*)



Salp (but *Salpa maggiore*)
(*Conaugh Fraser*)



Devil Ray/ Mobula
(*iStock*)



(*bestspotazores.com*)

Terrestrial Fauna of the Azores

As a volcanic archipelago in the North Atlantic, the Azores contains significant terrestrial biodiversity. The nine islands and surrounding sea combined contain approximately 450 endemic species, many of which are currently endangered [Fauna from the Lands, 2016]. The Azores is one of the safest tourist destinations as there are reportedly no known venomous animals there, and in fact, there has never been a snake observed on any of the nine islands. The islands were named after the only predatory bird of the Azores, the Common Buzzard. Early settlers arriving to the islands mistook it for a goshawk or “açor” [Rodebrand, 2017].

Of the terrestrial animals, arthropods account for most of the species endemic to the Azores with over 250 currently known and counting, as shown in Figure 1b [Rego et al., 2015]. With the increasing number of arthropod species discovered every year (greater than 1800 in 2008, Figure 1a), the number of publications on arthropods has also grown [Gaspar et al., 2008]. Of the more than 1800 species of insects discovered on the islands, humans are thought to have introduced approximately 43% of them, significantly altering the biodiversity of the island and reducing the number of resources available to native species.

Excluding livestock, there are only nine species of mammals found on the islands. Prior to their discovery in the 15th century, the only mammals existing on the Azores were two species of bats, and therefore humans introduced the remaining mammals. The only mammal endemic to the islands is a bat called the Azores Noctule *Nyctalus azoreum* (Figure 2), which can be found on all of the islands and roosts in caves, buildings, and hollowed-out trees [Trowbridge, n.d.]. The remaining mammals include an additional species of bat, three species of mice/rats, one rabbit species, one species of hedgehog, and two species of weasel/ferret.

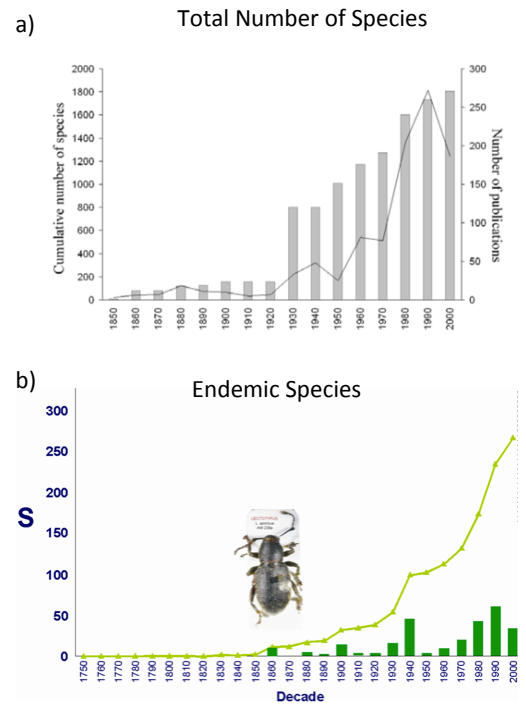


Fig 1. a) Cumulative number of total arthropod species discovered in the Azores plotted as gray bars along with number of arthropod related publications plotted as the black line [Gaspar et al., 2008]. b) The number of endemic species discovered each year is shown as green bars and the green line represents the cumulative total of endemic species [Rego et al., 2015].



Fig 2. Azores Noctule *Nyctalus azoreum* [https://upload.wikimedia.org/wikipedia/commons/thumb/f/f8/Nyctalus_azoreum.jpg/240px-Nyctalus_azoreum.jpg]

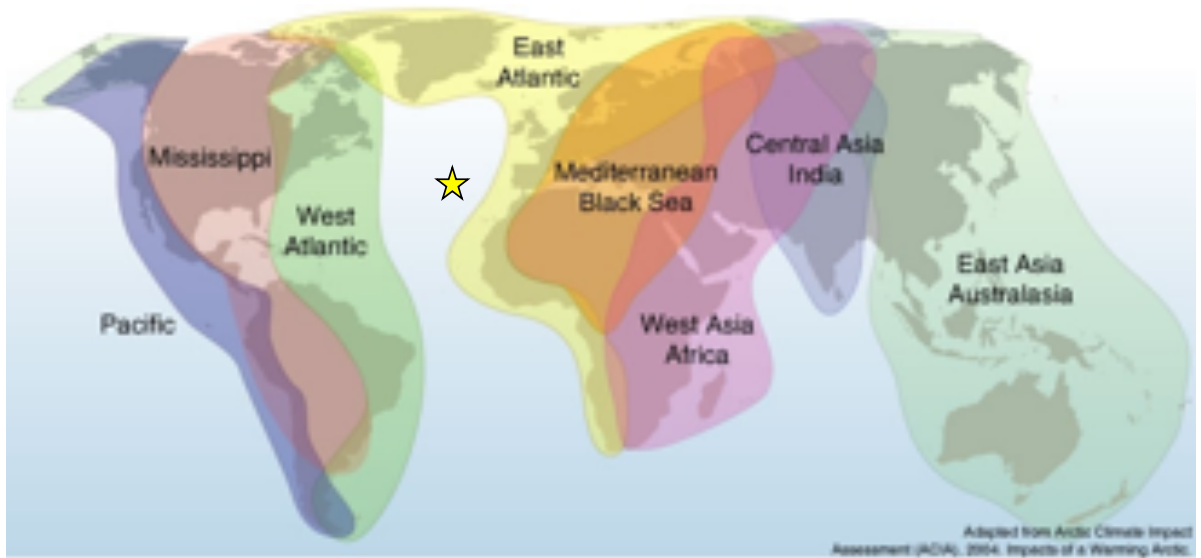


Fig 3. Bird migration flyways of the world. The Azores is represented by the gold star and is situated between the West Atlantic and East Atlantic flyways.

[<http://cliveg.bu.edu/greeningearth/ssnltydim/10-migration.jpg>]

Due to their unique location nearly halfway between the Americas and Eurasia, the Azores islands see birds from both the West Atlantic and East Atlantic flyways and therefore, have one of the most diverse bird populations in the world (Figure 3). There are approximately 380 species of birds recorded in the Azores but only 64 of which are considered “common” birds [Rodebrand, 2017]. There are 20 year-round residents, which include 2 endemic species (Azores Bullfinch and Monteiro’s Storm Petrel) and 9 endemic subspecies.

Additionally, there are approximately 30 migratory species that commonly pass through the Azores during spring and fall migration and 14 species which breed in the Azores during the summer months. The remaining 318 species are considered “vagrants” from the Americas or Eurasia/Africa who rarely find their way to the Azores.

The only bird endemic to São Miguel is the Azores Bullfinch *Pyrrhula murina*, found in the native laurel forest on the eastern edge of the island, as shown in Figure 4. It is the second rarest bird in the world with only an estimated ~775 individuals and less than 200 mating pairs left on the island [Rodebrand, 2017]. Populations have declined rapidly since the 1920s due to deforestation for grazing and agriculture as well as introduction of exotic vegetation [Monticelli et al., 2010]. Today, the entire range occupied by the Azores Bullfinch has been deemed a Special Protection Area (SPA) under the European Union Directive on the

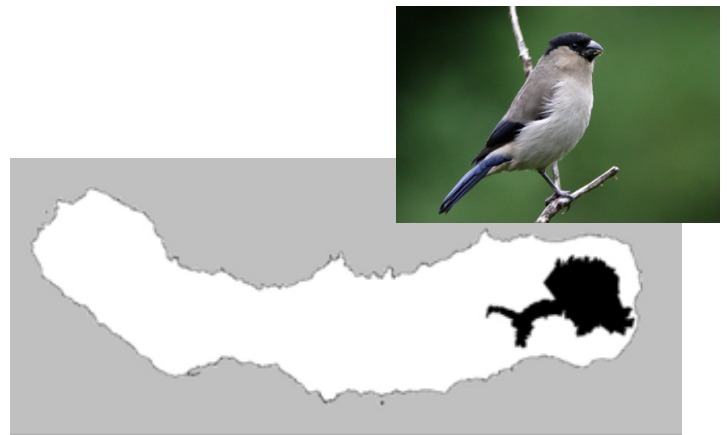


Fig 4. A map of São Miguel with the Azores Bullfinch range colored in black [Monticelli et al., 2010].

Conservation of Wild Birds. Current conservation efforts include captive breeding, removal of exotic vegetation, and replanting native vegetation.

The 4 main habitat types and birds we are likely to see in each, include [Pereira and Michielsen, 2013]:

- Marine – Yellow-legged Gull, Storm Petrel, Cory's Shearwaters, Common Tern
- Forested Areas – Azores Bullfinch, Goldcrest, Chaffinch, Woodpigeon, Eurasian Blackcap
- Bodies of Water – Moorhen, Eurasian Coot, Grey Egret, Eurasian Teal, Eurasian Wigeon
- Pastures – Azores Quail, Island Canary, Common Snipe, Common Buzzard

References

- Carla Rego, Mário Boieiro, Virgílio Vieira, and Paulo A.V. Borges. The biodiversity of terrestrial arthropods in Azores. 2015.
- Carlos Pereira and Gerbrand Michielsen. Bird watching in the Azores. 2013.
- Clara Gaspar, Paulo A.V. Borges, and Kevin J. Gaston. Diversity and distribution of arthropods in native forests of the Azores archipelago. *Arquipélago. Life and Marine Sciences* 25: 01-30. 2008.
- David Monticelli, Ricardo Ceia, Ruben Heleno, et al. High survival rate of a critically endangered species, the Azores Bullfinch *Pyrrhula murina*, as a contribution to population recovery. *J Ornithol.* 151:627–636. 2010.
- Fauna from the Lands of Priolo. (2016). Retrieved from <http://www.azores.gov.pt/Gra/srrn-cets-en/conteudos/livres/Fauna.htm>
- Leann Trowbridge. (n.d.). Azores temperate mixed forests. Retrieved from <https://www.worldwildlife.org/ecoregions/pa0403>
- Staffan Rodebrand. (2017). Birding Azores and the Birds of the Azores. Retrieved from <http://sr-oland.se/azores/index.html>

Agriculture in the Azores

Meg Frenkel

(1) Introduction: Azores climate

As in any part of the world, the agricultural industry of the Azores is largely defined by local climate conditions. Due to the Azores' proximity to the path of the Gulf Stream, seawater temperatures surrounding the Azores islands range only from 16-25°C and help to establish a subtropical maritime climate with humid forests and shrubland on land. For example, the annual average air temperature on the coast of Pico Island, the island with the greatest climatic diversity, is 18°C, ranging from 10.5°C in February to 26°C in August and only 6°C diurnally. Additionally, the Azores have fairly regular rainfall throughout the year, with heavier rain in autumn and winter, a short summer period (i.e.g, July, August), with a fairly constant wind that blows more heavily during the winter months. Despite the relatively static weather conditions, the geographic isolation of the islands, as well as the unique volcanic terrain do give rise to a wide variety of ecosystems and landscapes that establish the foundation for Azorean agriculture.

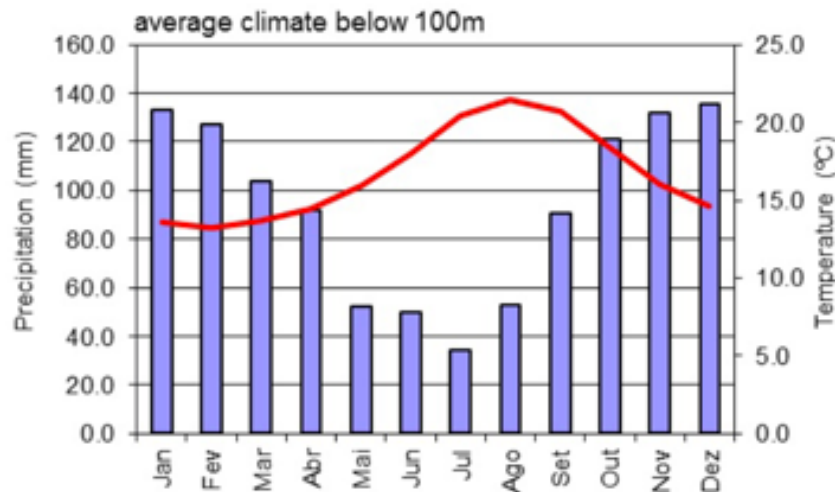


Figure 1. Monthly temperature and precipitation averages of the Azores (Madruga et al., 2015).

(2) Economics

Agriculture represents a critical component of the Azorean economy. Although the Azores contribute only 2.1% to the Portuguese economy as a whole, Azorean agriculture represents a disproportionate amount of the Portuguese agriculture/forestry/fishing sector (~9-10%). On the islands themselves, the agriculture industry employs more than 100,000 people (approximately ~12% of total Azores employment) and is particularly important on smaller islands where livestock farming is the primary economic activity and all

other industry is linked to the food sector. Most agriculture today still takes place in the form of small, family-based farms run by an aging population of farm owners. However, because of the small scale of these farms, most producers must supplement their income with other sources, including pensions, tourism, and other small businesses.

(3) Main agricultural products

The usable agricultural area on the Azores covers 120,400 Ha, about half of the total territory. Of this area, 88% is made up of permanent grassland and pasture that is good for extensive livestock farming, 10% is arable land used mostly to cultivate green maize to feed livestock, and only ~2% is occupied by other permanent crops. In addition to green maize, principle crops of the Azores include sugar beet, potatoes, sweet potatoes and yams (Table 1), as well as subtropical vegetables such as bananas, pineapple and tea. Vineyards, represent only (4%) of total agricultural production, though wine is culturally significant to the region.

The dominance of forage crops (~84%) strongly reflects the importance of the dairy industry in the Azores' agricultural economy. In fact, on the island of Terceira, the cow-to-human ratio has been cited as 2:1. Most of these cows live in small pastures divided by dry-stacked volcanic rock walls and are raised through a uniquely Azorean style of rotational grazing: the dairy cattle are rotated through pastures every day or every few days, but because many farmers do not own or rent adjacent fields, cattle must walk through the streets to get from one pasture to another. This resulting cow traffic is what locals refer to as 'cow jams.'

Table 1. Surface area and yield of principle crops from 2014.

Source: Statics Portugal INE (2015), 'Agricultural Statistics 2014'

	SURFACE AREA	YIELD
ANNUAL CROPS		
Green maize	9,342 Ha	270,775 t
Potato	599 Ha	11,142 t
Beetroot	354 Ha	13,320 t
Corn for grain	238 Ha	446 t
Sweet Potato	60 Ha	1,176 t
Azores yam	60 Ha	1,191 t
PERMANENT CROPS		

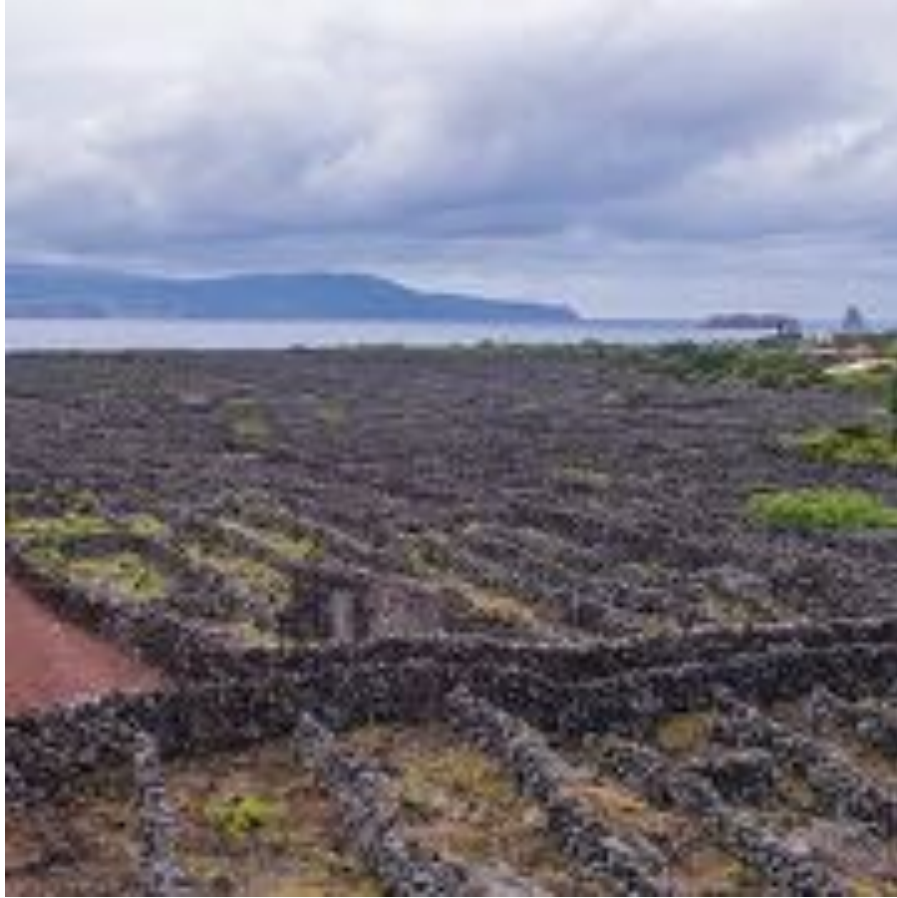
Wine products (2009)	926 Ha	12, 913 HI
Orange	366 Ha	3,754 t
Banana	291 Ha	5.129 t

With almost 90,000 dairy cows, the Azores produces approximately 250 million liters of milk per year, mainly on the island of São Miguel. Of this amount, only 57 million liters are used for direct human consumption and this milk is largely sent to markets in mainland Portugal (~75%) and other areas of the European Union. An increasing amount of milk is toward making cheese, such as the traditional “São Jorge” or “Queijo da Ilha.” Ilha has been produced since the 16th century and has a characteristic nutty, flavor, though it is also known to be quite smelly. Most Azoreans enjoy eating this cheese spread over a piece of bread for breakfast. São Jorge is a semi-hard cheese made of just three ingredients: cream, rennet (coagulate) and salt. It is made specifically on the island of São Jorge, but can be found through restaurants throughout the Azores. Eaters beware; São Jorge can commonly be produced in a ‘picante’ style of varying degrees of spiciness!

Though agriculture has been an economic boon to the Azores, such success has not ensued without concurrent environmental dilemmas. As grasses have replaced natural forests to support cattle grazing, the soil has become less effective at capturing rain, with implications for the amount of water available for distribution to urban areas. Meanwhile, soil erosion has also accelerated due to the spread of incenso, an imported shrub used by farmers to mark their territory. It is also important to note that a national quota system has allowed Azores dairy farming to maintain their stance in Portuguese markets, but these quotas have recently been removed. How the Azores respond to both modernization of agriculture and increased global competitiveness could determine how well the industry competes into the future.

(4) Vineyards and Wine

Wine has been produced in the Azores since the 15th century, only about 10 years after the first settlers arrived on the islands around 1439. The first of these winemakers were thought to be Franciscan friars who utilized the unique geology and particular soil conditions of the Azores to their advantage. For example, the basaltic lava fields of the Azores are a harsh environment for most crops, but grape wines can be grown on a variety of different soil types, including rocky terrain. Additionally, this early viniculture established the traditional Azorean practice of growing vines between basalt rock walls called “currais” which today delineate a maze of thousands of small, contiguous rectangular plots. In fact, the total length of these stone walls on the Azores could circle the Earth twice! This unique organization of grape vines is meant to protect the crops



from wind and sea salt. Additionally, the black basalt rocks can absorb heat during the day and give off heat at night, keeping the vines warm. The wines also benefit from the overall moderate climate of the Azores.

Generally speaking, some other characteristics for determining the ability to grow grapes and the quality of a

Figure 2. Vineyards of Pico Island, outlined by basaltic rock walls known as “currais.” (Vincent Ko Hon Chiu, UNESCO, 2015).

wine include (1) drainage and water holding capacity, and (2) pH. The volcanic material characterizing Azorean soils results in porous rocks that can store water up to 100% of their weight and then release the water slowly to the root systems of the vines, particularly important in years with little rainfall or drought. However, others suggest that such porosity and low organic content of basaltic soils allows for water to be rapidly removed, resulting in loss of excess water and resulting in grapes with a more concentrated, fruitful flavor. Meanwhile, pH can be considered a proxy for soil fertility. Moderately acidic soils (pH 4.5-5.8) are low in important plant nutrients like Ca^{+2} , Mg^{+2} , Na^{+} and K^{+} because the exchange complex in soils binds high amounts of non-nutrient cations (e.g., H^{+} , AlOH^{2+} , or $\text{Al}(\text{OH})_2^{+}$). However, moderately alkaline soils (pH 8-

10) contain growth-limiting salts and are often more dry that is optimal for grapes. The best soils fall somewhere in between the extremes and, fortunately, Azorean soils do.

The interplay between climatic and soil conditions have had a large role in determining the type of grapes grown on the Azores. Typically, Azorean wines are made from three different grape varieties: (1) *verdelho*, perhaps the most famous grape grown in the Azores and with a distinct sweet flavor, (2) *arinto*, a versatile variety used in blends/sparkling wines and (3) *terranhez*, a white Portuguese grape used in sweet fortified wines. These white wines have been more successful than red wines due to the lower heat demand for maturation of white grapes.

Additionally, three vineyard regions of the Azores have qualified for the status of “Quality Wines Produced in Specific Regions” (QWpsr) under European Union wine regulations: (1) Pico Island, (2) Biscoitos on the island of Terceira, and (3) Graciosa. Calling a wine a ‘QWpsr’ is a quality indicator on the basis of production method, management and geographic location, with the purpose of distinguishing these wines from table wines (TW) in a method adapted from a system originally employed by the French government. Moreover, Pico Island was named a World Heritage Site in 2004 for its exceptional preservation over the last 500 years, continuation of viticulture practices that are fully authentic in function, tradition, and techniques, and for existing as a “outstanding example of the adoption of farming practices to a remote and challenging environment.” The surrounding buildings, including manor houses, wine cellars, warehouses, conventional houses and churches, as well as pathways, wells, ports, and ramps also remain authentic to the first winemakers on the island.

Wine growing in the Azores has not been without its challenges, however. Because of the unique micro-parcel style of viticulture employed in the Azores, there is a high demand for human labor and mechanization is more difficult to achieve than at other vineyards. The remote location of the Azores also poses challenges to international shipping. Combined, these factors make wine production less efficient in an increasingly competitive global wine market. Additionally, wine production at Pico Island peaked in the 19th century and rapidly declined soon thereafter due to the spread of vine diseases and infestations such as *odium*, a powdery mildew found as a film on the surface of vines, and *phylloxera*, an aphid-like insect that draws juices from the roots of the grape plant and injects toxins that prevent healing. In fact, drought and infestation forced wine makers on Pico Island to turn to more disease-resistant grapes used in the United States, instead of their traditional *verdelho* grapes by the mid 1800s. Fortunately these more traditional grapes could be grown again, but not until the 1990s. While wine making is recovering in the Azores, locals are nevertheless concerned about the future of viticulture, as future generations appear less interested in

maintaining these authentic Azorean practices and traditions in favor of tourism and a growing service economy.

References:

Bogs, J. (2016), Grape Phylloxera, Buckeye Yard and Garden Online, The Ohio State University, <http://bygl.osu.edu/index.php/node/400>

Carvalho, A.C. (2015), Estatística Agrícolas 2014, Instituto Nacional de Estatísticas Statistics Portugal. https://www.ine.pt/xportal/xmain?xpid=INE&xpgid=ine_publicacoes&PUBLICACOESpub_boui=224773630&PUBLICACOESmodo=2

Kitsteiner, J. (2014), Rotational Grazing... Azores Style, Temperature Climate Permaculture, <http://tcpermaculture.com/site/2014/01/24/rotational-grazing-azores-style-2/>

Kitsteiner, J. (2014), Saying Goodbye to the Azores, Temperature Climate Permaculture, <http://tcpermaculture.com/site/2014/01/24/rotational-grazing-azores-style-2/>

Madruga, J., Azevedo, E.B., Sampaio, J.F., Fernandes, F., Reis, F., and Pinheiro, J. (2015) Analysis and definition of potential new areas for viticulture in the Azores (Portugal), *Soil*, 515-526.

Retallack, G.J., Bruns, S.F. The effects of soil on the taste of wine, *GSA Today*, 25(5):4-9.

Scheffler, D. (2015) Volcanic soils in Italy, Greece, Israel, Hawaii and Madeira produce unique wines, <http://www.scmp.com/magazines/style/article/1723887/volcanic-soils-produce-unique-wines>.

Festa, J. (2015), Exploring the Basalt Lined Vineyards and Historic Grapes of the Azores' Pico Island, Epicure and Culture, <https://epicureandculture.com/exploring-the-basalt-lined-vineyards-and-historic-grapes-of-the-azores-pico-island/>

UNESCO (2015), Landscape of the Pico Island Vineyard Culture, World Heritage Center, <http://whc.unesco.org/en/list/1117/>.

Oceanography

Changes in the Atlantic Meridional Overturning Circulation (AMOC) have been implicated in major climate changes of the past, and implications of the future state of ocean circulation under a warming climate are poorly understood. In the North Atlantic, warm surface waters flow to the north, where they lose heat to the atmosphere. The formation of sea ice and the associated cold brines that are formed sink in deepwater formation sites in the Greenland, Iceland, Norwegian, and Labrador Seas. This cold North Atlantic Deep Water returns to the South, and eventually is upwelled along the Antarctic continental margin. Overall, this general circulation pattern is responsible for net northward transport of heat in the Atlantic basin, which is the basis for the fabled “bi-polar seesaw” and is part of the “great ocean conveyor belt,” both terms coined by LDEO’s very own Wally Broecker.

The part of AMOC that anyone who has swum in the Atlantic on the East Coast of the US should care about is the Gulf Stream. The Gulf Stream current, which was originally charted by Benjamin Franklin in 1770, travels at a strength of 150 Sverdrups (Sv), or 150 million cubic meters per second. For comparison, all of the rivers that enter the Atlantic Ocean make up a combined 0.65 Sv of water. The Gulf Stream brings warm water from the tropics northward into the Gulf of Mexico, around Florida, and up the East Coast, and is also responsible for the relatively warm climates across Northern Europe.

Once the Gulf Stream leaves the East Coast of the US at Cape Hatteras in North Carolina, it begins to travel northwest out into the open ocean, where it branches into two main currents. One is the North Atlantic Current, which is the branch that later cools to become North Atlantic Deep Water, and the other is the Azores Current (Figure 1).

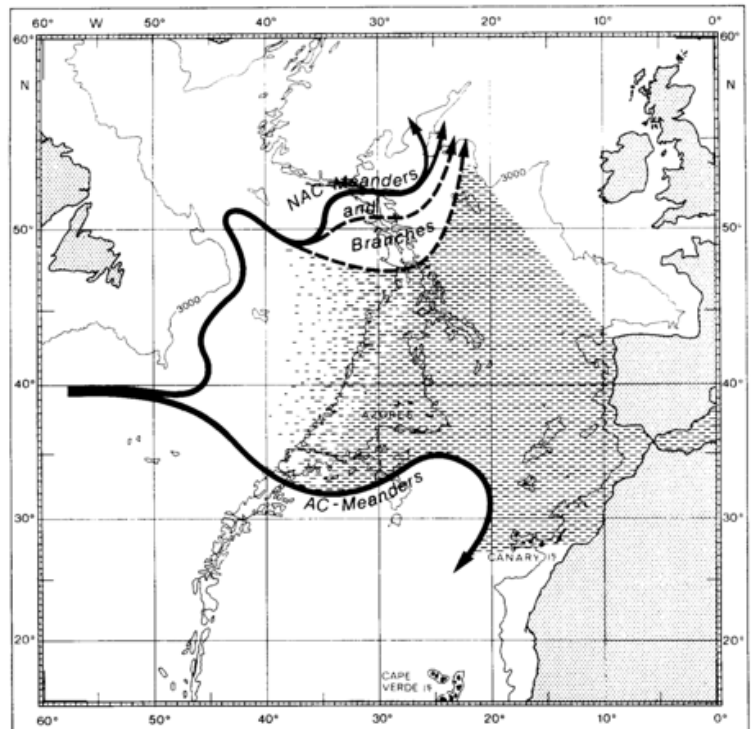


Figure 1. Map of the Gulf Stream extension currents (NAC and AC). From Sy, 1988.

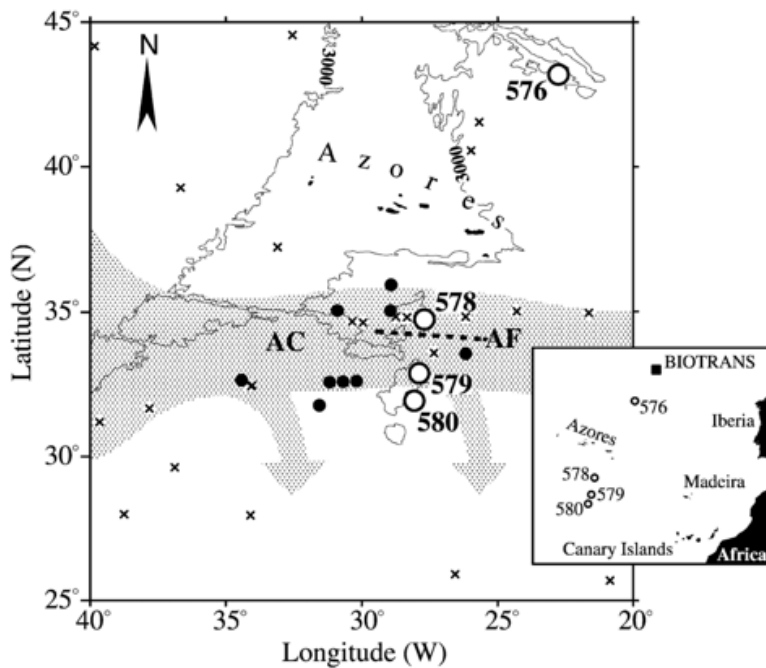


Figure 2. Map showing the location of the Azores Current (AC) and Azores Front (AF) relative to the Azores. From Scheibel et al., 2002.

the year. This suggests an alternative driving mechanism for the Azores Current. Outflow of very salty water from the Mediterranean Sea via the Strait of Gibraltar and Gulf of Cadiz has been proposed as a stabilizing mechanism that could have basin-wide effects on enhancing the strength of the Azores Current.

Coincident with the Azores Current is the Azores Front, which marks the boundary between African and European water masses (Figure 2). There is approximately a 4°C difference in temperature across the Azores Front (Gould, 1987) and a large change in water column structure (Fasham, 1985). Intensified local upwelling also allows for enhanced primary productivity, and the change in temperature and nutrient concentrations across the Azores Front leads to different plankton ecologies on either side (Scheibel et al., 2002). This difference in ecologies has been used to reconstruct variations in the Azores Front over glacial-interglacial cycles, which show that during glacial periods, the Azores Front moves southward significantly (Scheibel et al., 2002).

References

- Fasham, M.J.R., Platt, T., Irwin, B., and Jones, K., 1985, Factors Affecting the Spatial Pattern of the Deep Chlorophyll Maximum in the Region of the Azores Front: *Prog. Oceanog.*, v. 14, p. 129–165.
- Gould, W.J., 1985, Physical Oceanography of the Azores Front: *Prog. Ocean.*, v. 14, no. 1972, p. 167–190.

The Azores Current was relatively recently discovered and first published on in the mid- to late-1980s (Gould, 1985). Previously, it was unclear where exactly the return flow to the south occurred—many believed it to be west of the Mid-Atlantic Ridge (Worthington, 1976). Hydrographic surveys revealed a primarily zonal flow from the Grand Banks of Newfoundland to the Gulf of Cadiz. The eastward transport of the Azores Current is 8-12Sv, most of which is in the top 1000m of the ocean. Despite seasonal variation in the latitude of wind fields, the Azores Current does not vary on seasonal timescales, but instead meanders randomly throughout

- Ozgokmen, T.M., Chassignet, E.P., and Rooth, C.G.H., 2001, On the Connection between the Mediterranean Outflow and the Azores Current: *Journal of Physical Oceanography*, p. 461–480.
- Schiebel, R., Waniek, J., and Zeltner, A., 2002, Impact of the Azores Front on the distribution of planktic foraminifers, shelled gastropods, and coccolithophorids: v. 49, p. 4035–4050.
- Schiebel, R., Schmuker, B., Alves, M., and Hemleben, C., 2002, Tracking the Recent and late Pleistocene Azores front by the distribution of planktic foraminifers: *Journal of Marine Systems*, v. 37, p. 213–227.
- Sy, A., 1988, Investigation of large-scale circulation patterns in the central North Atlantic: the North Atlantic Current, the Azores Current, and the Mediterranean Water plume in the area of the Mid-Atlantic Ridge: *Deep-Sea Research*, v. 35, no. 3, p. 383–413.
- Worthington, L. Valentine, 1976, On the north Atlantic circulation. *Johns Hopkins Oceanographic Studies*, 6.

Marine Boundary Layer

The marine boundary layer is the lowermost portion of the atmosphere that interacts with

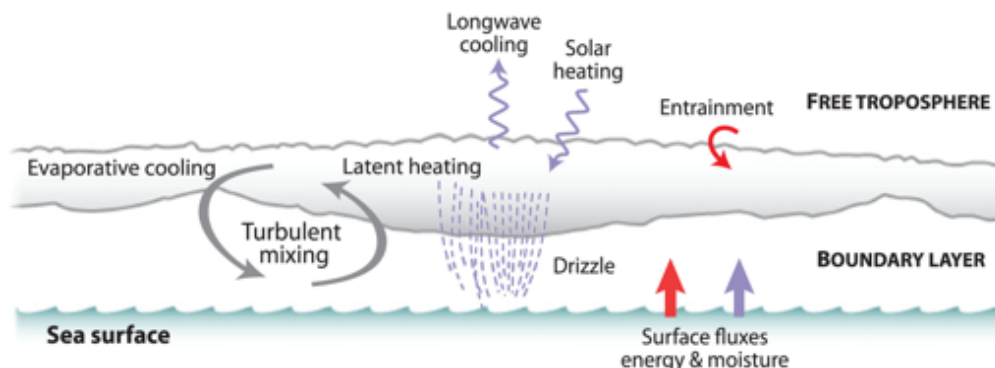


Figure 1. Schematic depicting the processes that occur in the Marine Boundary Layer.

the ocean's surface (Figure 1). It is generally 1-2 km thick and is usually topped by stratocumulus clouds. Marine boundary layer clouds are important in boundary layer dynamics, but they also are a key part of the earth's radiation budget (Rémillard et al., 2012). Their radiative impact is dependent on their macro- and microscopic properties, however observations of marine boundary layer clouds are usually limited in time from a couple of weeks to a month. These short-duration studies don't allow for climatology to be assessed as a factor in the formation of stratocumulus clouds or their properties.

In 2009, the Clouds, Aerosol, and Precipitation in the Marine Boundary Layer (CAP-MBL) field campaign took place on Graciosa Island in the Azores. The U.S. Department of Energy Atmospheric Radiation Measurement Program Mobile Facility, which includes more advanced instrumentation than previous MBL cloud studies, was deployed there for 21 months.

The goals of the program were to detect the presence of clouds in the overlaying atmospheric column, in addition to climatological measurements including temperature and precipitation amount and type. This led to a variety of findings—data included in Figure 3 showed that while upper level clouds show a seasonal signal, lower level clouds are common throughout the year. High radar reflectivity at low levels from October to May (Figure 3) is indicative of wintertime rain.

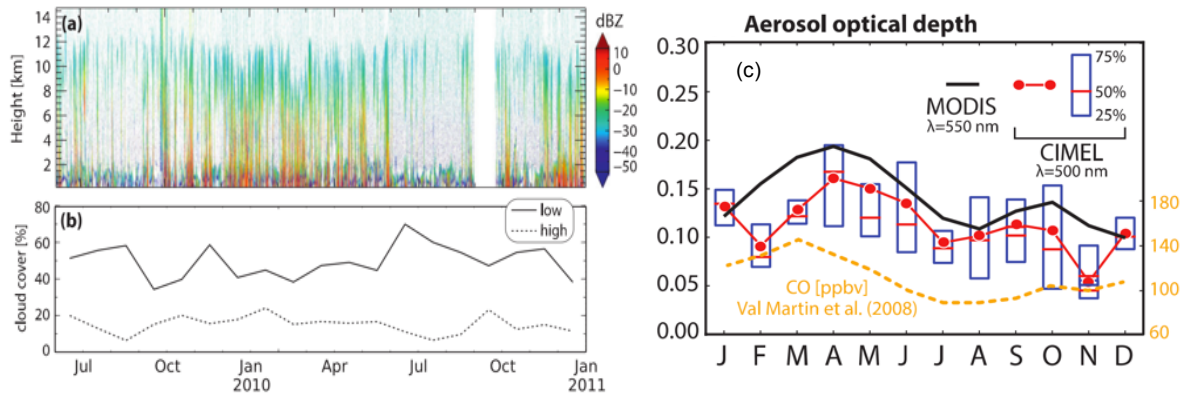


Figure 2. A) Height-time series of radar reflectivity from the CAP-MBL mobile ARM deployment. B) Monthly cloud cover determined using the data from A. From Wood et al., 2015. C) Measured Aerosol optical depth at the Azores (red lines/blue boxes) and satellite-measured (MODIS) aerosol optical depth (black).

The success of the temporary field station led to the establishment of a permanent monitoring station in 2013, also on Graciola Island. The initial studies revealed a wide variety of cloud types representative of most over Earth as a whole, which made the Azores the preferred location for the establishment of a new permanent monitoring system. Future monitoring aims to provide data to evaluate and improve global weather and climate models.

References

- Remillard, J., Kollias, P., Luke, E., and Wood, R., 2012, Marine Boundary Layer Cloud Observations in the Azores: *Journal of Climate*, v. 25, p. 7381–7398, doi: 10.1175/JCLI-D-11-00610.1.
- Wood, R., Wyant, M., Bretherton, C.S., Remillard, J., Kollias, P., Fletcher, J., Stemmler, J., Szoek, S. de, Yutter, S., Miller, M., Mechem, D., Tselioudis, G., Chiu, J.C., Mann, J.A.L., et al., 2015, Clouds, Aerosols, and Precipitation in the Marine Boundary Layer: An ARM Mobile Facility Deployment: *Bulletin of the American Meteorological Society*, no. March, p. 419–440, doi: 10.1175/BAMS-D-13-00180.1.

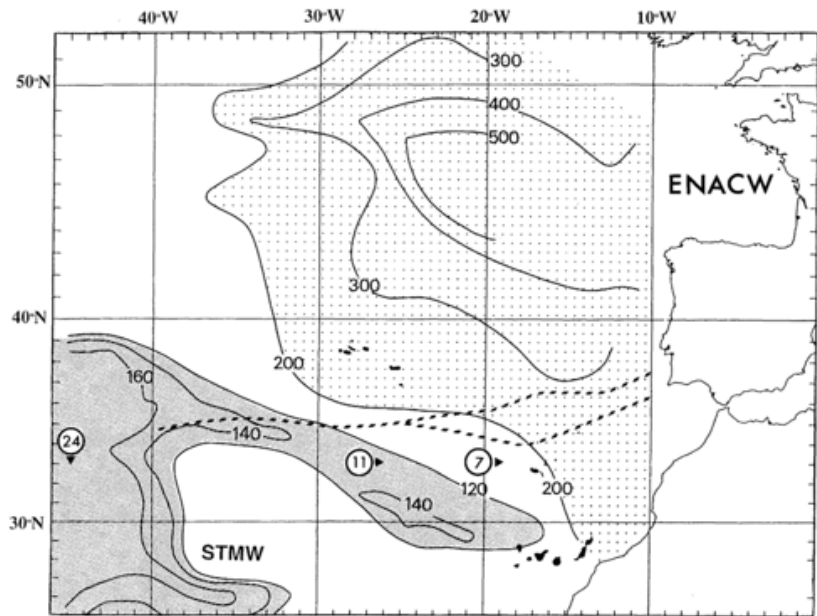


Figure 1. Winter thickness (m) of Eastern North Atlantic Central Water (ENACW) Mode Water with $27.0 < \sigma_\theta < 27.2 \text{ kg m}^{-3}$, with maximum winter thickness near $\sim 46^\circ\text{N } 16^\circ\text{W}$ (WOA94 data) and Subtropical Mode Water (STMW) with $26.4 < \sigma_\theta < 26.6 \text{ kg m}^{-3}$ (which contains Sargasso Sea Water ($\sim 18^\circ\text{C}$) with $\sigma_\theta \sim 26.45 \text{ kg m}^{-3}$). The STMW has a maximum winter thickness (240 m) in the Western Basin at $\sim 36^\circ\text{N } 52^\circ\text{W}$, near the position of minimum thickness (80 m) of water with $27.0 < \sigma_\theta < 27.2 \text{ kg m}^{-3}$, located near $37^\circ\text{N}, 55^\circ\text{W}$. The dashed lines represent mean positions of the Subtropical Front derived from the infrared imagery (see text for details). Ringed values are transport (in Sv, reference level 2000 dbar) associated with the STF (see text for details).

Around the first century AD, the Roman historian Plutarch visited Macaronesia, the area of the eastern Atlantic that includes Cape Verde, the Canary Islands, Madeira, the Savage Islands and the Azores. He remarked that there was “an air that is salubrious, owing to the climate and the moderate changes in the seasons, prevails on the islands.” [Cropper, 2013] Today the Azorean climate is relatively mild with annual temperature variations of only 6 degrees (Figure 1) and is likened to the Mediterranean climate [Hernández *et al.*, 2016]. However, the Azores are vulnerable to changes in precipitation patterns that can yield flash floods, droughts, and landslides.

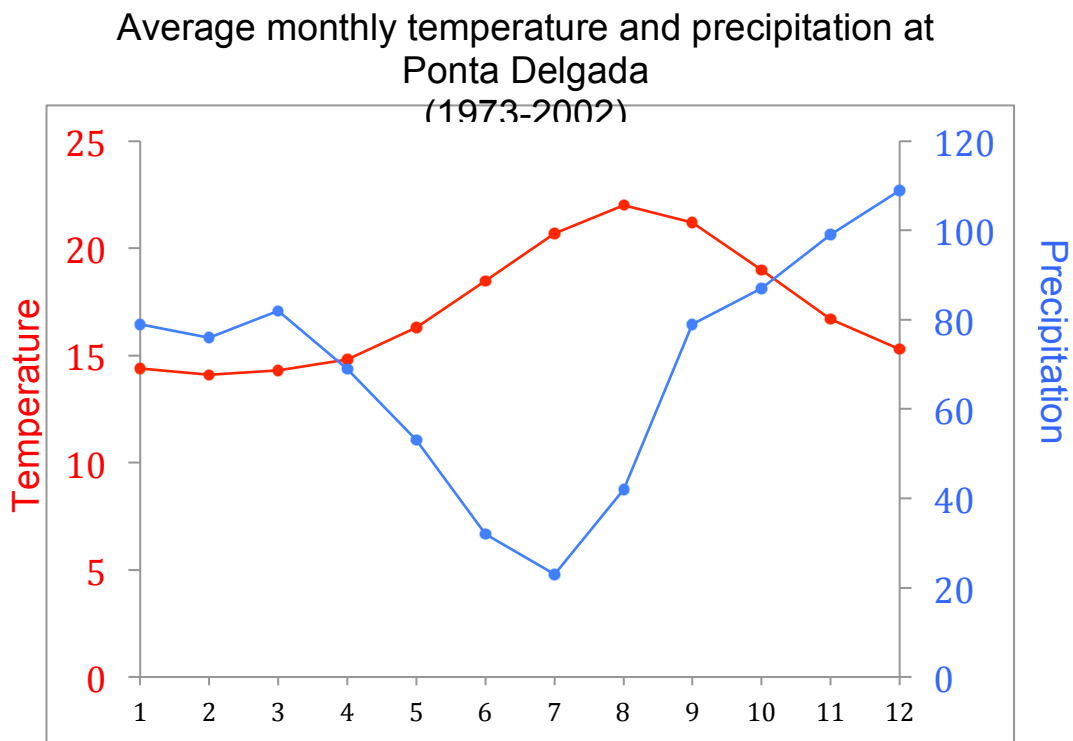


Figure 1 Plotted from Cropper [2013].

Located ~35 deg North, the Azores sit between the Hadley and Ferrel Cells under a semi-permanent high-pressure system called the Azores High (sometimes referred to as the Bermuda High). Farther to the north, the Iceland Low, a subpolar semi-permanent low-pressure system, is recorded. Together, the Azores High and Iceland Low define the North Atlantic Oscillation index (NAOi), a climate index that tracks the position and intensity of these semi-permanent pressure systems.

A weather station at Ponta Delgada on Sao Miguel has been recording temperature and precipitation since 1873, and records of sea level pressure (SLP) go back to 1850. From 1973-2002 mean annual precipitation was 829 mm/yr [Cropper, 2013]. For comparison, New York City’s mean precipitation rate is around 1175 mm/yr. However stable in general, precipitation patterns at Ponta Delgada strong seasonal cycle as well as clear interannual

variability (Figure 1). Winter (ONDJFM) marks the rainy season while summers are generally dry. Precipitation data from Ponta Delgada from 1873-2012 show two distinct periods (Figure 2). From 1873-1942, the drier period, average precipitation was 893.3 mm/yr. From 1942-2012, average precipitation increased to 1001 mm/yr. Extreme precipitation events have increased throughout the period, with almost 35% of extreme events occurring from 1992-2012.

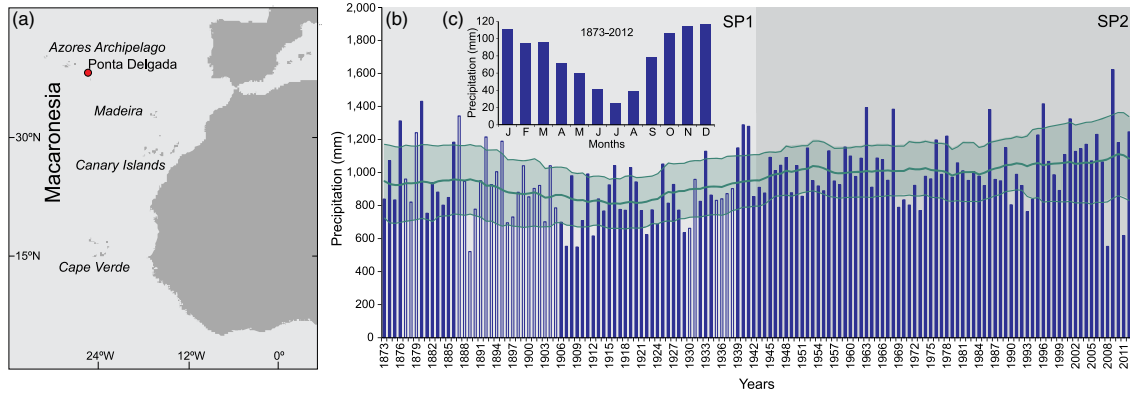


Figure 2 from *Hernández et al.* [2016].

The NAO is the leading mode of climate variability in the North Atlantic [*Hurrell, 1995*]. It is characterized by shifts in the strength and position of the Azores High and Iceland Low pressure systems in the north Atlantic. Other modes of climate variability include the Atlantic Multidecadal Oscillation (AMO), Pacific Decadal Oscillation (PDO), which both describe sea surface temperature changes, and the most famous El Niño Southern Oscillation (ENSO). Just as ENSO is known to have teleconnections with other parts of the globe, the NAO impacts precipitation in the eastern United States, western Europe and Greenland as well as the Azores.

The North Atlantic Oscillation index (NAOi) is a SLP anomaly (SLPa) difference that tracks the NAO. The NAOi is defined as:

$$\text{NAOi} = \text{SLPa}_{\text{Azores}} - \text{SLPa}_{\text{Iceland}}$$

There is no distinct periodicity in the NAO (Figure 3).

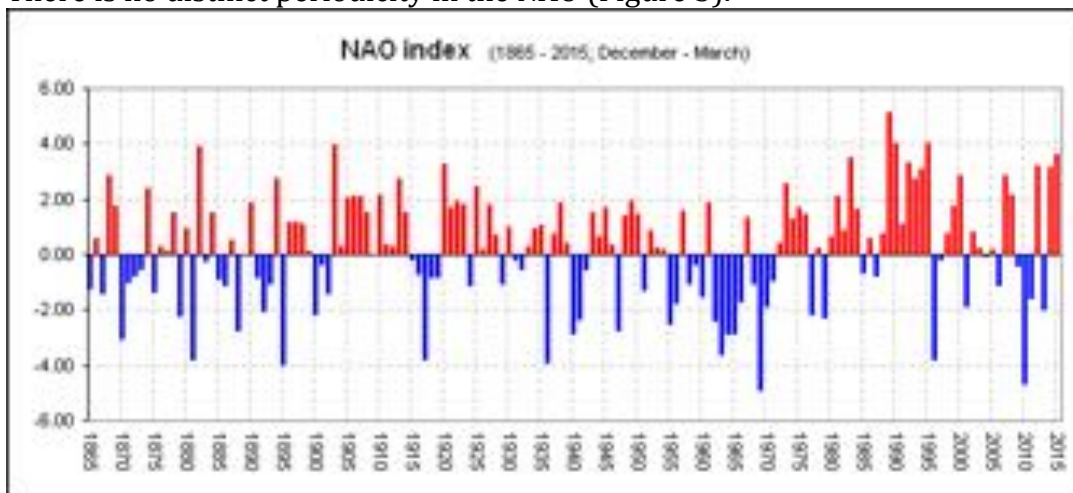


Figure 3

The positive/negative phase of NAO (NAO+/NAO-) occurs when the Azores High is anomalously high/low and the Iceland Low is anomalously low/high. During the positive/negative phase of the NAO, winter rainfall generally decreases/increases in the Azores.

The NAO has a strong correlation with winter precipitation at Ponta Delgada, but a weaker correlation with summer precipitation (Figure 4). Up to 50% of the variance in winter precipitation patterns can be explained by the NAO [Hernández *et al.*, 2016]. Patterns in summer precipitation may be instead governed by the AMO, PDO and ENSO. However, it is still true that precipitation throughout the year is higher during NAO- years than NAO+ years.

A. HERNÁNDEZ *et al.*

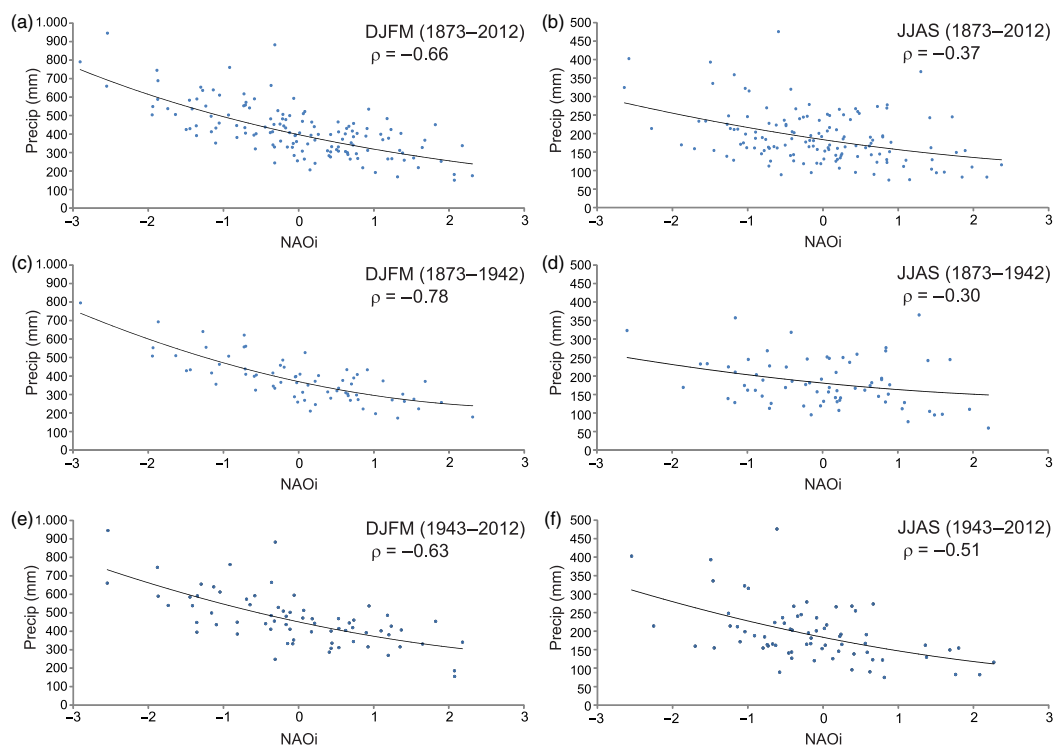


Figure 4 Correlation between the NAOi and precipitation for winter (left) and summer (right) from [Hernández *et al.*, 2016]

In addition, severe precipitation conditions correspond with the NAO- phase. However, the magnitude of the NAOi does not correlate with the amount of precipitation, it is only the sign of the NAO that is linked with severe precipitation. The NAO- phase does correlate with high severe precipitation during summer months [Hernández *et al.*, 2016]. In addition, there is a link between hurricane conditions and daily severe precipitation. The May-June NAOi sign is indicative of increased hurricanes (NAO- phase corresponds to more hurricanes crossing the Atlantic) that bring rain to Ponta Delgada during the summer (6 out of 10 days with precipitation exceeding 110 mm correspond to tropical storms in the North Atlantic.) [Hernández *et al.*, 2016]

Cropper, T. (2013), The weather and climate of Macaronesia: past, present and future, *Weather*, 68(11), 300-307, doi:10.1002/wea.2155.

Hernández, A., H. Kutiel, R. M. Trigo, M. A. Valente, J. Sigró, T. Cropper, and F. E. Santo (2016), New Azores archipelago daily precipitation dataset and its links with large-scale modes of climate variability, *International Journal of Climatology*, 36(14), 4439-4454, doi:10.1002/joc.4642.

Hurrell, J. W. (1995), Decadal Trends in the North Atlantic Oscillation: Regional Temperatures and Precipitation, *Science*, 269(5224), 676-679, doi:10.1126/science.269.5224.676.

Volcanic Emissions Climate and Health

In addition to ash and lava, volcanoes emit large masses of gas during eruptions. The majority of this gas is water, with large portions of CO₂, and SO₂ and minor components of HF, CO, N₂, Ar, He, H₂O (Shinohara, 2013). Particular gas volumes and ratios are geographically dependent on the volatile concentrated in the melting source region. Globally, volcanoes emit a combined average of 0.26 billion metric tons of CO₂ per year. (Gerlach, 2011). Volcanoes are a key component of long term global carbon cycles. The majority of emissions are released during an eruptive event, but hazardous amounts of gas can still be released in the quiet stages of volcanic cycle (Viveiros *et al.*, 2015). Gases emitted during an eruption can potentially impact global climate while quiescent emissions often effect the health and safety of people living near and visiting volcanic centers.

Climate Effects

Common misconceptions about global warming

Climate change deniers often scapegoat volcanic CO₂ emissions as the cause of global warming. They erroneously state human fossil fuels emissions pale in comparison to volcanic emissions. The truth is that total volcanic CO₂ outputs globally (0.26 Gt) amount to only the equivalent of anthropogenic emission in the state of Ohio alone (Gerlach, 2011). The 1991 eruption of Mount Pinatubo in Indonesia was the largest volcanic eruption in the last 100 years. For volcanic emissions to match annual human CO₂ emissions, 700 equally sized eruptions would need to occur every year. Figure 1 compares annual human emissions and volcanic emissions since 1750.

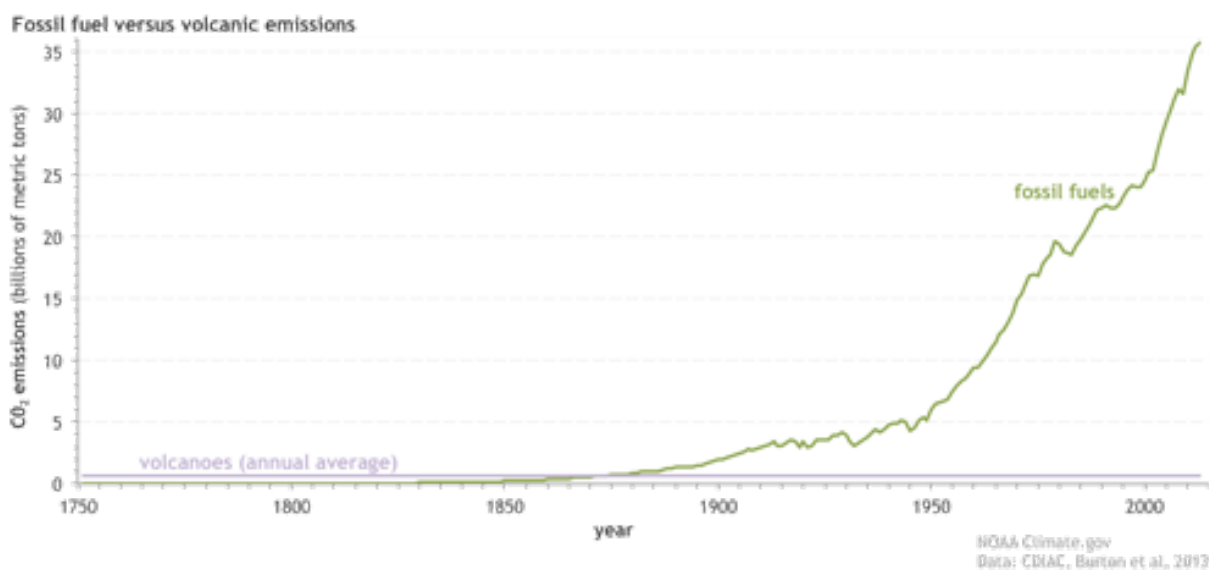


Figure 1. Annual CO₂ emissions for anthropogenic and volcanic sources (NOAA Climate.GOV, 2016)

Cooling effects on Climate

Sulfur gases released during volcanic eruptions can potentially reduce global average temperatures by several degrees Celsius. This effect can last for up to several years. The immediate climate effect of an eruption is local cooling associated with ash clouds. (~2°C) (Niemeier *et al.*, 2009). This cooling is short lived, as ash quickly settles out of the atmosphere. Sulfur Dioxide injected into the stratosphere during a plinian eruption has the potential to cool the atmosphere by several degrees for reduced global mean temperatures (USGS, 2016). SO₂ in the atmosphere undergoes photochemical reactions with water to produce sulfuric acid (H₂SO₄). Sulfuric acid reacts to form sulfate aerosols which increases albedo and cools the earth (USGS, 2016). Reactions associated with the formation of sulfate aerosols also deplete the ozone layer. Figure 2 details these processes and reactions (USGS, 2016). Particles can stay in and cool the atmosphere for several years.

The June 15th 1991 eruption of Mount Pinatubo emitted 17 Mt of SO₂ into the stratosphere. This spread around the world in 3 weeks and took one year to reach uniform coverage. It produced 25 Mt of sulfate aerosols and reduced global average temperatures by up to 0.5°C (Self *et al.* 1999). The climate effect was enough to negate warming associated with either el Niño or anthropogenic climate change from 1991 to 1993.

Health Hazards of Quiescent Emissions in the Azores

Gas emissions from the soil and fumaroles are the biggest concern for everyday life in the hydrothermal regions of the Azores (Wallenstein *et al.*, 2015). Carbon dioxide released from the soil tends to concentrate in topographic lows and unventilated structures creating asphyxiation risks. Additionally, radon gas is commonly associated with elevated CO₂ output which has been correlated with elevated cancer risks. All three volcanos on São Miguel contain hydrothermal areas where potentially hazardous CO₂ concentrations can manifest (Viveiros *et al.*, 2015).

On our trip to São Miguel, we will be visiting Furnas Village which is located in a caldera of the Furnas Volcano complex. The area is well known for the many geysers and smoking fumaroles around the village. The hydrothermal systems and stunning natural beauty are a large draw for tourism. The village's signature dish, Cozido das Furnas, consists of a variety of meats and vegetables slowly cooked in a cloth covered pot buried in the steaming hydrothermally active ground.



Furnas Village (Wikimedia Commons author: José Luis Ávila Silveira and Pedro Noronha e costa)



Furnas Village, São Miguel, Azores. (Wikimedia Commons author: Eduardo Manchon)



Fumarole in the Center of Furnas Village (Wikimedia Commons photo by José Luis Ávila Silveira and Pedro Noronha e costa)



Cozido das Furnas is cooked by burying a pot filled with the stew in the smoking ground and letting it sit for several hours. (Wikimedia Commons: Ravi Sarma)



Cozido Das Furnas: pork, beef, chicken, blood sausage, potatoes, sweet potatoes, kale, yams, carrots and cabbage, slowly cooked in a pot buried in hydrothermally active soil. (Wikimedia Commons author: Schnobby)

The entire Furnas Volcano emits ~1030 tons of CO₂ a day through its fumaroles, soil and hot springs (Pedone *et al.*, 2015). The main gases emitted are H₂O, CO₂, H₂S, N₂, O₂, CH₃ and Ar (Pedone *et al.*, 2015).

While there have been no reported deaths linked to asphyxiation from carbon dioxide emissions at Furnas village, gas emissions still represent a significant health hazard for the hydrothermal regions. As seen in Table 1, CO₂ concentrations above 15% by volume are quickly lethal, but concentrations as low as 0.5 vol% can cause difficulty breathing and headaches (Viveiros *et al.*, 2015).

CO ₂ concentration (percentage in air)	Exposure time	Health effects	Occupational exposure limit	Observations
0.039	–	–	–	Atmospheric air
0.5	–	–	8 h/day in a work environment	Permissible exposure limit
0.5–3.0	Several hours	Difficulty in breathing Increase in the cardiac rhythm Headache		
3.0	– > 15 min	– 100% breathing rhythm accelerates Headache Muscle weakness	15 min	Short-term exposure limit
5.0	–	300% breathing rhythm accelerates Headache Muscle weakness Depression Sickness Vertigo Noise in the ears Somnolence		
10.0	Several minutes	Unconsciousness, Quick recovery when the person is moved to a ventilated environment		
>15.0	–	Lethal concentration. Unconsciousness and death		

Based on NIOSH/OSHA (1981), Le Guern *et al.* (1982), Blong (1984), Wong (1996) and Williams-Jones & Rymer (2000).

Table 1 from Viveiros *et al.* (2015) Lists of risks for CO₂ hazards at various concentrations.

In Furnas Village, there have been reports of small animals dying, such as birds, cats and dogs. On Graciosa Island in 1992, two tourists died due to carbon dioxide asphyxiation in a lava cave where CO₂ concentrations were greater than 15% of the air by volume (Viveiros *et al.*, 2015). On some trails in the Furnas Caldera, CO₂ reaches concentrations of 80 vol% when measured 20 cm above the ground. (Viveiros *et al.*, 2010)

Asphyxiation is a pernicious problem because there is no simple way to tell where concentrations are hazardous and topography and weather cause concentrations to fluctuate wildly (USGS, 2017). Figure 3 demonstrates how sharp the boundary for lethal CO₂ concentrations can be. The flame is quickly suffocated when lowered only several inches and there are no visible signs in the air to distinguish the boundary.



Figure 3. The flame is quickly extinguished when lowered closer to the source of the carbon dioxide (USGS, 2017).

Homes in these hydrothermal regions can achieve hazardous carbon dioxide concentrations. This is most likely in buildings where there is little ventilation with fresh air between the building's foundation and the soil. Viveiros et al. (2015) recommend that the safest procedure would be to use maps of soil CO₂ degassing to zone for building codes. In hazardous populated areas, mitigation measures should be installed such as ventilated spaces between buildings and the soil, the use of fans and other air conditioning systems to create positive pressures beneath the floors, and installing impermeable membranes above the soil (Viveiros *et al.*, 2015).

Spikes in indoor CO₂ levels also correlate with barometric low pressures and rain soil (Viveiros *et al.*, 2015). This is thought to be because soil gas permeability is reduced in wet soil allowing more CO₂ to be emitted through the dry soil under buildings.

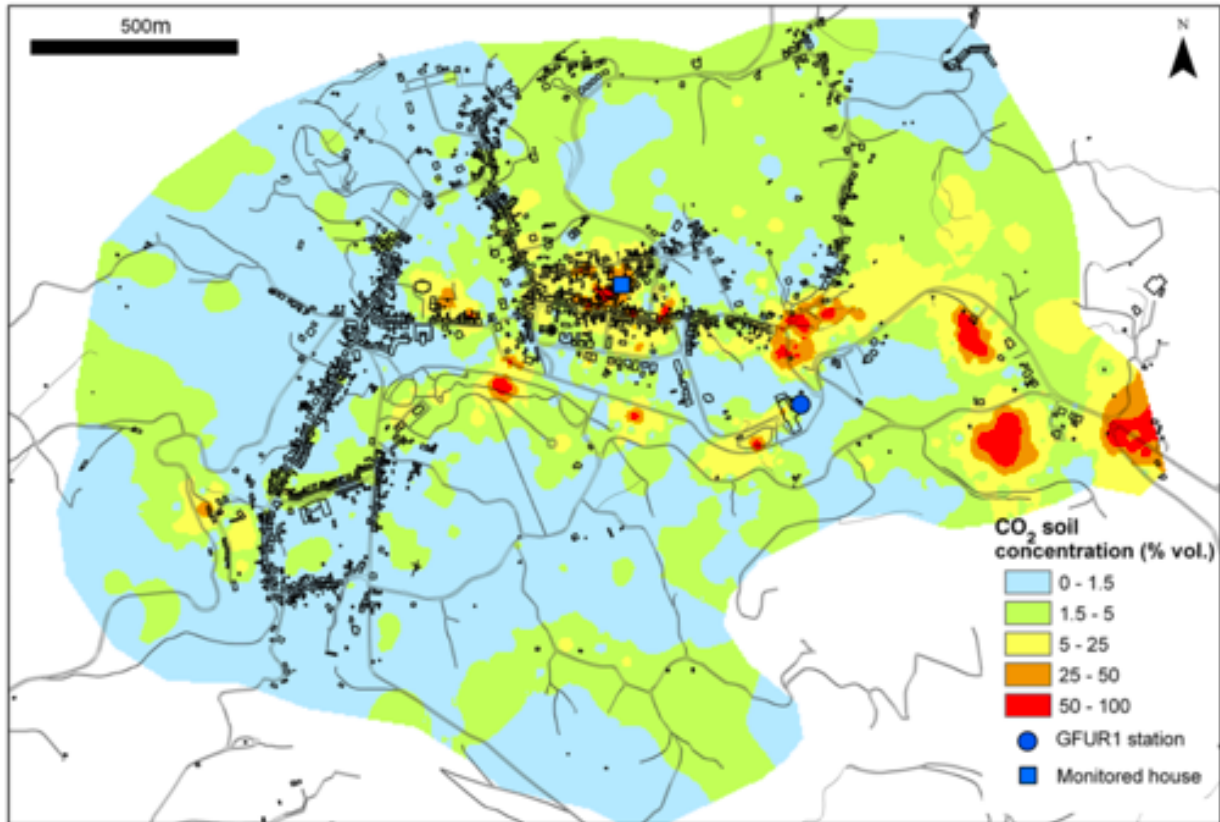


Figure 4. Map of soil CO₂ concentrations and locations of buildings in Furnas Village, São Miguel, Portugal from (Viveiros *et al.*, 2015). According to Viveiros *et al.* (2015), at soil CO₂ concentrations above 50 vol% there is a high risk of asphyxiation indoors; above 25 vol% underground spaces will accumulate lethal concentrations; above 5 vol% there is low risk of asphyxiation but poorly ventilated spaced below ground can possibly reach lethal levels.

Long-term exposure to volcanic air pollution from diffuse soil degassing has also been correlated to living in a volcanically active region (Linhares *et al.*, 2015). The Azores have the second highest death rate from respiratory diseases in all of Portugal. In the Azores, 195.8 deaths per 100,000 inhabitants are due to respiratory diseases, higher than the European average of 150 per 100,000 inhabitants (Linhares *et al.*, 2015). Linhares *et al.* (2015) found that the inhabitants of the hydrothermally active town of Ribeira Quente had a 4.4 times greater occurrence of respiratory defects than a reference area which was non-hydrothermally active.

Trace amounts of radon (²²²Rn) gas is also hazard in the hydrothermally active areas. Silva *et al.* (2015) found that in Furnas village and Ribeira Quente village respectively, 38% and 22% of buildings are built on soil that puts them at risk for elevated indoor ²²²Rn concentrations above the legal limit in the Azores (Silva *et al.*, 2015). Recent epidemiological studies of Ribeira

Quente village found that residents had a relative risk of 1.71 for developing chromosomal damage in mouth epithelial cells when compared to a control group with lower radon exposure. This type of chromosomal damage is used as a biomarker for cancer risk (Linhares *et al.*, 2016). The suggestions for mitigating ^{222}Rn exposure were comparable to those for CO_2 : mapping soil concentrations; increasing ventilation between soil and building foundations; and installing impermeable layers above soil (Silva *et al.*, 2015).

Gerlach, T. (2011) 'Volcanic versus anthropogenic carbon dioxide', *Eos*, 92(24), pp. 201–202. doi: 10.1029/2011EO240001.

Linhares, D. *et al.* (2015) 'Air Pollution by Hydrothermal Volcanism and Human Pulmonary Function', *BioMed Research International*, 2015. doi: 10.1155/2015/326794.

Linhares, D. P. S. *et al.* (2016) 'DNA damage in oral epithelial cells of individuals chronically exposed to indoor radon (^{222}Rn) in a hydrothermal area', *Environmental Geochemistry and Health*, pp. 1–12. doi: 10.1007/s10653-016-9893-2.

Niemeier, U. *et al.* (2009) 'Initial fate of fine ash and sulfur from large volcanic eruptions', *Atmospheric Chemistry and Physics Discussions*, 9(4), pp. 17531–17577. doi: 10.5194/acpd-9-17531-2009.

Pedone, M. *et al.* (2015) 'Total (fumarolic + diffuse soil) CO_2 output from Furnas volcano', *Earth, Planets and Space*. *Earth, Planets and Space*, 67(1), p. 174. doi: 10.1186/s40623-015-0345-5.

Shinohara, H. (2013) 'Composition of volcanic gases emitted during repeating Vulcanian eruption stage of Shinmoedake, Kirishima volcano, Japan', *Earth, Planets and Space*, 65(6), pp. 667–675. doi: 10.5047/eps.2012.11.001.

Silva, C. *et al.* (2015) 'Diffuse soil emanations of radon and hazard implications at Furnas Volcano, São Miguel Island (Azores)', *Geological Society, London, Memoirs*, 44(1), pp. 197–211. doi: 10.1144/M44.15.

Viveiros, F. *et al.* (2010) 'Soil CO_2 emissions at Furnas volcano, São Miguel Island, Azores archipelago: Volcano monitoring perspectives, geomorphologic studies, and land use planning application', *Journal of Geophysical Research: Solid Earth*, 115(12), pp. 1–17. doi: 10.1029/2010JB007555.

Viveiros, F. *et al.* (2015) 'Mapping of soil CO_2 diffuse degassing at São Miguel Island and its public health implications', pp. 185–195. doi: 10.1144/M44.14.

Wallenstein, N. *et al.* (2015) "'Chapter 16 Volcanic hazard vulnerability on São Miguel Island, Azores'", *Geological Society, London, Memoirs*, 44(1), pp. 213–225. doi: 10.1144/M44.16.

Webpages:

Scott, M., & Lindsey, R. (2016, June 15). Which emits more carbon dioxide: volcanoes or human activities? Retrieved August 15, 2017, from <https://www.climate.gov/news-features/climate-ga/which-emits-more-carbon-dioxide-volcanoes-or-human-activities>

Stephen Self, Jing-Xia Zhao, Rick E. Holasek, Ronnie C. Torres, Alan J. King. (1999, November 06). The Atmospheric Impact of the 1991 Mount Pinatubo Eruption. Retrieved August 15, 2017, from <https://pubs.usgs.gov/pinatubo/self/>

USGS Volcano Hazards Program. (2017, May 10). Volcanic Gas. Retrieved August 14, 2017, from <https://volcanoes.usgs.gov/vhp/gas.html>

USGS Volcano Hazards Program. (2016, February 26). Volcanic Gas: Climate Change. Retrieved August 14, 2017, from https://volcanoes.usgs.gov/vhp/gas_climate.html

Geothermal

Yen Joe Tan

The Earth's geothermal energy originates from during its original formation and from the decay of radioactive materials. This can be exploited to generate electricity. The three main type of geothermal power plants are dry steam, flash steam, and binary cycle. Dry steam power plants use steam directly from geothermal reservoirs to power turbines. It is the first type of geothermal power plant built. Flash steam power plants take deep, high-pressure water to the surface. This produces a blast of steam which is then used to power turbines. This remains the most common type of power plant. Binary cycle power plants allow exploitation of lower temperature geothermal reservoir by transferring the heat to a second liquid that has a lower boiling temperature. The vaporized liquid is then used to power turbines.

Azores is the major geothermal energy resource in Portugal. Every island except Corvo and Santa Maria has reported surface geothermal manifestation [Carvalho et al., 2015]. However, the Ribeira Grande geothermal field in Sao Miguel is the only high-temperature field exploited for the generation of electricity (Figure 1).

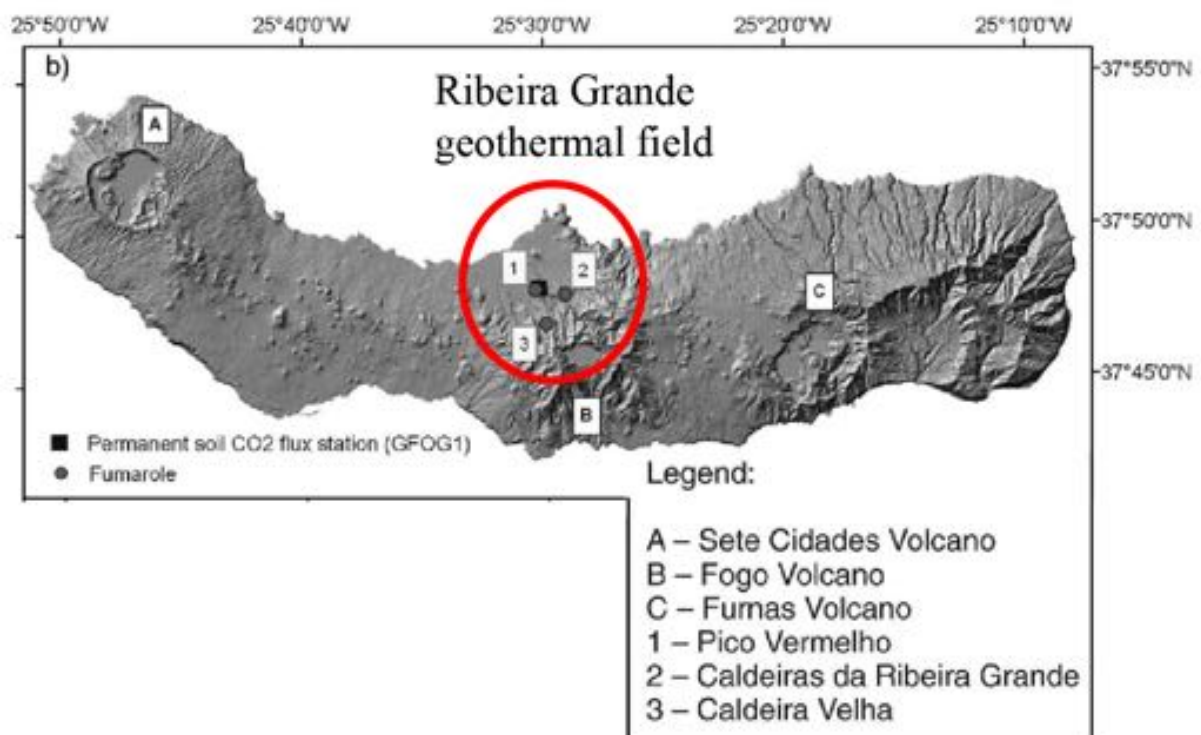


Figure 7. Location of the Ribeira Grande geothermal field on Sao Miguel, Azores, Portugal [Martini et al., 2009].

At the Ribeira Grande geothermal field, the Pico Vermelho pilot plant was started in 1980 with a 3 MW capacity. In 2006, a new power plant was started at Pico Vermelho that has a 10 MW capacity. In 2014, this was further expanded to have a > 10 MW capacity. The Ribeira Grande power plant was started in 1994 with a 5 MW capacity (Figure 2). This was further expanded in 2000 to a capacity of 13 MW. These development projects mean that the geothermal energy

production from the Ribeira Grande geothermal field has been steadily increasing over the years (Figure 3). In 2008, the energy production from the two power plants total 165 GWh. This represents ~ 39% of the electricity consumption in Sao Miguel (Figure 4). In 2014, the energy production from the two power plants total 196 GWh. This represents ~ 42% of the electricity consumption in Sao Miguel and ~ 22% that of the Azores archipelago [Carvalho et al., 2015].



Figure 8. Ribeira Grande power plant.

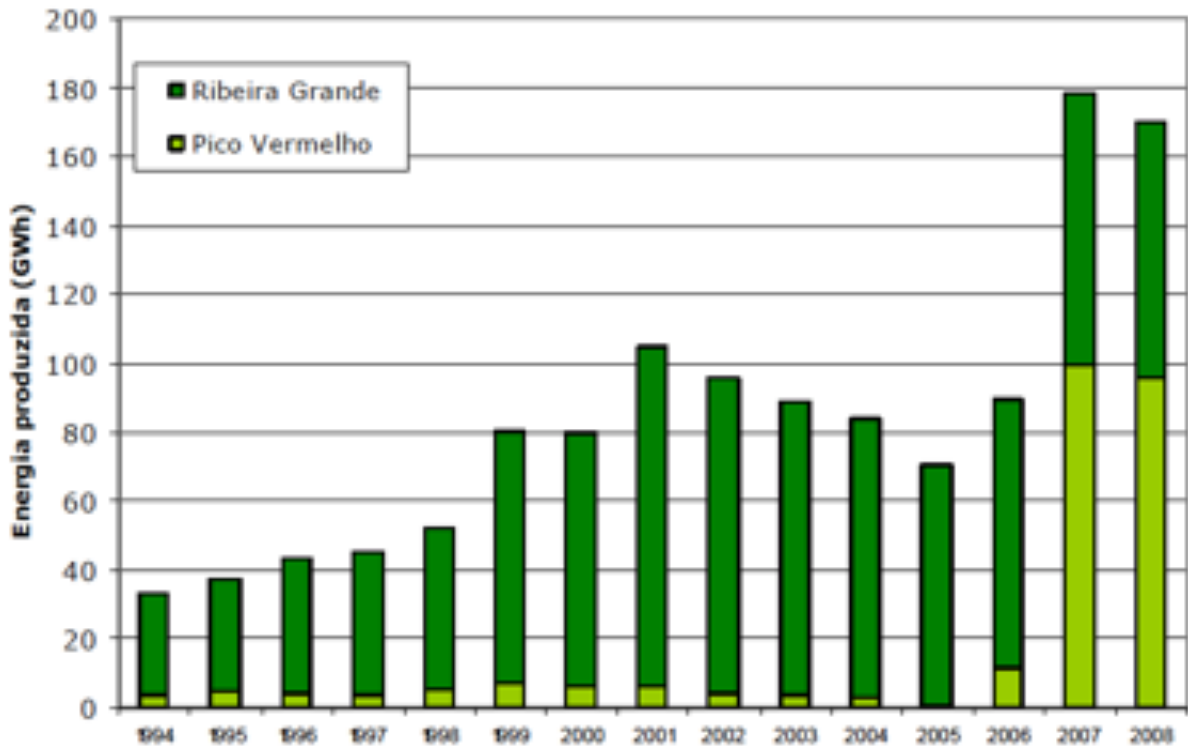


Figure 9. Annual geothermal energy production from Ribeira Grande geothermal field [SOGEO, 2017].

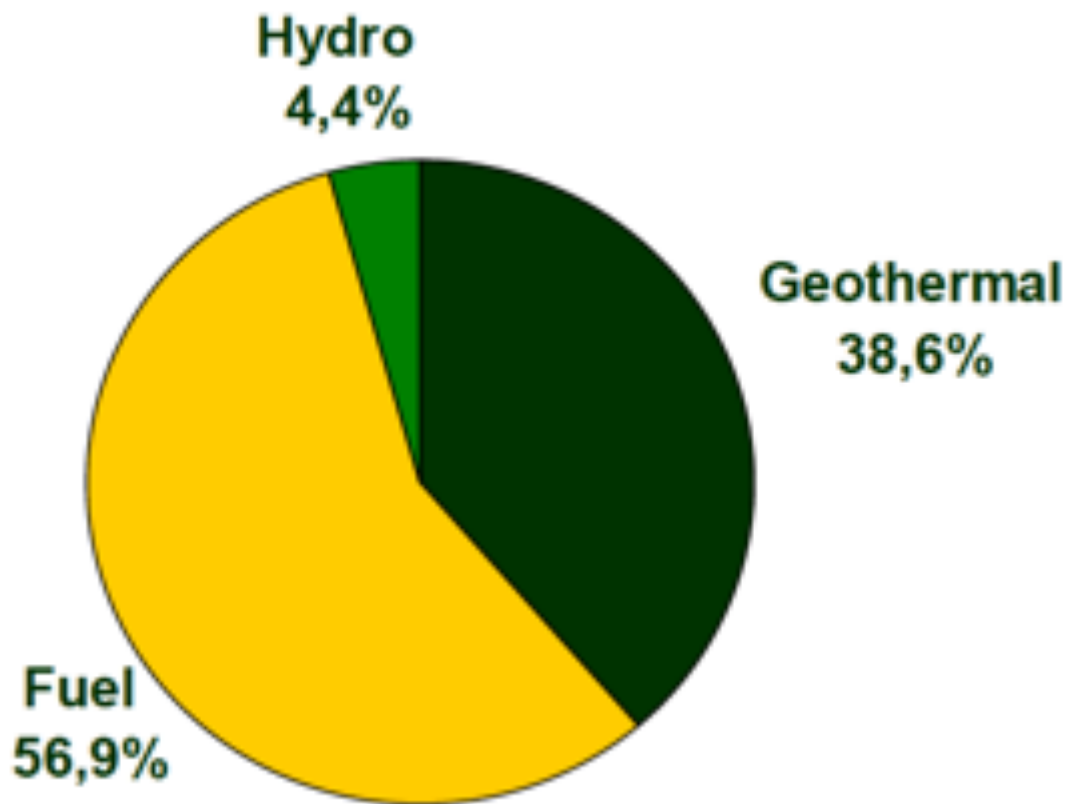


Figure 10. Energy consumption in Sao Miguel from different sources in 2008 [SOGEO, 2017].

In 2016, the construction of the Pico Alto pilot plant with 3 MW capacity was started in the Terceira Island (Figure 5). The power plant is expected to be completed in 2017.



Figure 11. Pico Alto power plant under construction in Terceira.

References:

Carvalho, J. M. et al. Portugal country update 2015 in *Proceedings World Geothermal Congress*, 2015.

Martini, F. et al. Seasonal cycles of seismic velocity variation detected using coda wave interferometry at Fogo volcano, Sao Miguel, Azores, during 2003-2004. *Journal of Volcanology and Geothermal Research*, 181:231-246, 2009.

SOGEO. Use of geothermal resources in the Azores islands. www.aegean-energy.gr/pdf/milos-conf2009/Geothermal_resources_in_the_Azores.pdf, last accessed August 2017.

Hydroelectric power

Bar Oryan

Hydro power has been used for at least 2000 years. It is not clear who were the first people to start using hydro power. The first usage of water as a source of power is documented to be around the 4th-3rd centuries B.C.E in various places in Eurasia. The main functions were water lifting for irrigation and grinding wheat into flour.

Hydroelectric power has come a long way since. The largest hydroelectric plant is the Three Georges dam in China (Figure 1). It has a generating capacity of 22,500 MW. In 2014, the dam generated 98.8 terawatt-hours breaking the world record for that time. With an average power consumption of 10,812 kWh per year, the Three Georges dam can provide power for about 9 million American households. With an average power consumption of about one tenth of the American household the Three Georges dam has the capacity to provide power for about 90 million Chinese households. The dam also reduces coal consumption by 31 million tons per year, avoiding 100 million tons of greenhouse gas emissions.

Dams benefit the environment by reducing greenhouse gas emissions and by providing cheap energy. However, dams have a devastating impact on the ecosystem of rivers and on the erosion and sedimentation deposition regime of a river. Subject to extensive research this would be out of scope for this guidebook.



Figure 12 - The Three Gorges dam in China.

Hydroelectric power: How it works

The basic principal of generating electricity using hydropower is simple. Using the earth's water cycle, a dam is most efficient when built on a river featuring a large drop of elevation. The potential energy of flowing water is harnessed and converted to electric energy using an electric generator. Water flow from the reservoir through the penstock drive the turbine that generates electricity as illustrated by figure 2.

The generation of electricity in the generator is based on Faraday's law of induction. Electric generators function in a similar in all

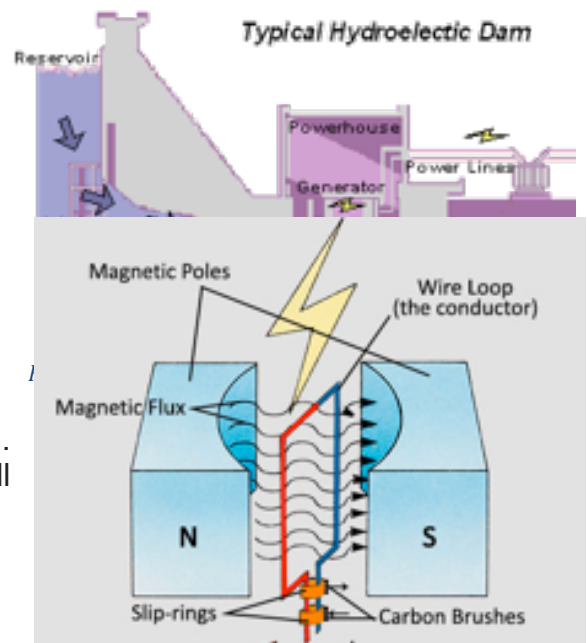


Figure 14 - illustration of a typical electric aenerator.

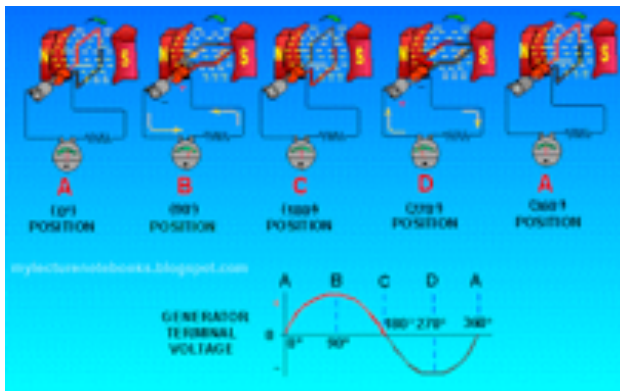
types of power plants and are based on the same principal. The major difference between different types of power plants is the driving force of the turbine. Faraday's law of induction can be described by the following equation:

$$\epsilon = \frac{d\Phi_{\beta}}{dt}$$

where ϵ is, the electromotive force generating the induced current and Φ_{β} is the magnetic flux and is denoted by:

$$\Phi_{\beta} = \oiint \vec{B} \cdot d\vec{S}$$

As can be seen above electromotive force will generate an induced current on a conductor only when the magnetic flux changes with time. There are two ways magnetic flux can change with time. The magnetic field denoted by \vec{B} can change. Also, the area perpendicular to the magnetic field could change. The second option is easier to accomplish using flow of water. In hydroelectric plants the flow of water is rotating a turbine that is rotating a conductor as illustrated in figure 3.



The direction of the induced current on the conductor that is driven by the turbine is determined by Fleming right hand rule. The induced current flows in the direction of the cross product of the direction of motion and direction of the magnetic field. The way the turbine moves the conductor generates an alternating current as shown in figure 4. It is possible

to generate a direct current using a commutator with the same principles.

Figure 15 - Generation of alternating current

Hydroelectric power in Portugal and in the Azores

February 2016 marked a peak in power produced by renewable sources in Portugal. 95% of the power produce was the product of renewable sources. However, less than 25% of the power generated by renewable sources is to be credit to hydroelectric power (Eurostat, 2015). The biggest hydroelectric power plant in Portugal is the Alto Lindoso dam (figure 5). It has a capacity of 630MW which is about 3% of the capacity of the Three Georges dam. There are about 100 hydroelectric power plants in Portugal most of them are small with some feeding local business. We will visit a small hydroelectric power feeding a tea planation.

Only 4% of the power produced in the Azores is generated by hydroelectric power plants. The island of San Miguel has the largest hydroelectric capacity with 7 hydroelectric plants able to produce 5.1MW which is 5% of the island demand



Figure 16 - Alto Lindoso dam

(Cross-Call, 2013; Nazari,2013). 4 hydroelectric plants are

responsible for 1.65 MW which is about 35% of the demand in Flores island (Cross-Call, 2013; Nazari,2013). Around 2% of the demand of Terceira and Faial is fulfilled by a number of hydroelectric plants producing 1.4 MW and 0.3MW respectively (Cross-Call, 2013; Nazari,2013).

Bibliography (APA)

Cross-Call, D. F. (2013). *Matching energy storage to small Island electricity systems: a case study of the Azores* (Doctoral dissertation, Massachusetts Institute of Technology).

Eurostat, E. U. (2015). Share of renewables in energy consumption up to 15% in the EU in 2013. Accessed: March.

Nazari, M. H. (2013). Electrical networks of the Azores Archipelago. In *Engineering IT-Enabled Sustainable Electricity Services* (pp. 99-118). Springer US.